Course Notes for SIGGRAPH 2016

Capturing the Human Body: From VR, Consumer, to Health Applications

Hao Li Lingyu Wei Anshuman Das Tristan Swedish Pratik Shah Ramesh Raskar

 SIGGRAPH '16 Courses, July 24-28, 2016, Anaheim, CA, ACM 978-1-4503-4289-6/16/07.
http://dx.doi.org/10.1145/2897826.2927371

Capturing the Human Body: From VR, Consumer, to Health Applications

Abstract: Modeling the human body is of special interest in computer graphics to create "virtual humans", but material and optical properties of biological tissues are complex and not easily captured. This course will cover the major topics and challenges in using image acquisition to model the human body.

Takeaways (what's in it for the reader): This course provides an overview of human body capture methodologies. Attendees will receive an overview of the bio-physics which create the variability in appearance of the eye, ear, skin, mouth, and hair among individuals. Instructors will then present state of the art methods used to create more accurate models by incorporating tools used in biomedical imaging. Such techniques use physical measurement to produce visually accurate human anatomy. Finally, we will explore health applications of image acquisition and modeling.

Course Schedule

8:30 am -- 9:00 am	Introduction to Body Shape and Human Performances [Li, Wei]
9:00 am -- 9:30 am	Biomedical Imaging and Human Image Capture [Das, Swedish, Shah]
9:30 am -- 9:50 am	Visual Computing in Health Technologies [Raskar]
9:50 am -- 9:55 am	Conclusion and Q&A session [All]
10:00 am	Close

Speaker's Bio

Hao Li, Assistant Professor, University of Southern California

Hao Li joined the University of Southern California in 2013 as a tenure-track assistant professor of computer science. Before his faculty appointment he was a research lead at Industrial Light & Magic, where he developed the next generation real-time performance capture technologies for Star Wars Episode VII. Prior to joining the force, Hao spent a year as a postdoctoral researcher at Columbia and Princeton Universities. His research lies in geometry processing, 3D reconstruction, and performance capture. While primarily developed to improve real-time digital content creation in film production, his work on markerless dynamic shape reconstruction has also impacted the field of human shape analysis and biomedicine. His algorithms are widely deployed in the industry, ranging from leading visual effects studios to manufacturers of state-of-the-art radiation therapy systems. He has been named top 35 innovator under 35 by MIT Technology Review in 2013 and NextGen 10: Innovators under 40 by CSQ in 2014. He was also awarded the Google Faculty Award in 2015, the SNF Fellowship for prospective researchers in 2011, and best paper award at SCA 2009. He obtained his PhD from ETH Zurich in 2010 and received his MSc degree in Computer Science in 2006 from the University of Karlsruhe (TH). He was a visiting professor at Weta Digital in 2014 and visiting researcher at EPFL in 2010, Industrial Light & Magic (Lucasfilm) in 2009, Stanford University in 2008, National University of Singapore in 2006, and ENSIMAG in 2003.

Anshuman Das, Postdoctoral Associate, MIT

Anshuman Das is a postdoctoral associate at MIT and the Tata Center for Technology and Design. Anshuman is interested in creating rapid diagnostics that are smart, predictive, and accessible and will improve the way diagnostics are carried out. Within the health diagnostics field he is exploring intersections with health diagnostics and optics, lasers, UV-VIS, soft x-ray, Raman, and terahertz spectroscopy. He is also interested in super-resolution optical imaging and soft matter based optical elements. He is currently working on electrical and optical sensing of infections, wide-angle endoscopy and designing smart otoscopes. Before coming to MIT Anshuman received his Ph.D. from JNCASR in India where he researched on light management, degradation, and electrode design in organic solar cells.

Tristan Swedish, Technical Assistant, MIT

Tristan Swedish is a Technical Assistant at MIT. He received his BS in Electrical Engineering and Physics at Northeastern University, where he created computational models of light propagation in lung tissue and worked on an optical device to measure the biomechanics of the cornea. Tristan has also worked at BBN Technologies on a project to detect signals in non-stationary environments and more efficient solutions to inverse problems in shock wave propagation. At the MIT Media Lab, Tristan is building new types of imaging devices for retinal and skin diagnostics.

Pratik Shah, Research Scientist, MIT

Pratik, a research scientist in the Camera Culture group at the MIT Media lab, works at the intersection of nanotechnology, imaging, low cost diagnostics, entrepreneurship and scalable solutions for improving human health. Pratik has experience in vaccine design and discovery, applying throughput OMICS, nanotechnology and nucleic acid sequencing for biomedical research and drug discovery, microbial signaling systems, start-up and non-profit ventures. He also works on clinical images, with graphical interfaces, to isolate disease features and develop neural nets, which can automatically label and overlay high-dimensional medical images. Pratik has a BS, MS and a Ph.D in microbiology and completed fellowship training at the Broad Institute, Massachusetts General Hospital and Harvard Medical School.

Ramesh Raskar, Associate Professor, MIT

Ramesh Raskar joined the Media Lab from Mitsubishi Electric Research Laboratories in 2008 as head of the Lab's Camera Culture research group. His research interests span the fields of computational photography, inverse problems in imaging and human-computer interaction. Recent projects and inventions include transient imaging to look around a corner, a next generation CAT-Scan machine, imperceptible markers for motion capture (Prakash), long distance barcodes (Bokode), touch+hover 3D interaction displays (BiDi screen), low-cost eye care devices (Netra,Catra), new theoretical models to augment light fields (ALF) to represent wave phenomena and algebraic rank constraints for 3D displays(HR3D). In 2004, Raskar received the TR100 Award from Technology Review, which recognizes top young innovators under the age of 35, and in 2003, the Global Indus Technovator Award, instituted at MIT to recognize the top 20 Indian technology innovators worldwide. In 2009, he was awarded a Sloan Research Fellowship. In 2010, he received the Darpa Young Faculty award. Other awards include Marr Prize honorable mention 2009, LAUNCH Health Innovation Award, presented by NASA, USAID, US State Dept and NIKE, 2010, Vodafone Wireless Innovation Project Award (first place), 2011. He holds over 40 US patents and has received four Mitsubishi Electric Invention Awards. He is currently co-authoring a book on Computational Photography.

Modeling and Capturing the Human Body: for rendering, health and visualization

Hao Li	Anshuman Das	Tristan Swedish	Pratik Shah	Ramesh Raskar
USC	MIT	MIT	MIT	MIT

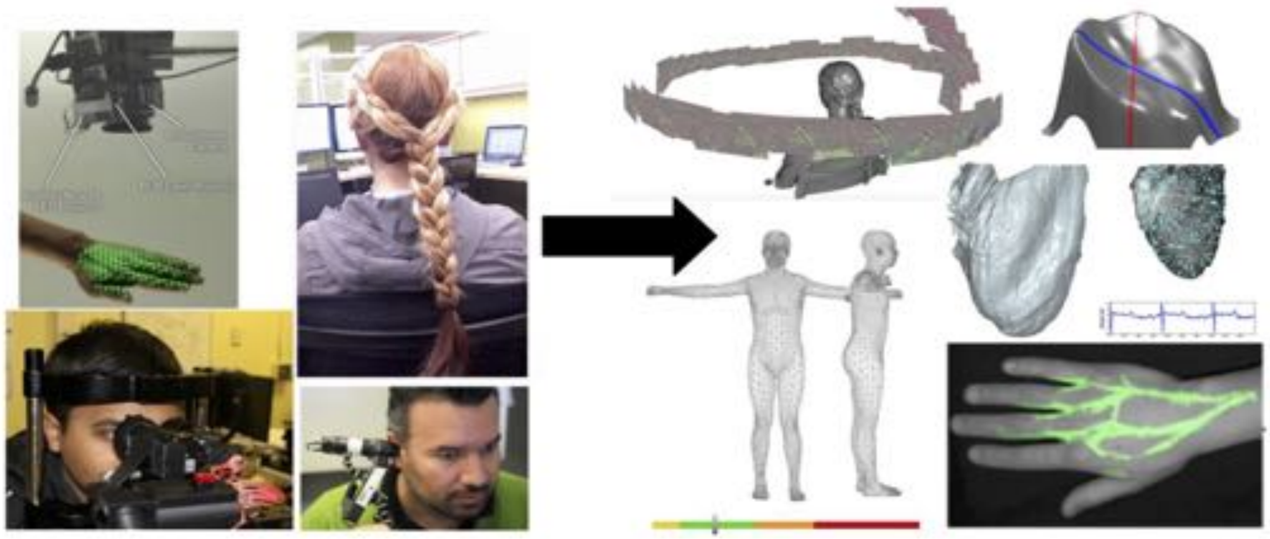

Figure 1: *This course offers an overview of modeling and capturing methodologies that have applications in rendering pipelines and health. We provide a survey of state of the art and emerging capturing modalities (left) in which the data produced can be transformed to visualize health, form, and performance (right).*

Abstract

Modeling the human body is of special interest in computer graphics to create "virtual humans", but material and optical properties of biological tissues are complex and not easily captured. This course will cover the major topics and challenges in using image acquisition to model the human body. Attendees will receive an overview of the bio-physics which create the variability in appearance of the eye, ear, skin, mouth, and hair among individuals. Instructors will then present state of the art methods used to create more accurate models by incorporating tools used in biomedical imaging. Such techniques use physical measurement to produce visually accurate human anatomy. Finally, we will explore health applications of image acquisition and modeling.

Module I: Introduction to Human Body Dynamics and Visual Appearance

In this module we will discuss the motivations for reproducing human appearance using computer graphics. We will introduce visually distinct anatomical features (eye, ear, skin, mouth and hair) their state of the art reproductions and relevance in health assessment. We will cover the biological reasons for dynamic appearance of humans such as blood perfusion in skin, breathing rates, and perspiration.

Module II: Biomedical Imaging and Human Image Capture

Image capture of real scenes is integral to creating visually believable models. We provide an overview of capturing techniques in the literature. Examples of the capabilities of biomedical imaging traditionally used in clinical settings will be provided. We will then examine how measurements made using biomedical devices are used for diagnosis and the shared problem domain of human appearance capture and health assessment.

Module III: Rendering the Human Body

This module explores how data captured from images can be incorporated in graphics rendering pipelines. Shape from image, light-tissue interaction physics and light transport models will be discussed.

Module IV: From Models to Health

Techniques developed to model the human body have applications in health. We will examine methods developed in both computer graphics and biomedical imaging communities to solve problems in cancer detection and heart monitoring.

Luo, L. et al. 2013. ACM Trans. Graph. 32, 4.
Pamplona, V. et al. 2011. ACM Trans. Graph. 30, 4.
Hu, L. et al. 2014. ACM Trans. Graph. 33, 4.
Pamplona, V. et al. 2010. ACM Trans. Graph. 29, 4.
Das, A. et al. 2015. SPIE Photonics West. 9303-302.
Li, H. et al. 2013. ACM Trans. Graph. 32, 4.
Swedish, T. et al, 2015, ACM Trans. Graph. 32, 4.
Kadambi, A. et al. 2013. Computational Optical Sensing and Imaging.

Course Outline

Part 1	Introduction to Human Body Shapes and Performances	Hao Li and Lingyu Wei
Part 2	Biomedical Imaging and Human Image Capture 1	Tristan Swedish
Part 3	Biomedical Imaging and Human Image Capture 1	Anshuman Das
Part 4	Biomedical Imaging and Human Image Capture 1	Pratik Shah
Part 5	Visual Computing in Health Technologies	Ramesh Raskar
	Closing Comments	

INTRODUCTION TO HUMAN BODY SHAPES AND PERFORMANCES

Hao Li and Lingyu Wei
MIT Media Lab

3D Scanning

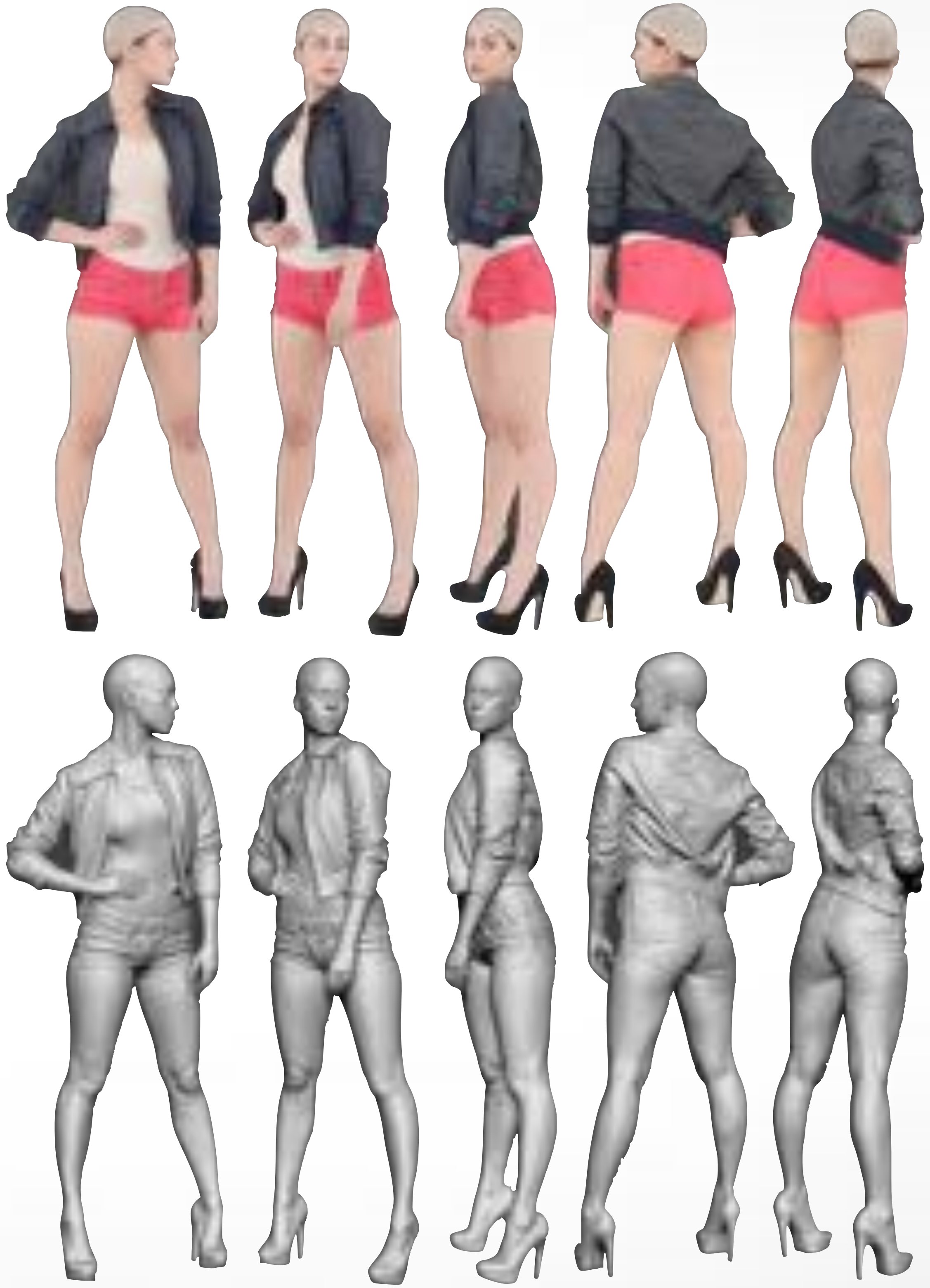

Realtime 3D Scanning

Democratization

Geometric Data

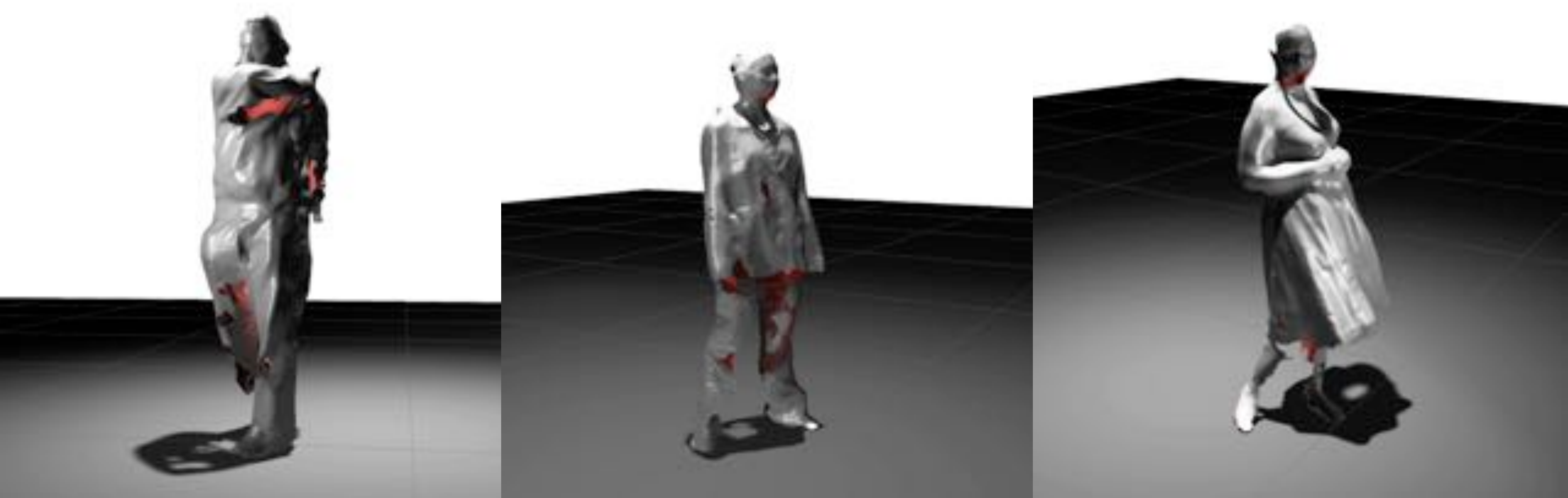

Research Agenda

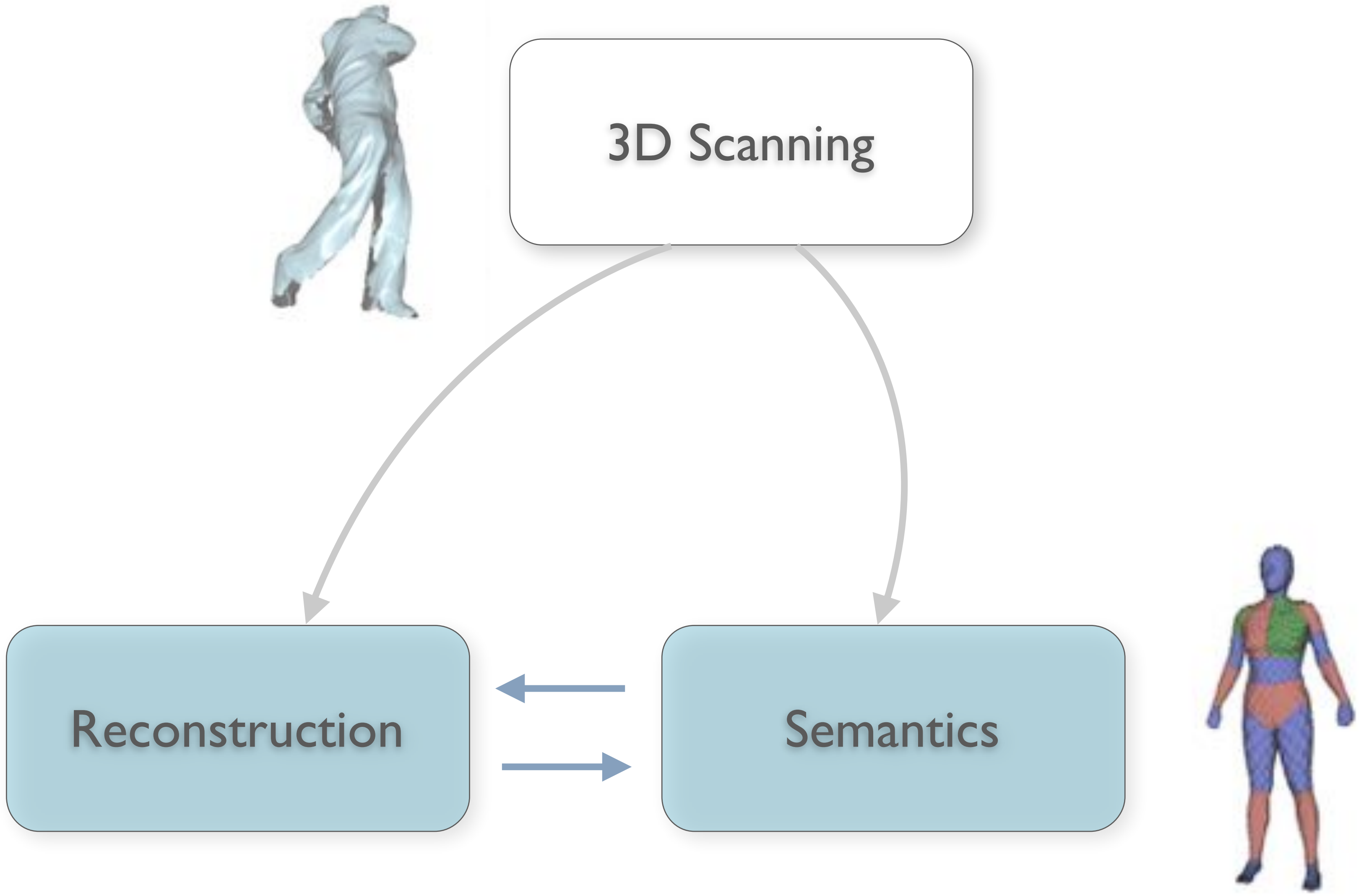

Correspondences

Dynamic Shapes

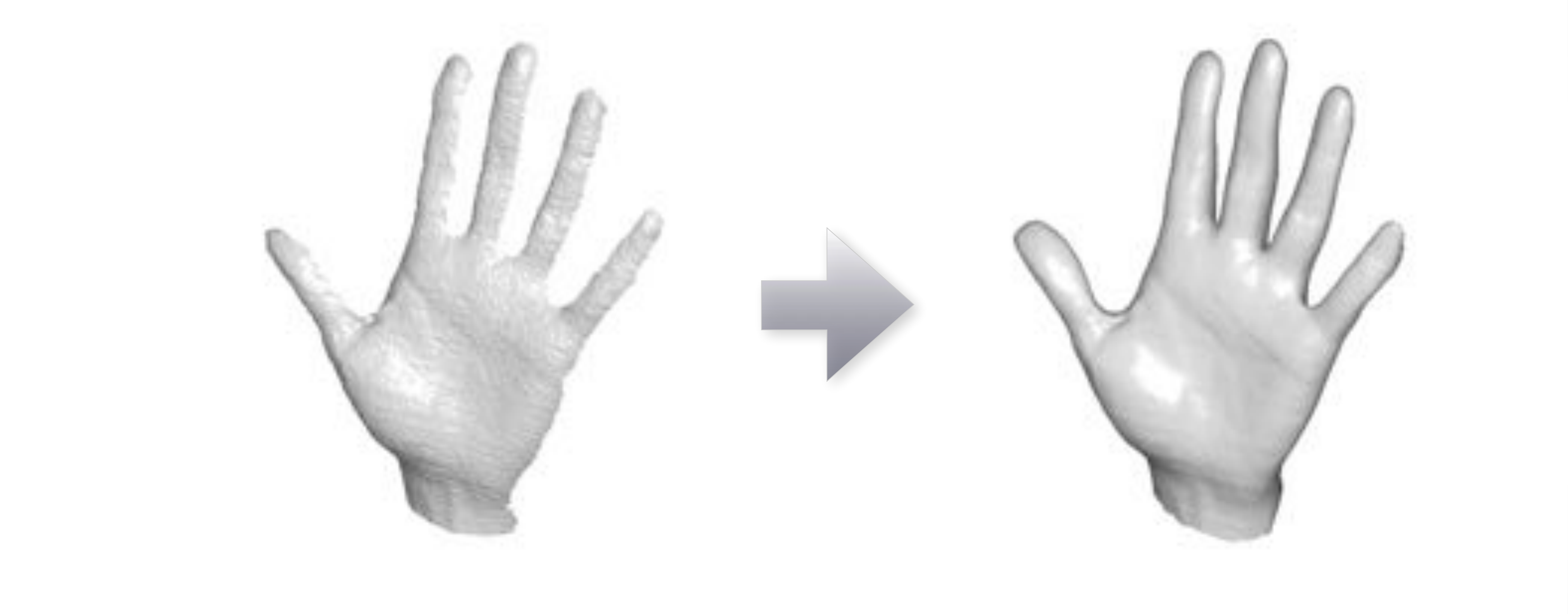

Correspondence Problem

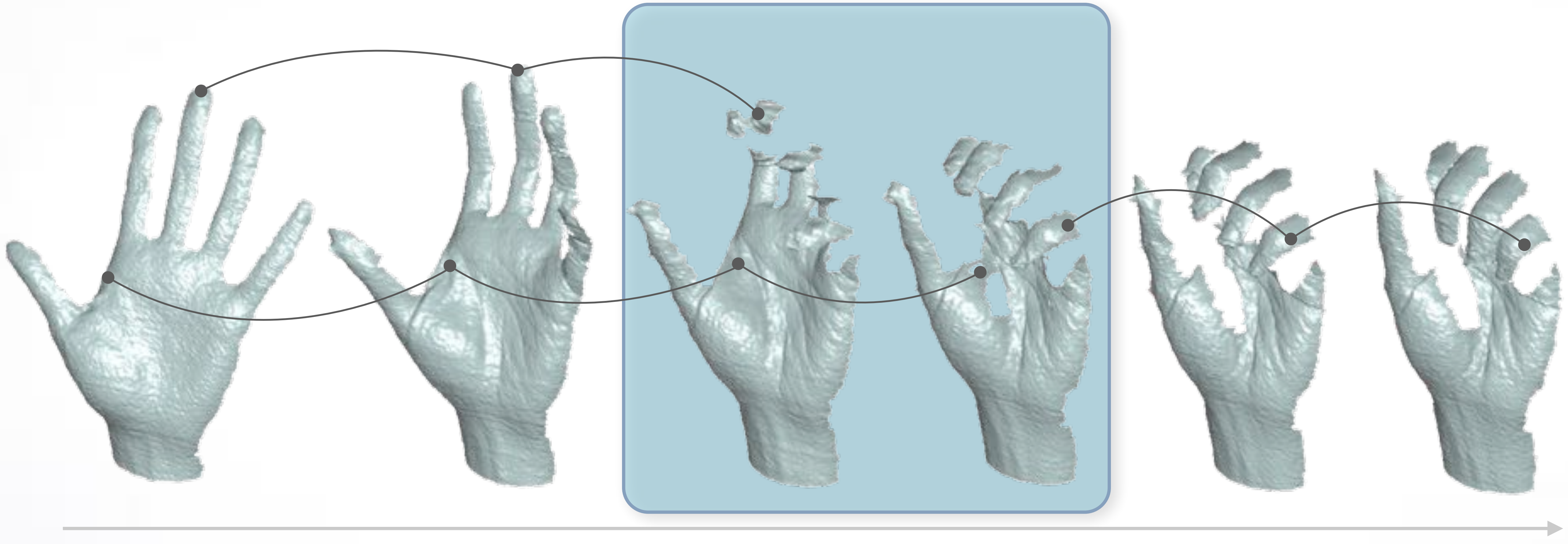

Non-Rigid Registration

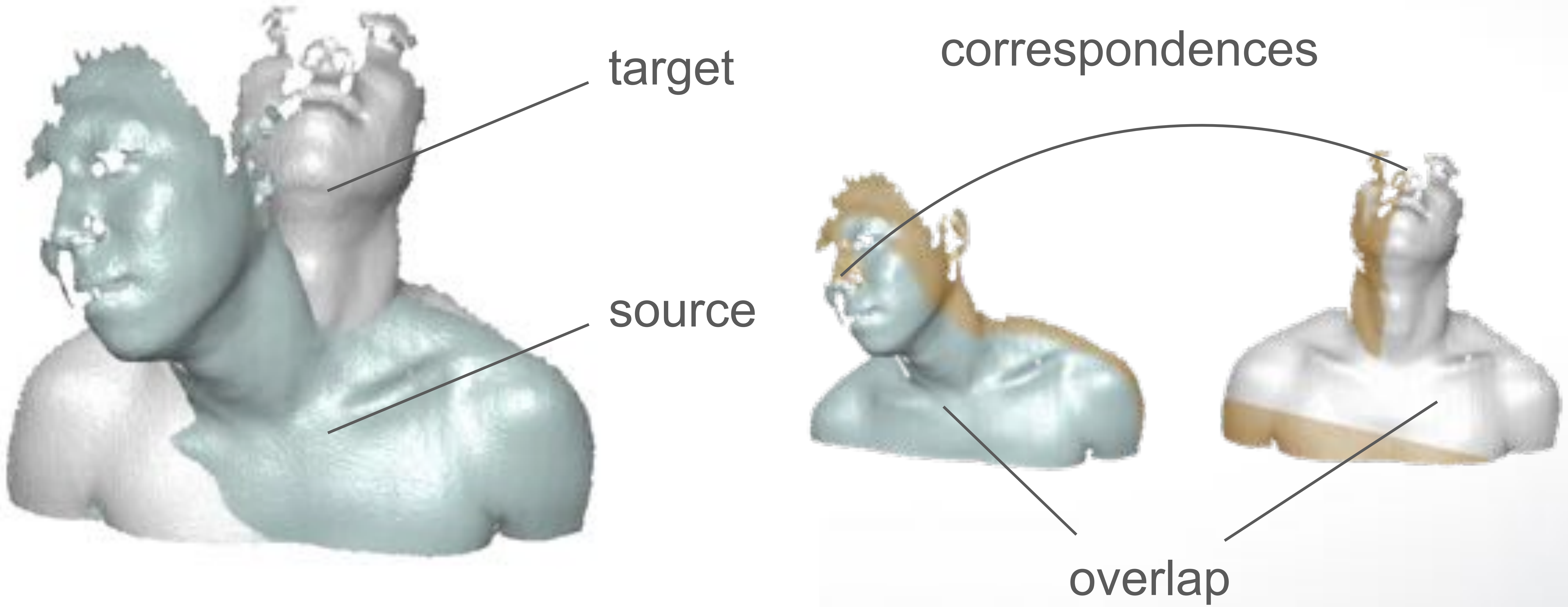

Understanding Shapes

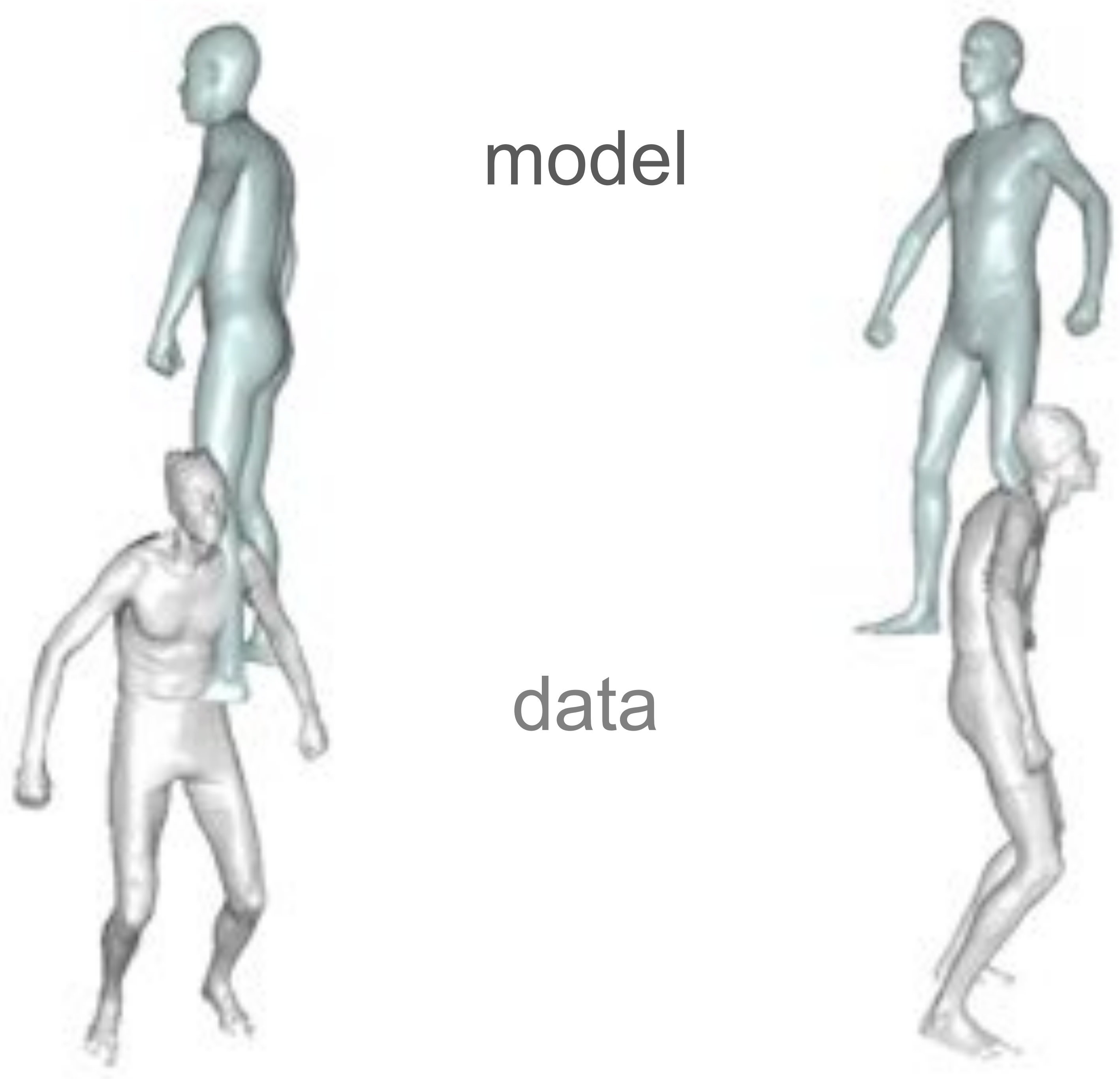

Other Applications

MPI IS, Embodee

entertainment

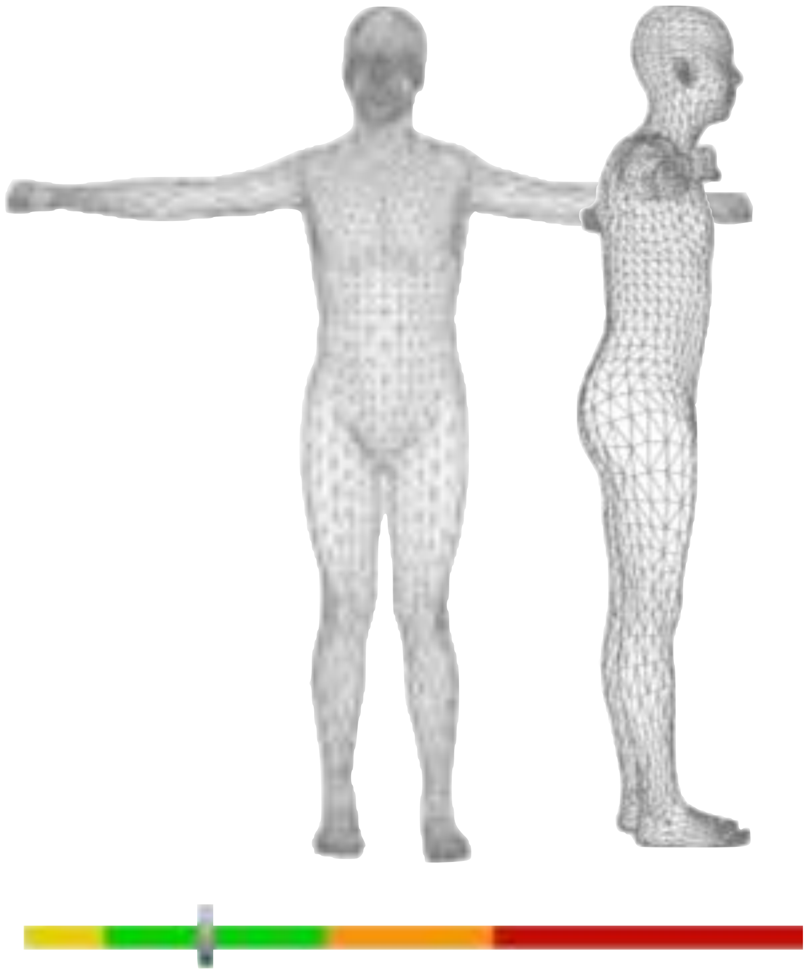

fitness

digital garment

3D **Self-Portraits**

Shapify.me

3D **Self-Portraits**

Pipeline

Overview

frame

scanning

fused scan

fusion &
segmentation

initial
alignment

non-rigid
registration

Overview

non-rigid registration

merging

texturing

3D print

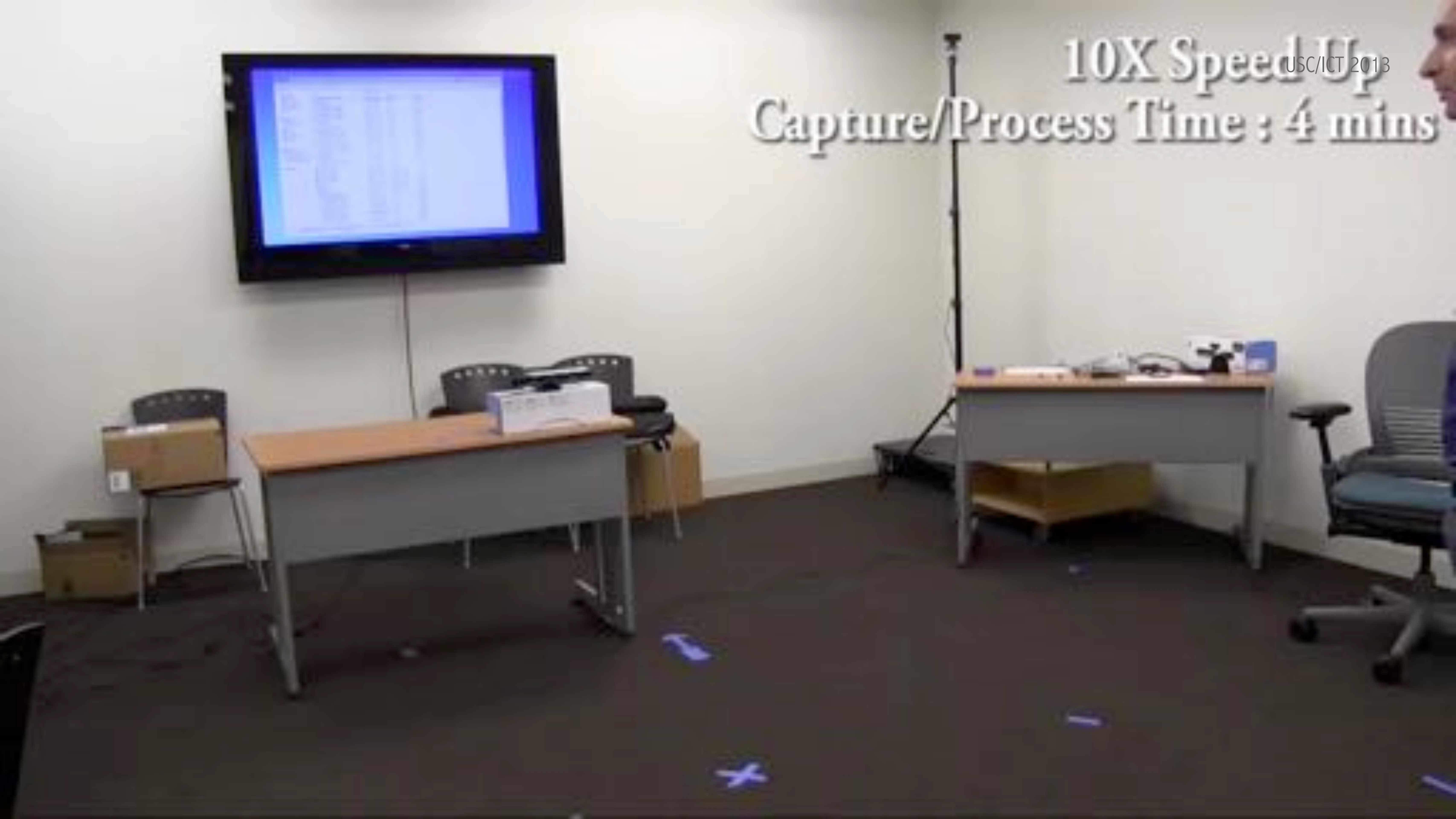
10X Speed Up
USC/ICT 2013
Capture/Process Time : 4 mins

Faces

Realtime 3D Scanning

Weise et al. 2009

Pipeline Overview

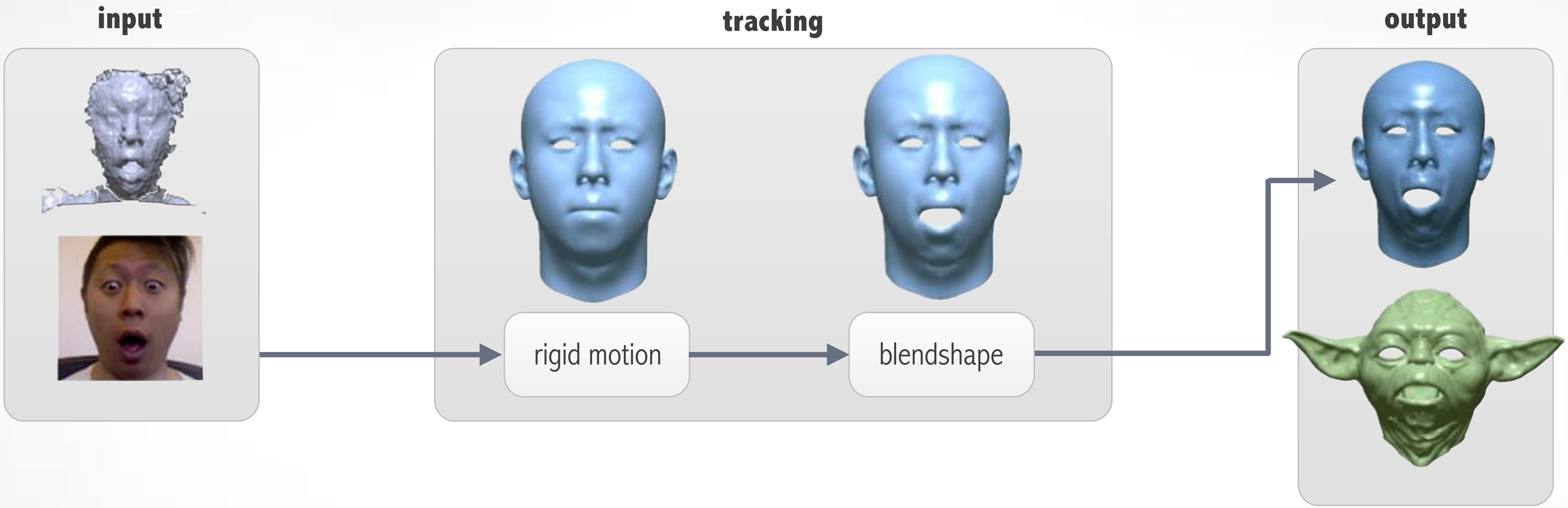

$$\mathbf{v}_i(\mathbf{x}) = \mathbf{v}_i^{(0)} + \sum_l \mathbf{v}_i^{(l)} x_l$$

$$x_l \in [0, 1]$$

Pipeline Overview

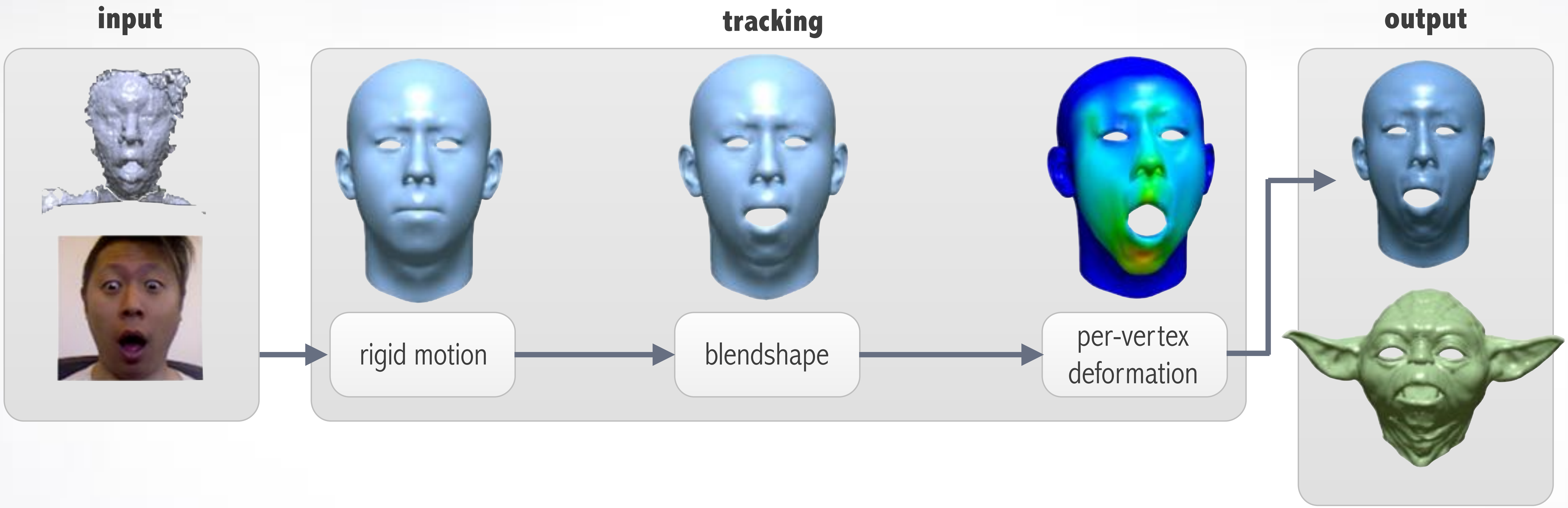

$$\tilde{\mathbf{v}}_i(\Delta\mathbf{v}_i) = \mathbf{v}_i + \Delta\mathbf{v}_i$$

Tracking **Basic Emotions**

Li et al. SIGGRAPH 2013

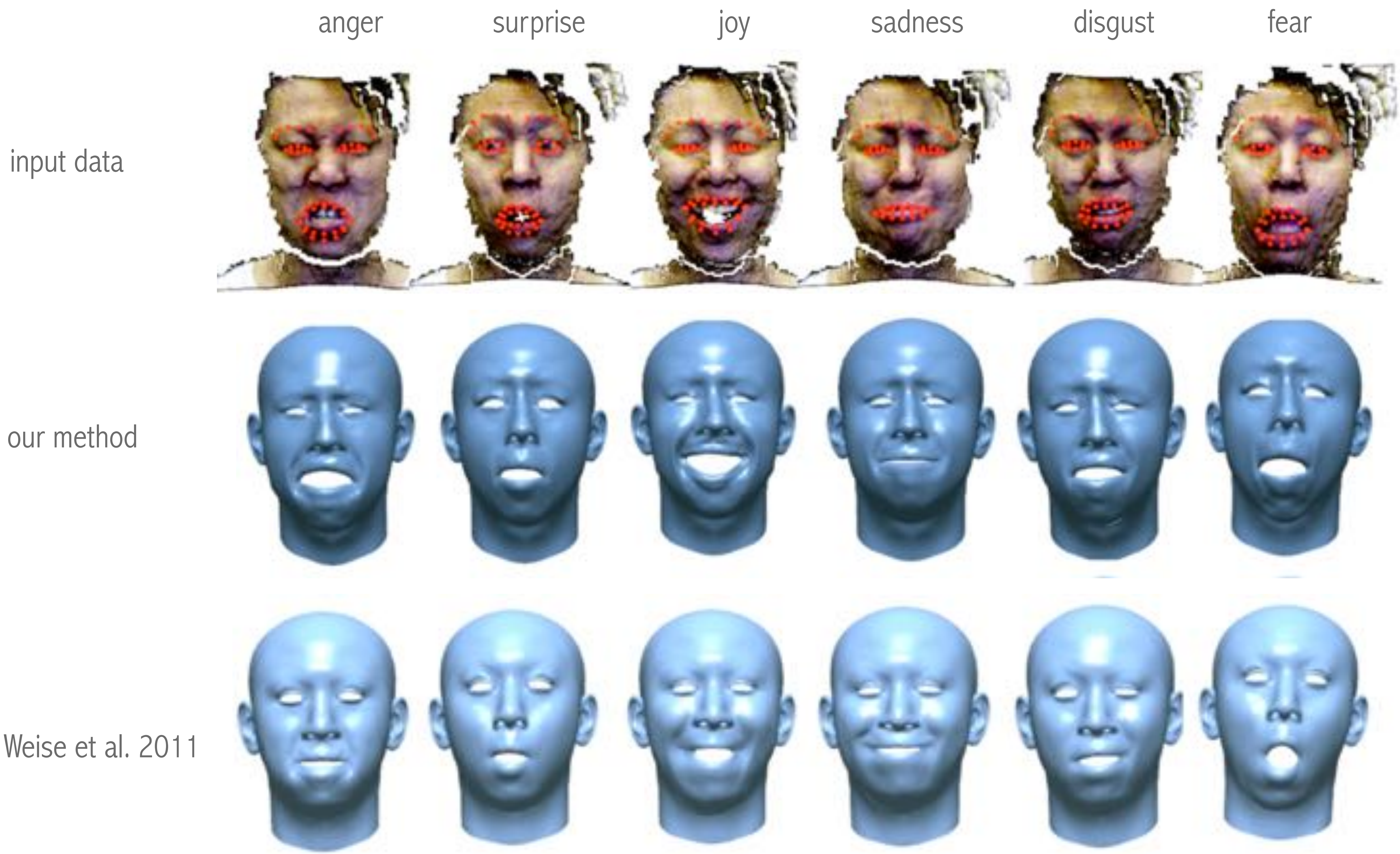

Facial Performance Capture

Li et al. SIGGRAPH 2013

Fast **Calibration**

Li et al. SIGGRAPH 2013

Capturing **Hair**

Hu et al. SIGGRAPH 2014

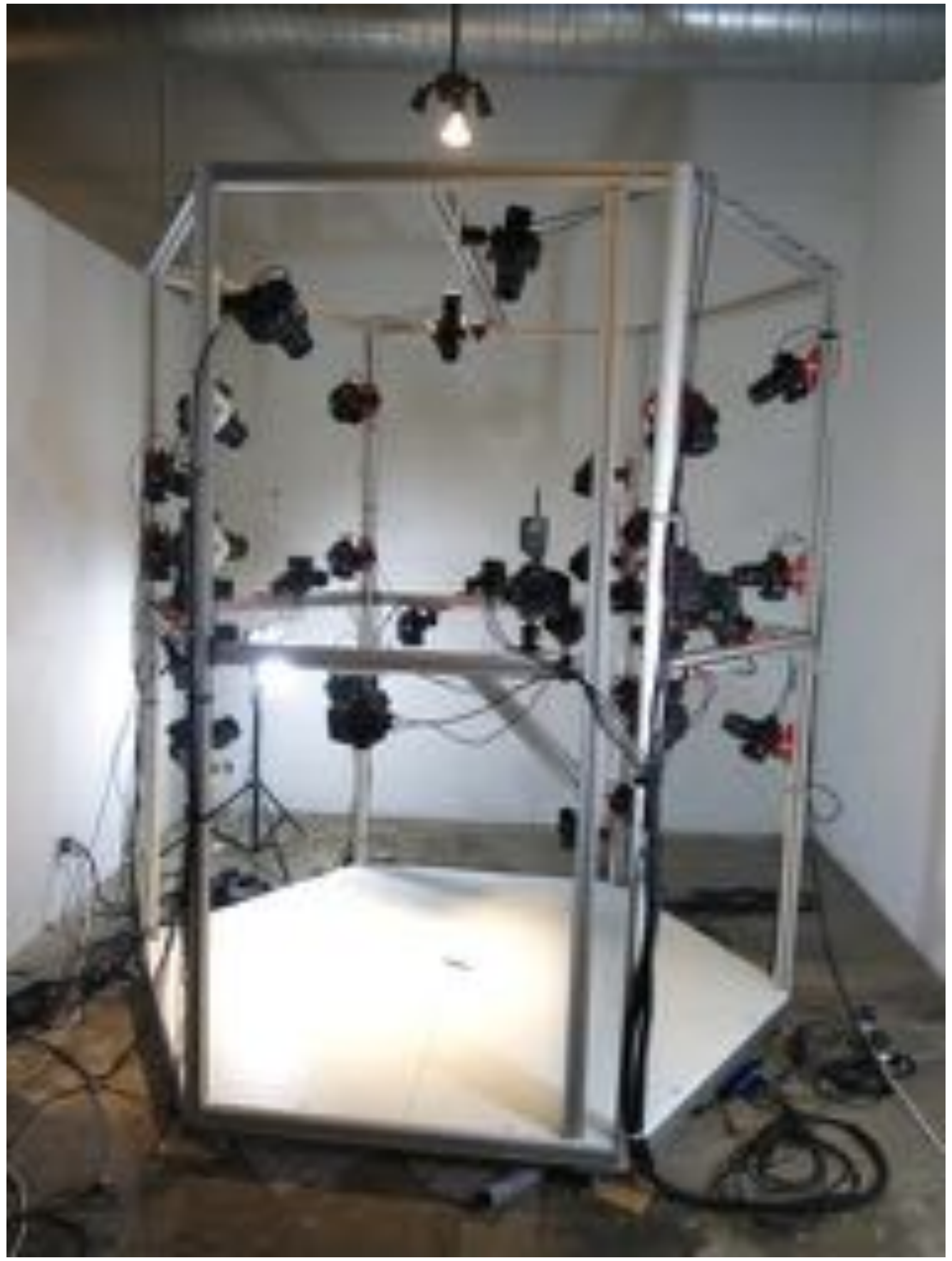

2D Orientation Map

Luo et al. SIGGRAPH 2013

- Detect local dominant orientation using rotated filters [Paris04]

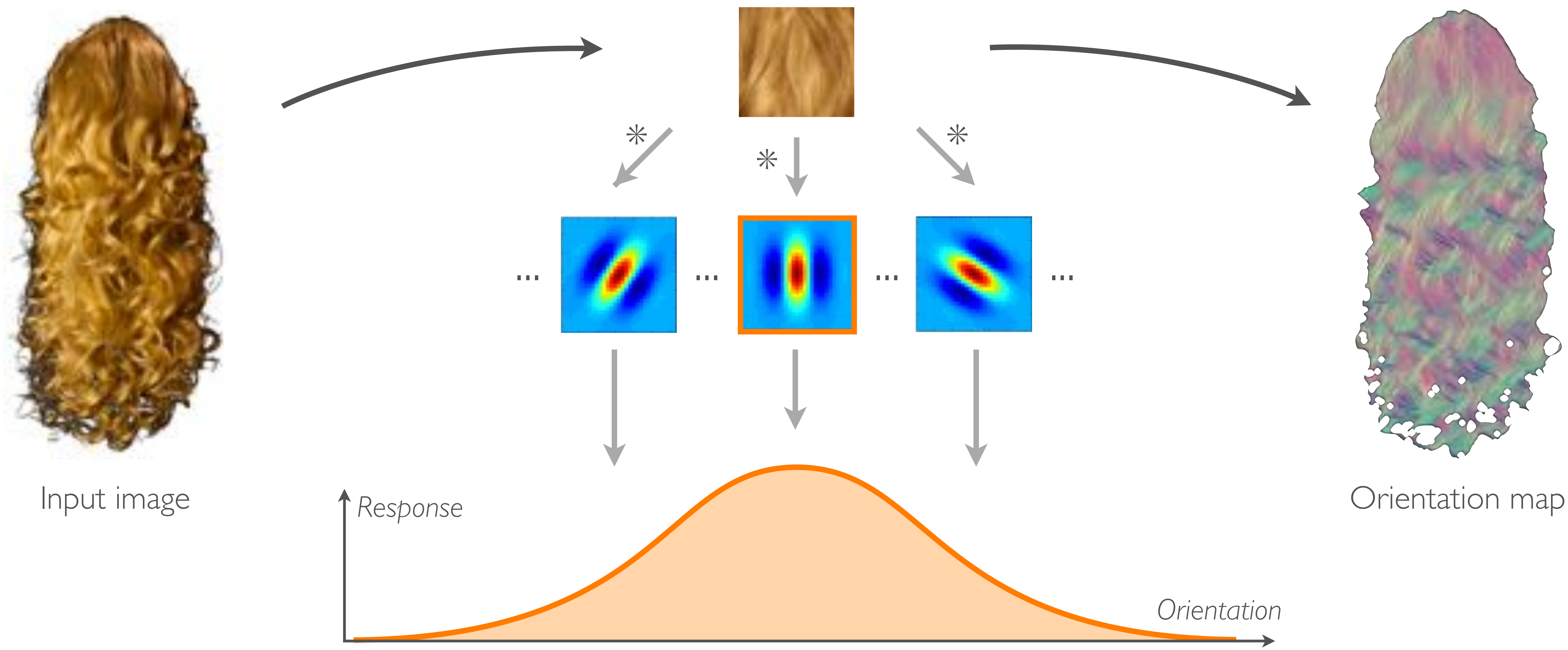

3D Orientation Field

Luo et al. SIGGRAPH 2013

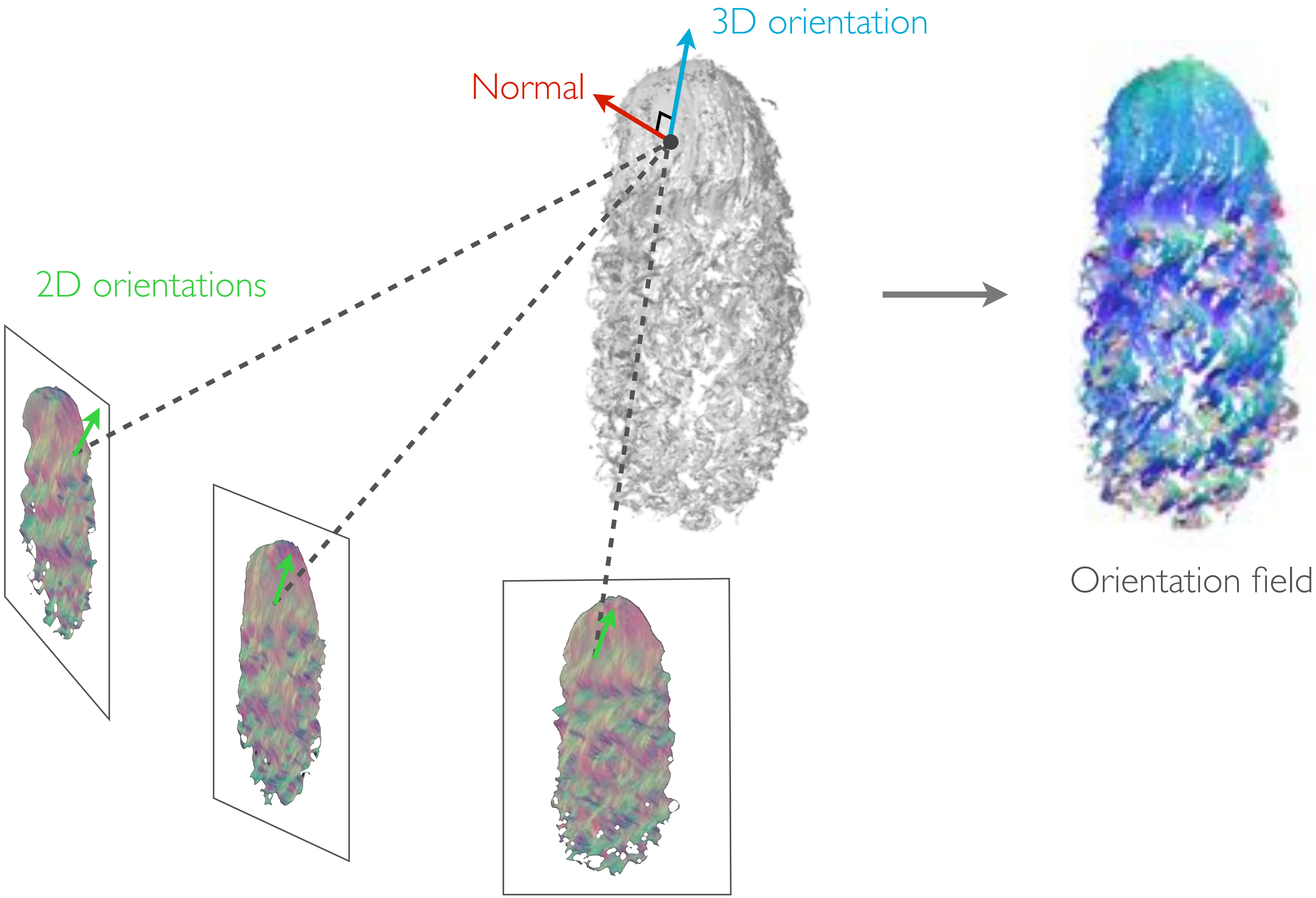

Pipeline

Luo et al. SIGGRAPH 2013

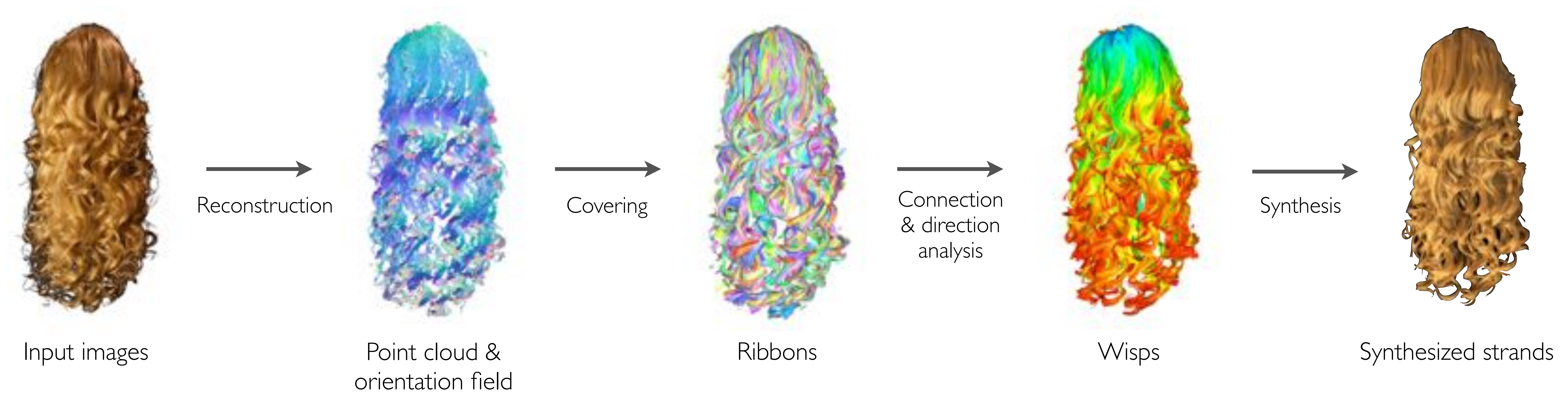

Local Minima

Implausible structures in the output [Luo et al. 2013]

Captured Data

Reconstruction with Simulated Examples

Hu et al. SIGGRAPH 2014

Simulated example

Reference photo

Our result

Reconstruction with Simulated Examples

Hu et al. SIGGRAPH 2014

Simulated example

Reference photo

Our result

Reconstruction with Simulated Examples

Hu et al. SIGGRAPH 2014

Simulated example

Reference photo

Our result

Reconstruction Priors

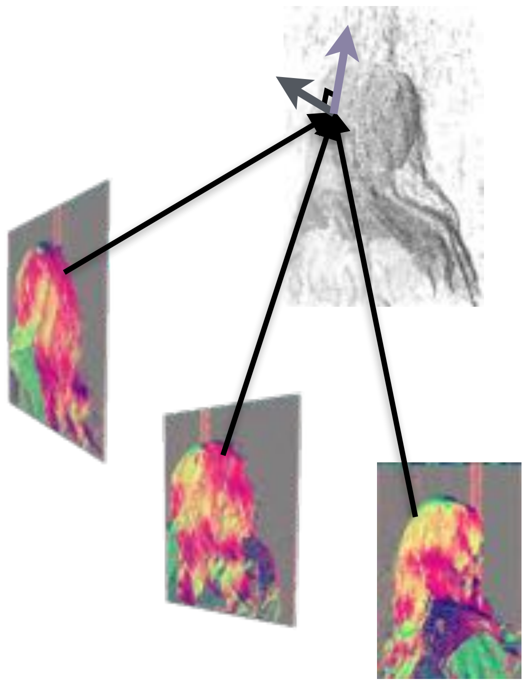

appearance

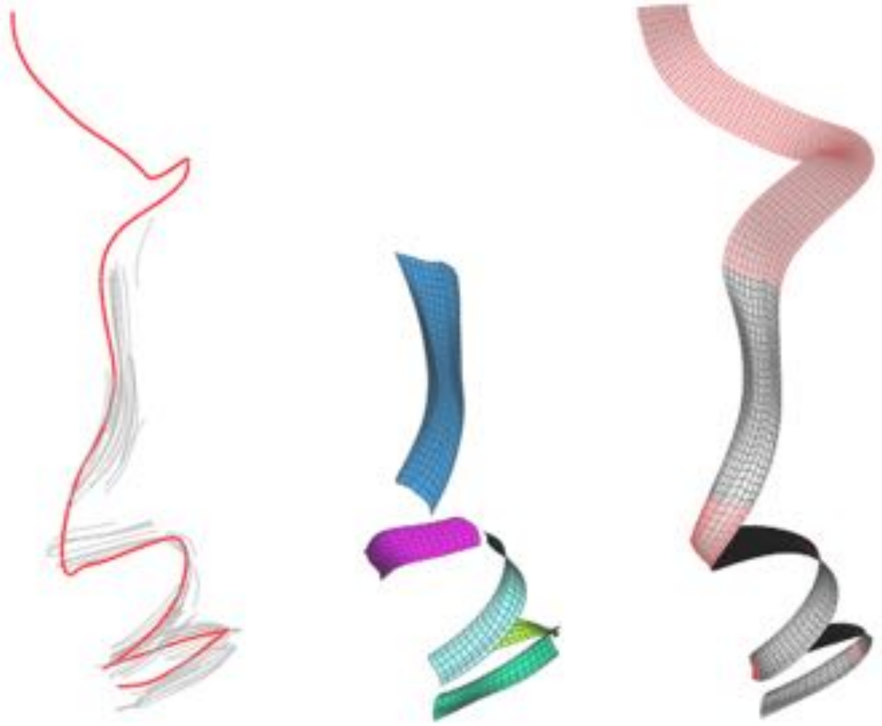

geometry

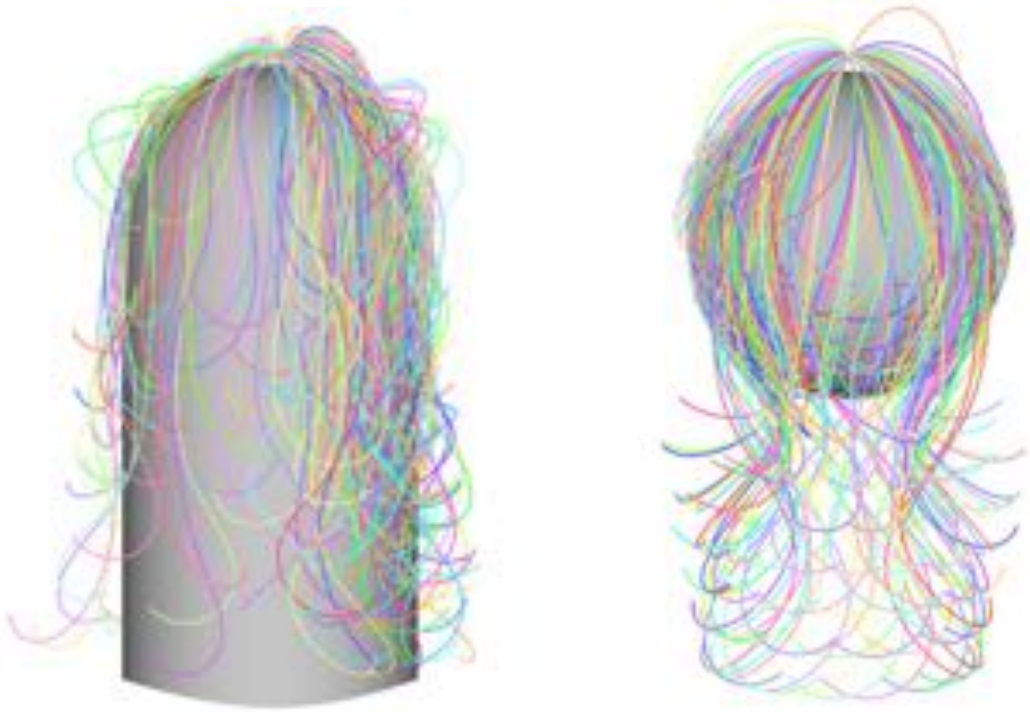

physics

Capturing **Hair**

Braid Capture

Kinect Fusion [Newcombe et al. 2011]

Braid Capture

Orientation field extraction

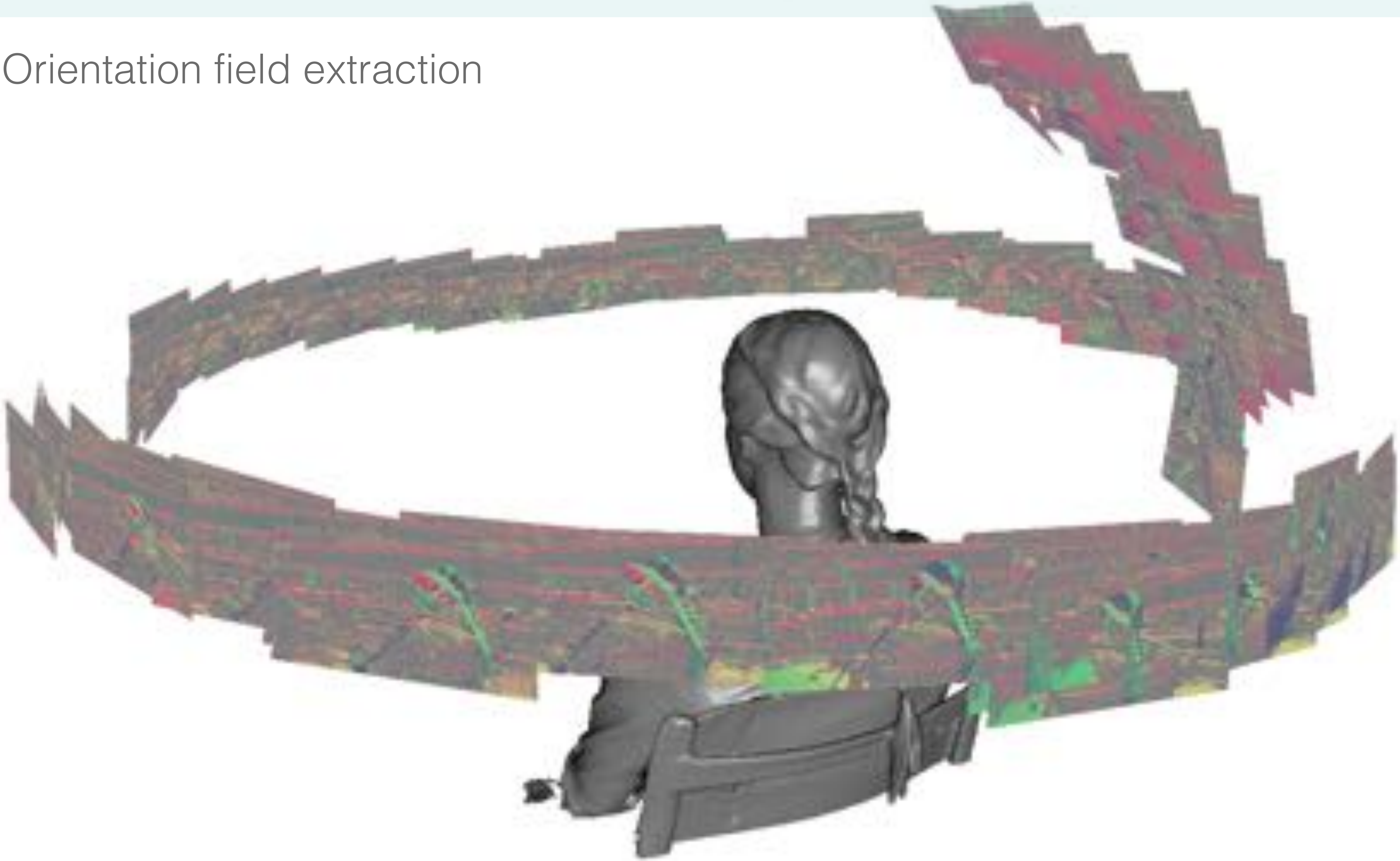

Braid Capture

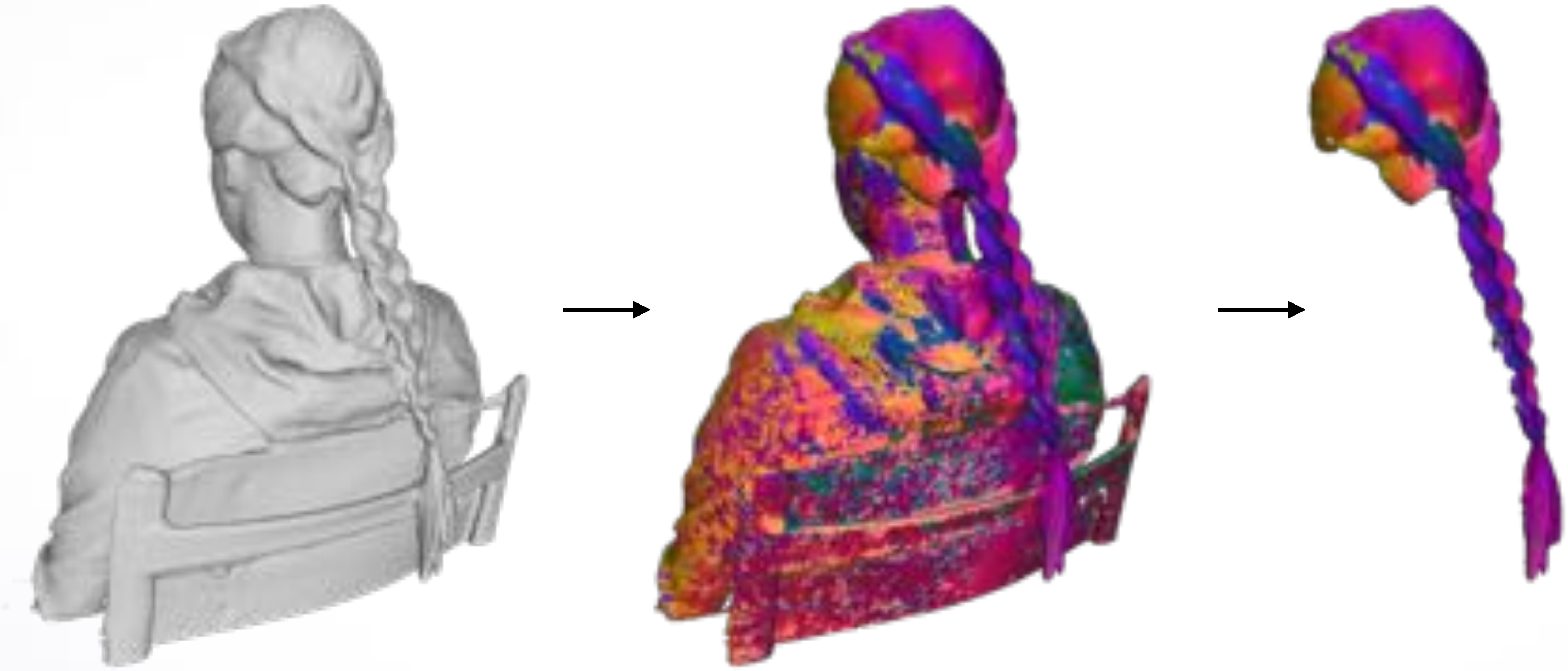

Input mesh　　3D orientation field　　Cleaned mesh

Structure Analysis

Cleaned mesh

Patch fitting

Labeling

Structure extraction

Braid Theory [Artin 1947]

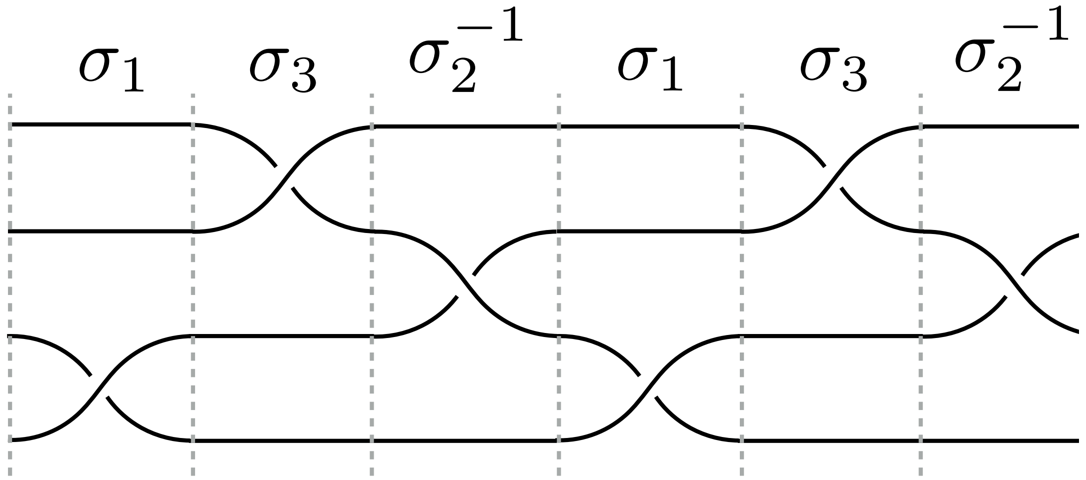

4-strand basic braid

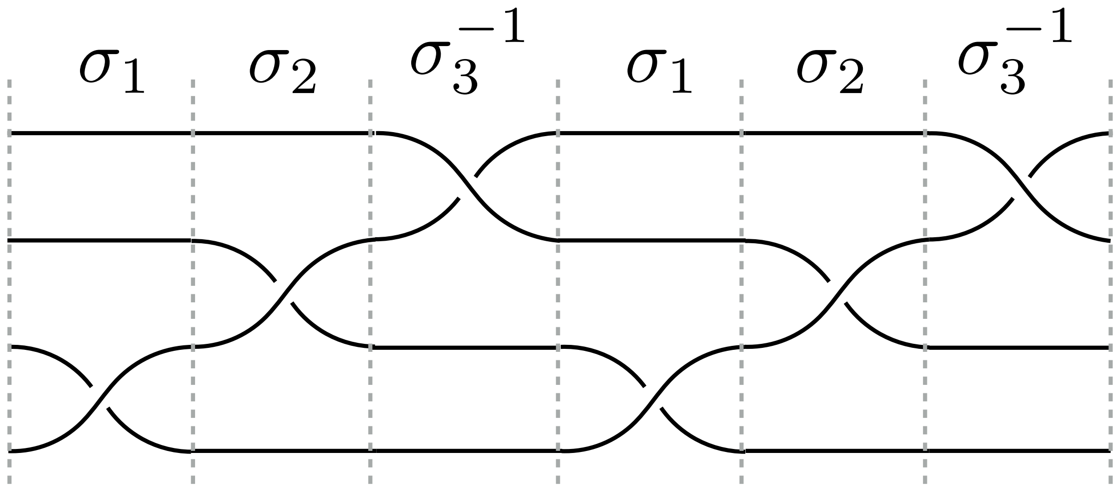

4-strand fishtail

Procedural Modeling

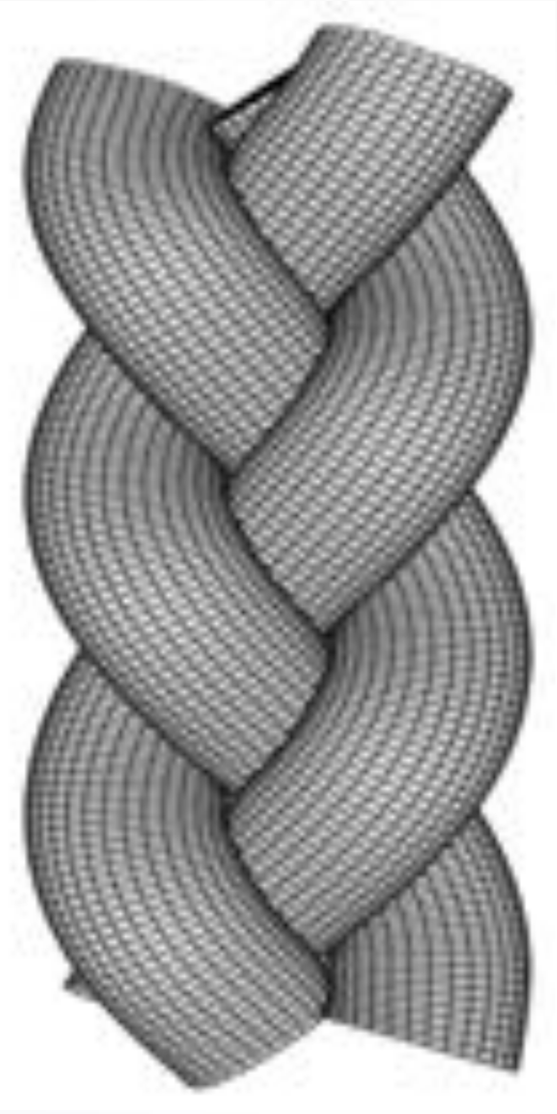

Basic
braid

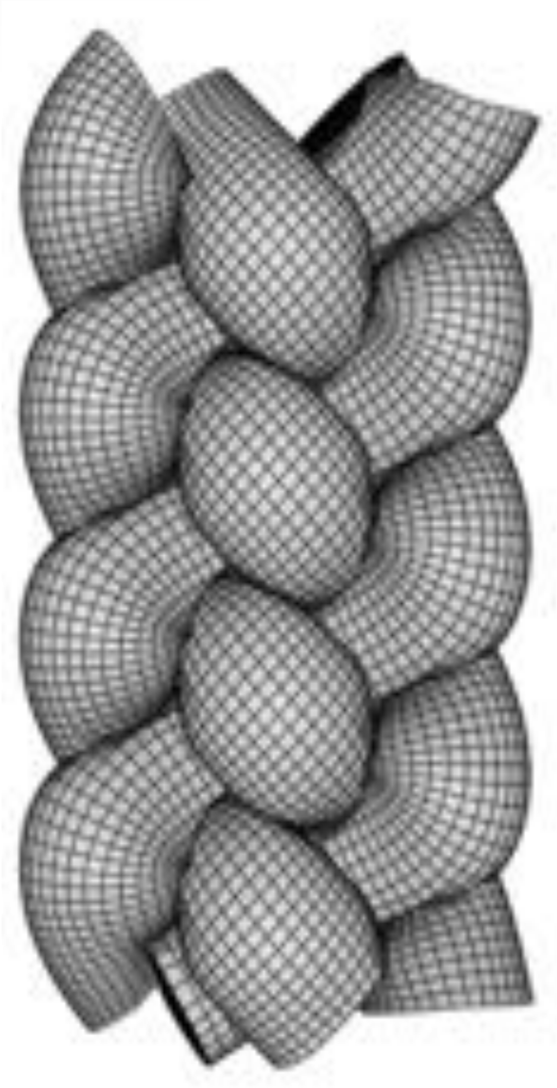

Four-strand
braid

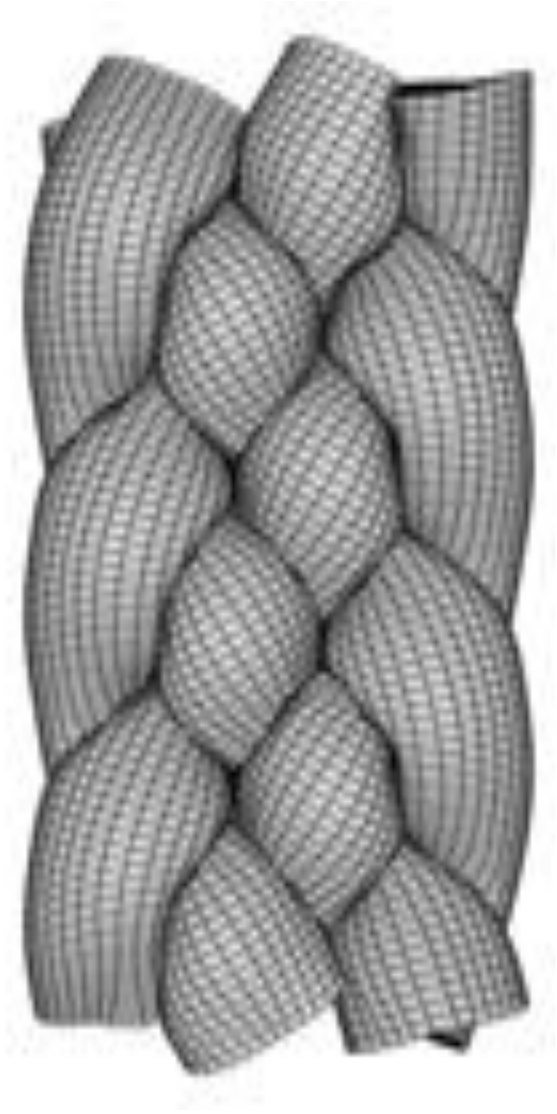

Five-strand
Dutch braid

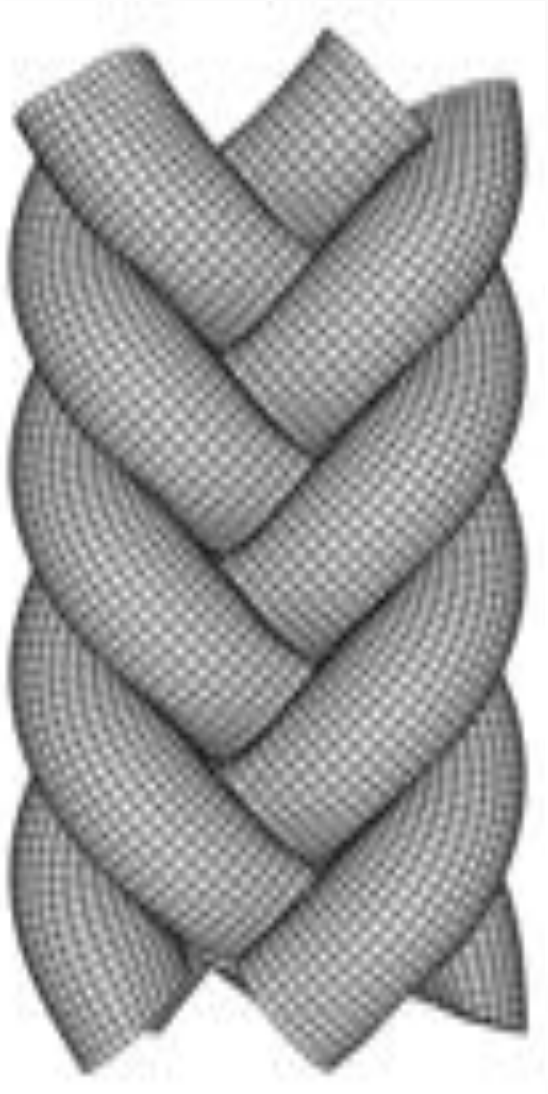

Fishtail
braid

Braid Capture

Five-strand Dutch braid

Braid Capture

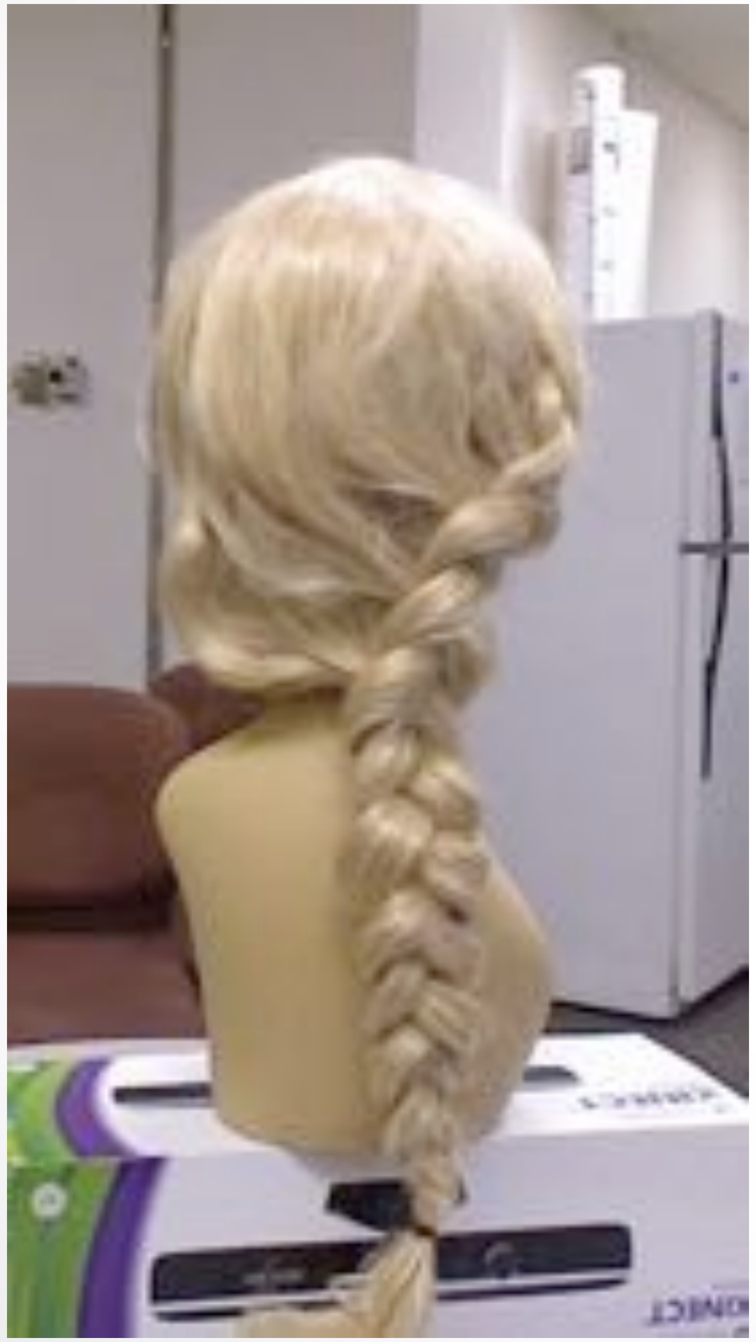

Braid Capture

Braid Capture

Impacting **Science**


Science
AAAS

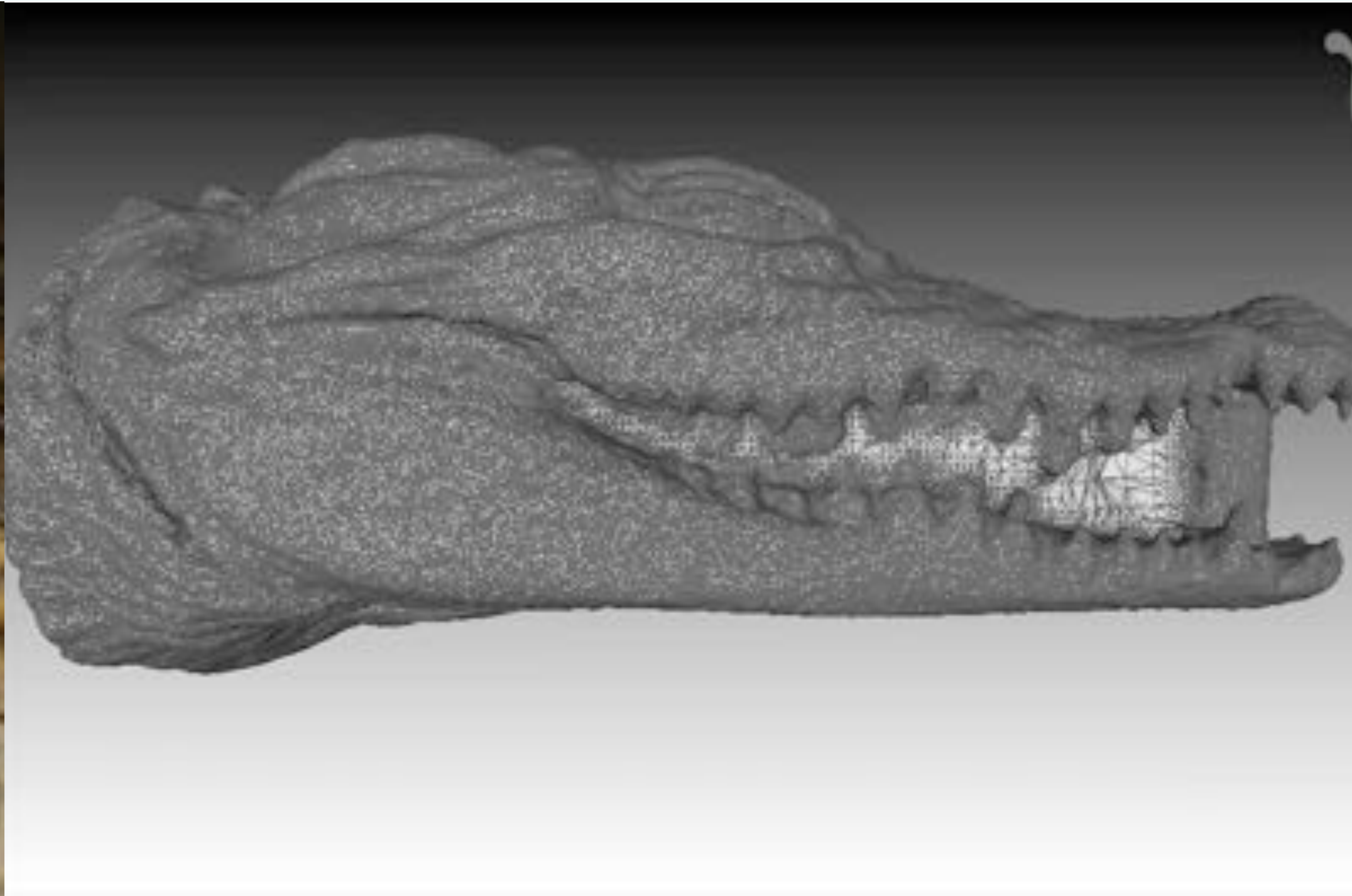

Cardiology

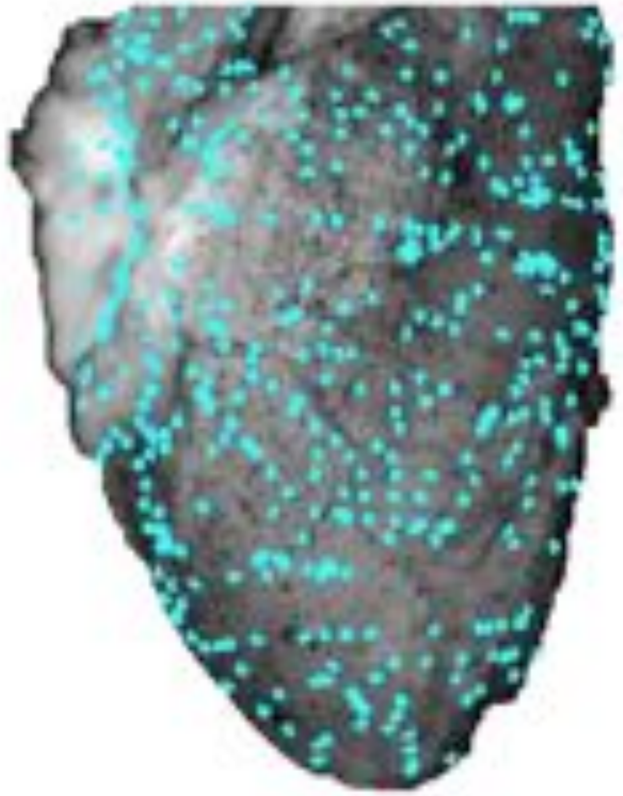

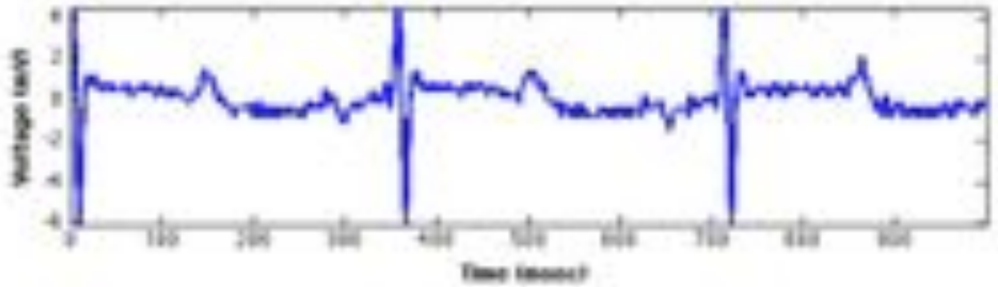

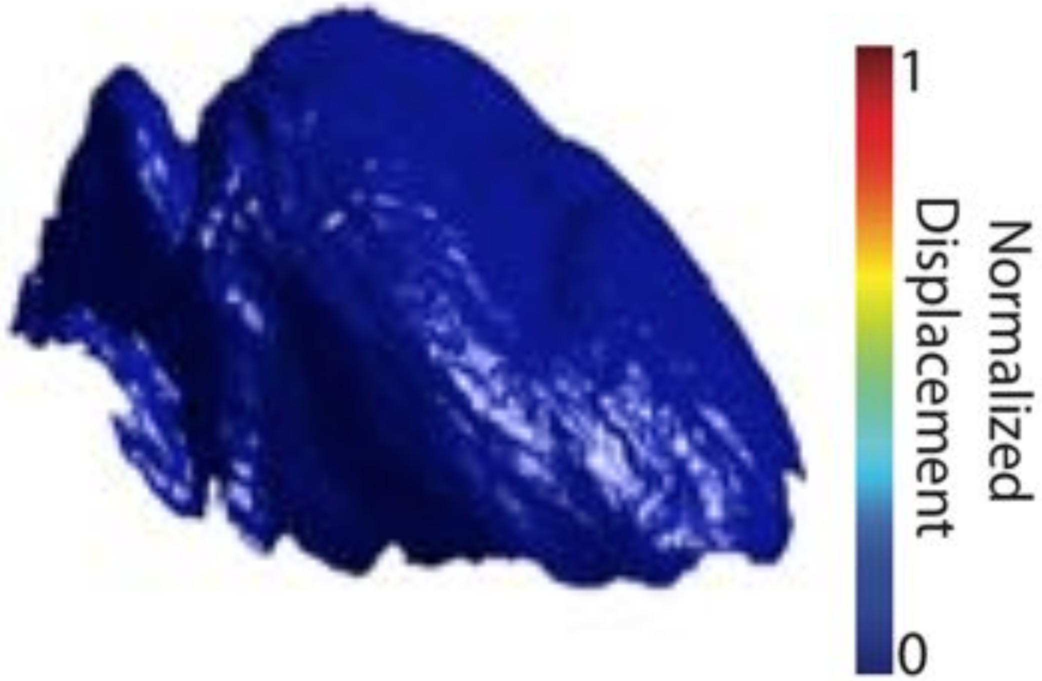

Cancer Treatment

C-Rad 2011

http://hao.li

IMAGE CAPTURE FOR VIRTUAL REALITY AND INTERACTION

Tristan Swedish
MIT Media Lab

Alignment Displays and Imaging for Interaction and Health

Eye box trade offs

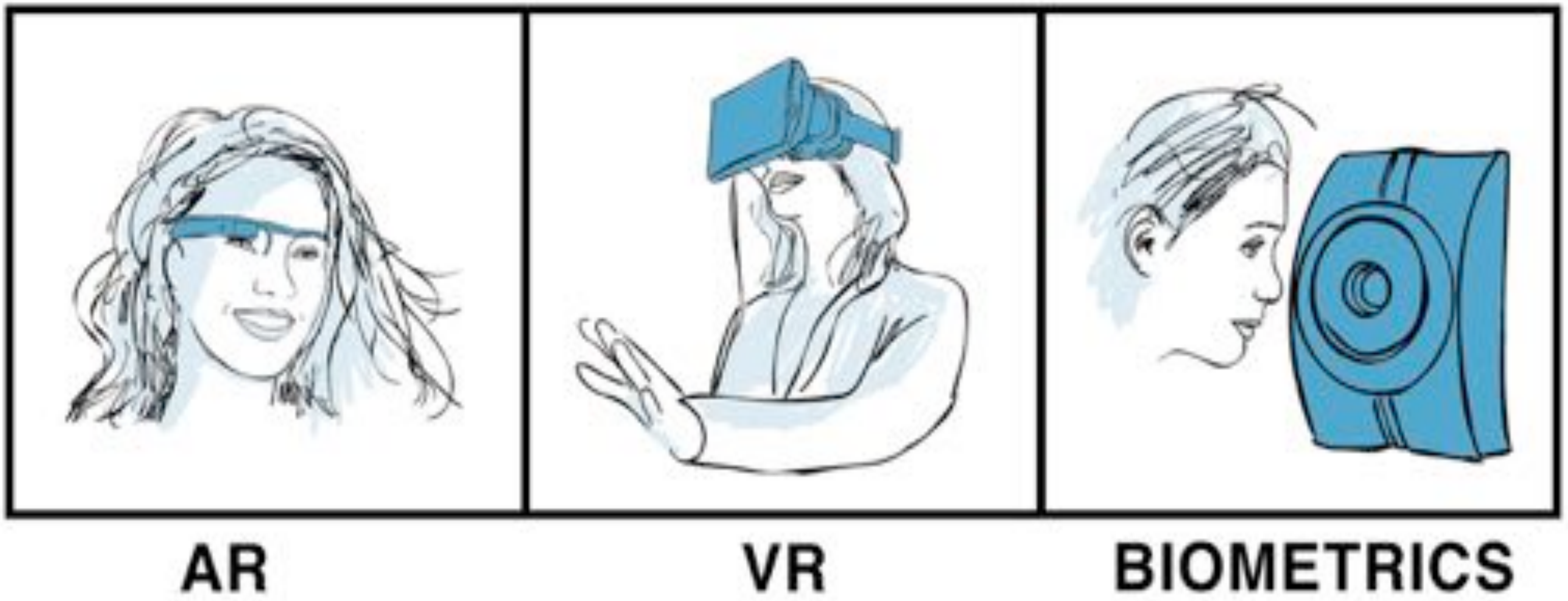

eyeSelfie: solve the user guidance problem

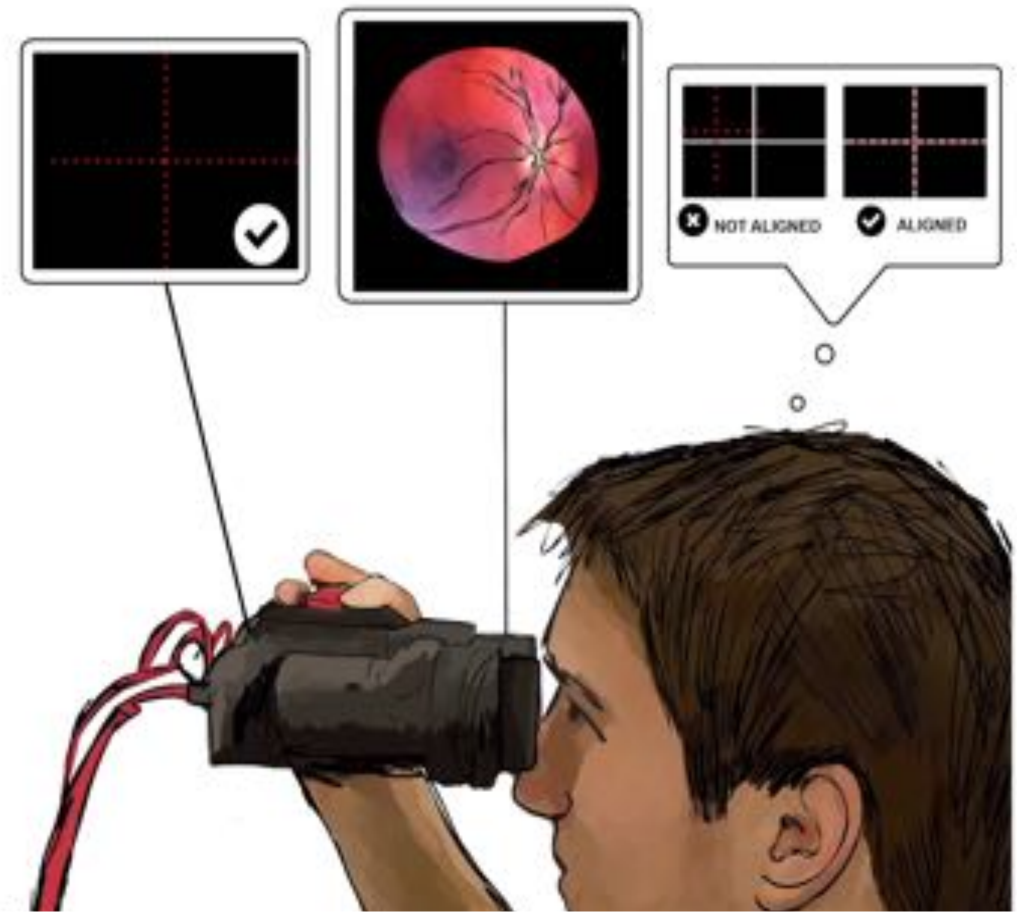

[T. Swedish, et al. eyeSelfie. ACM Trans. Graph (34, 4), 2015.]

Directed rays as perceptual cues

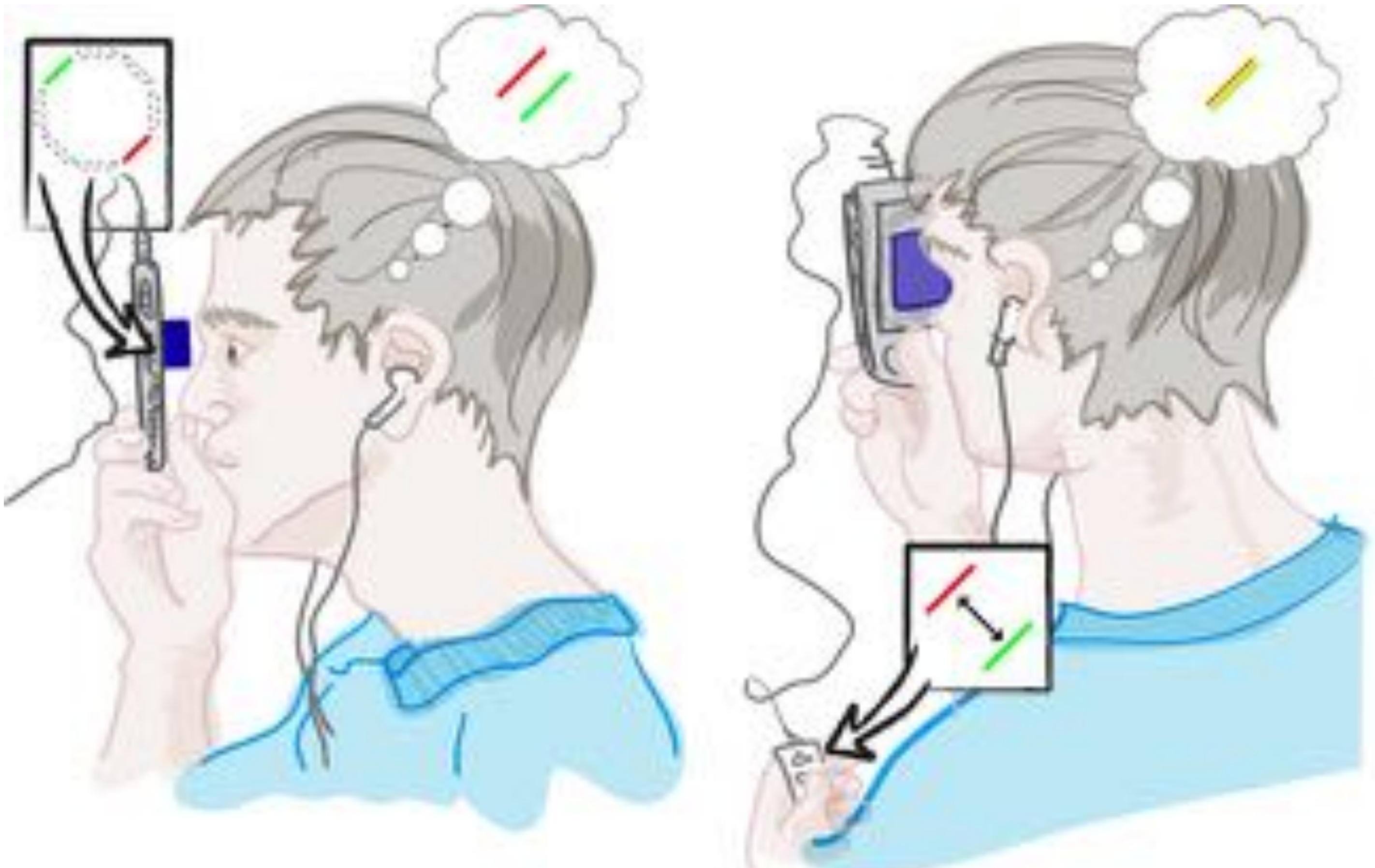

NETRA

Pamplona et al, Siggraph, 2010

Directed rays as perceptual cues

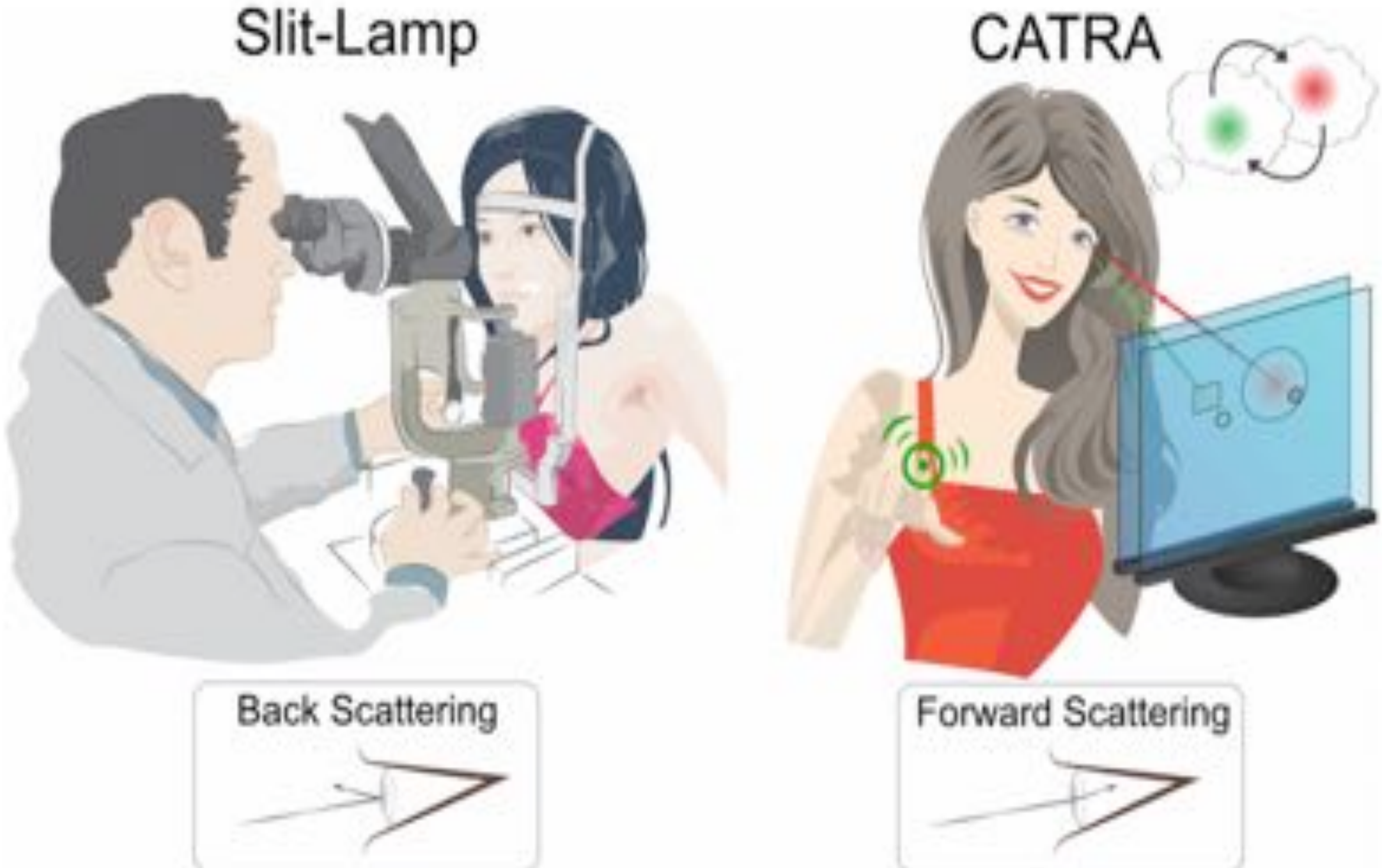

CATRA

Pamplona et al, Siggraph, 2011

Retinal Alignment Challenge

Retinal imaging challenge: field of view

Retinal imaging challenge: reflections

Eye Alignment Displays

Eye box: near eye pinhole projector

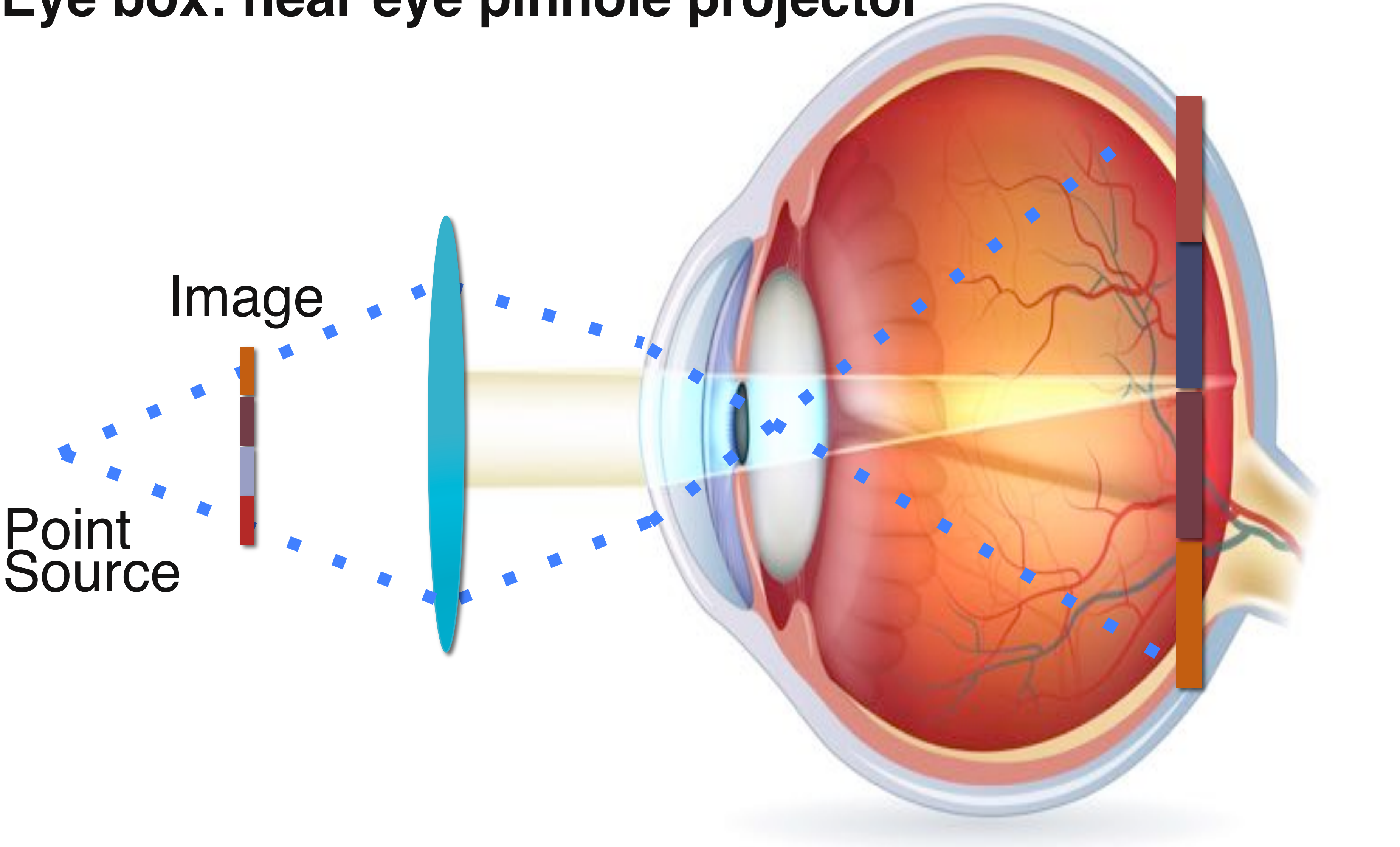

Eye box: near eye pinhole projector

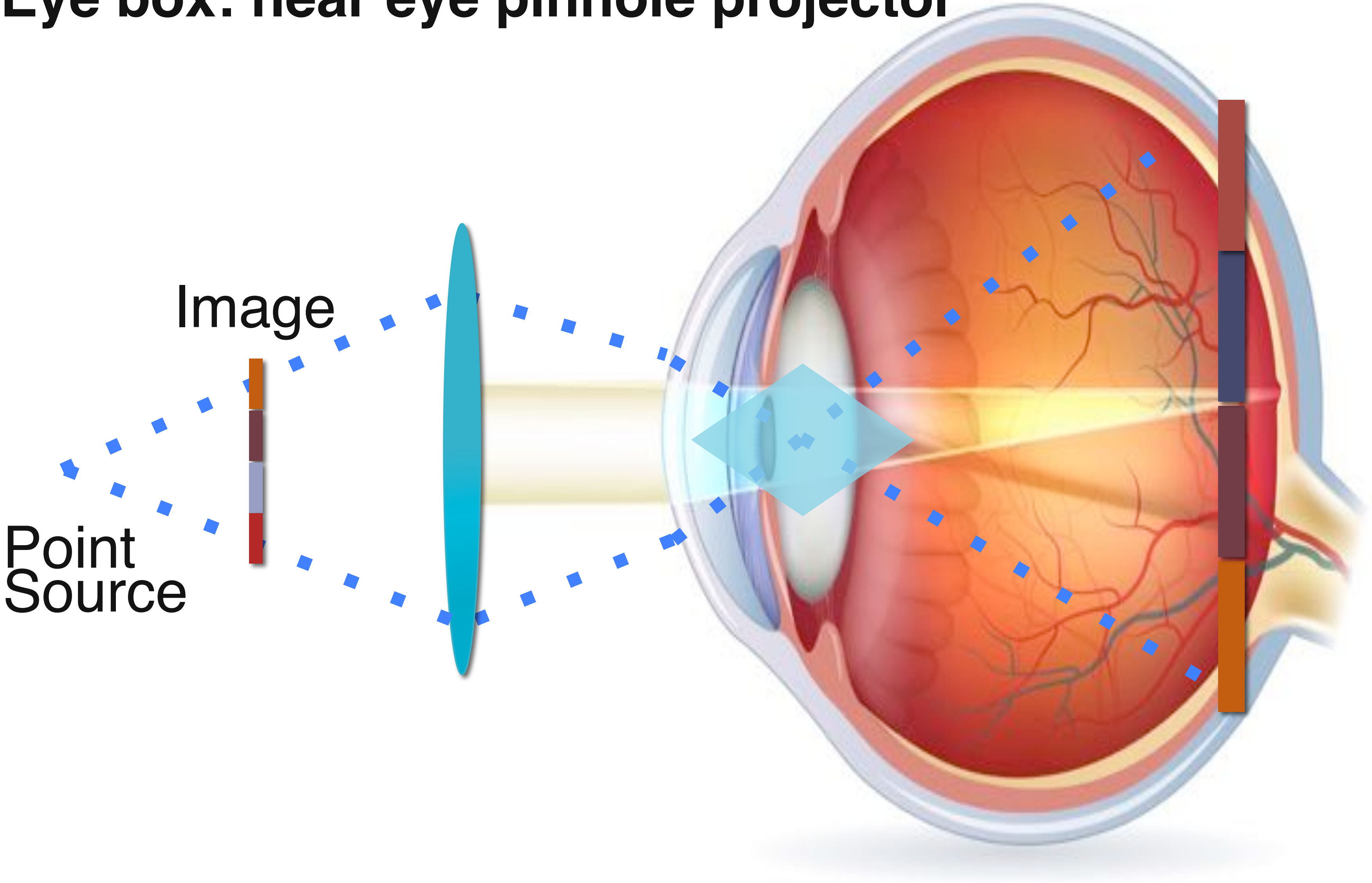

Eye box: near eye pinhole projector

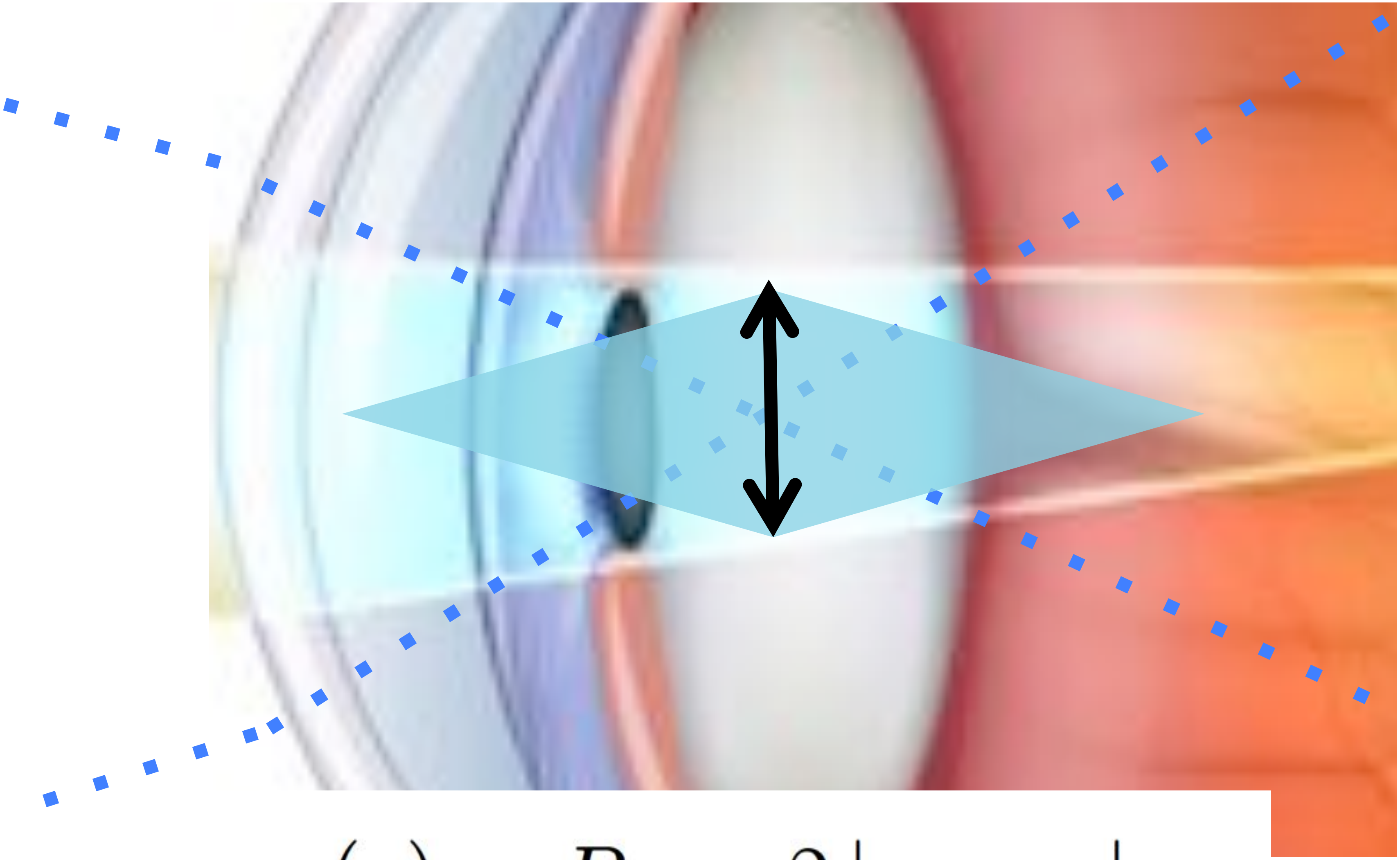

$$\omega_e(z) = P_D - 2\left|z - z_0\right| u_\alpha$$

Pupil forming display

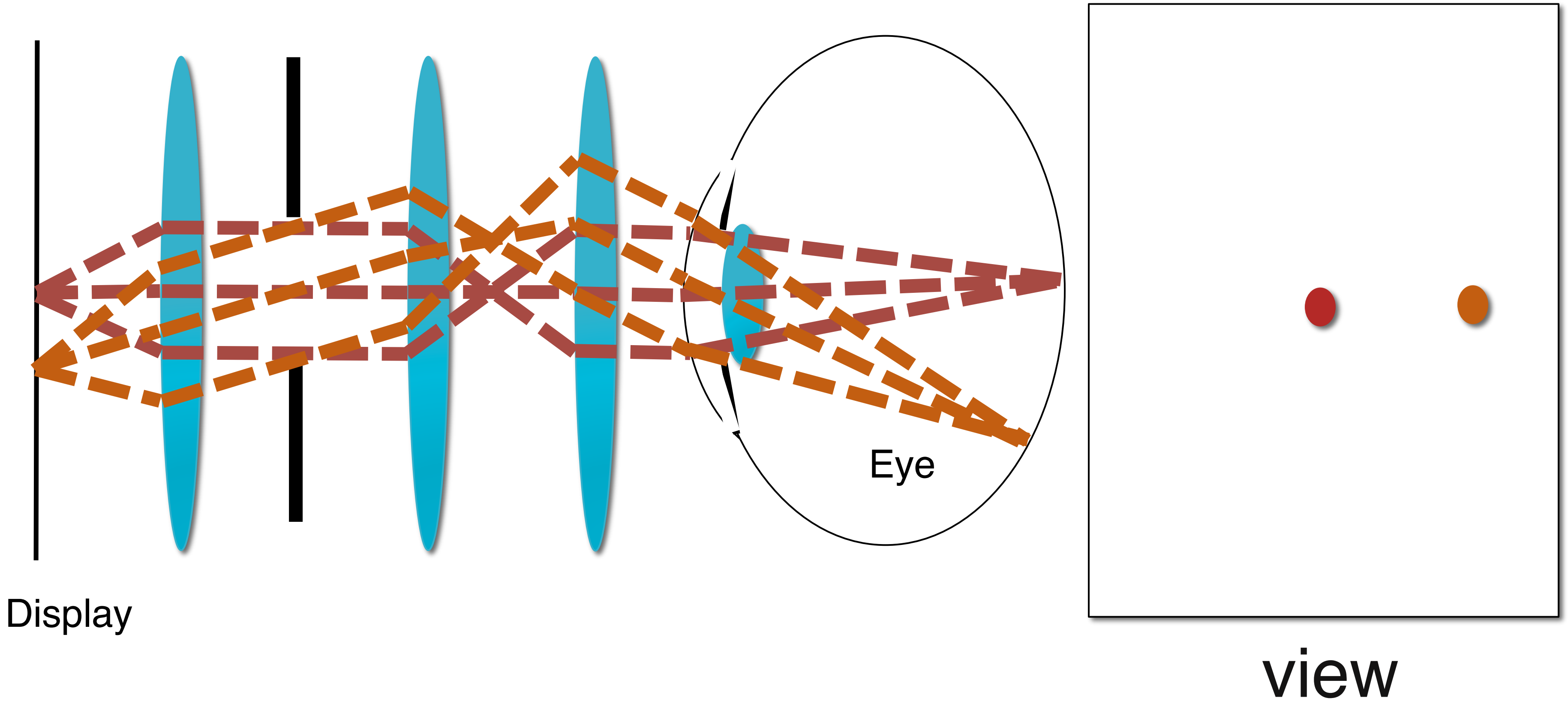

Pupil forming display

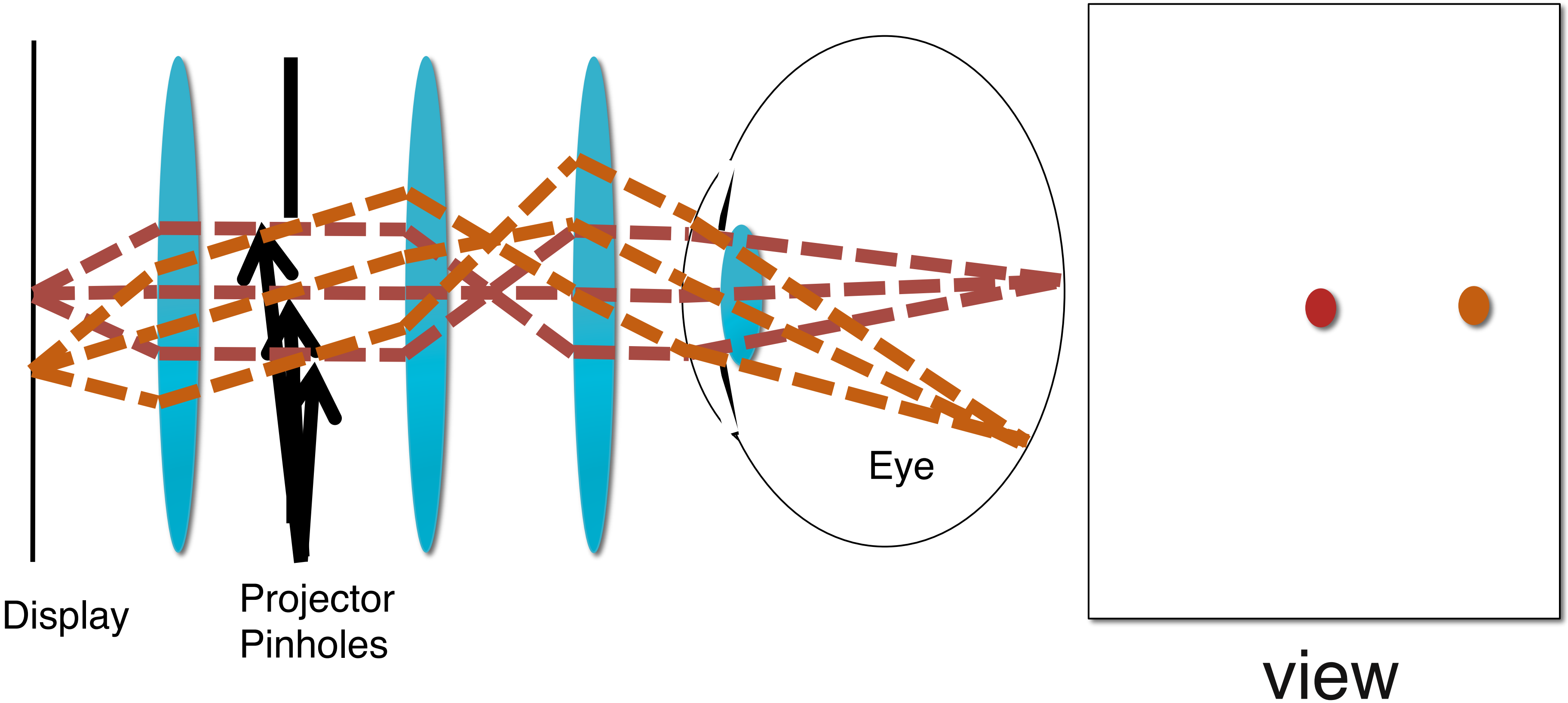

Pupil forming display

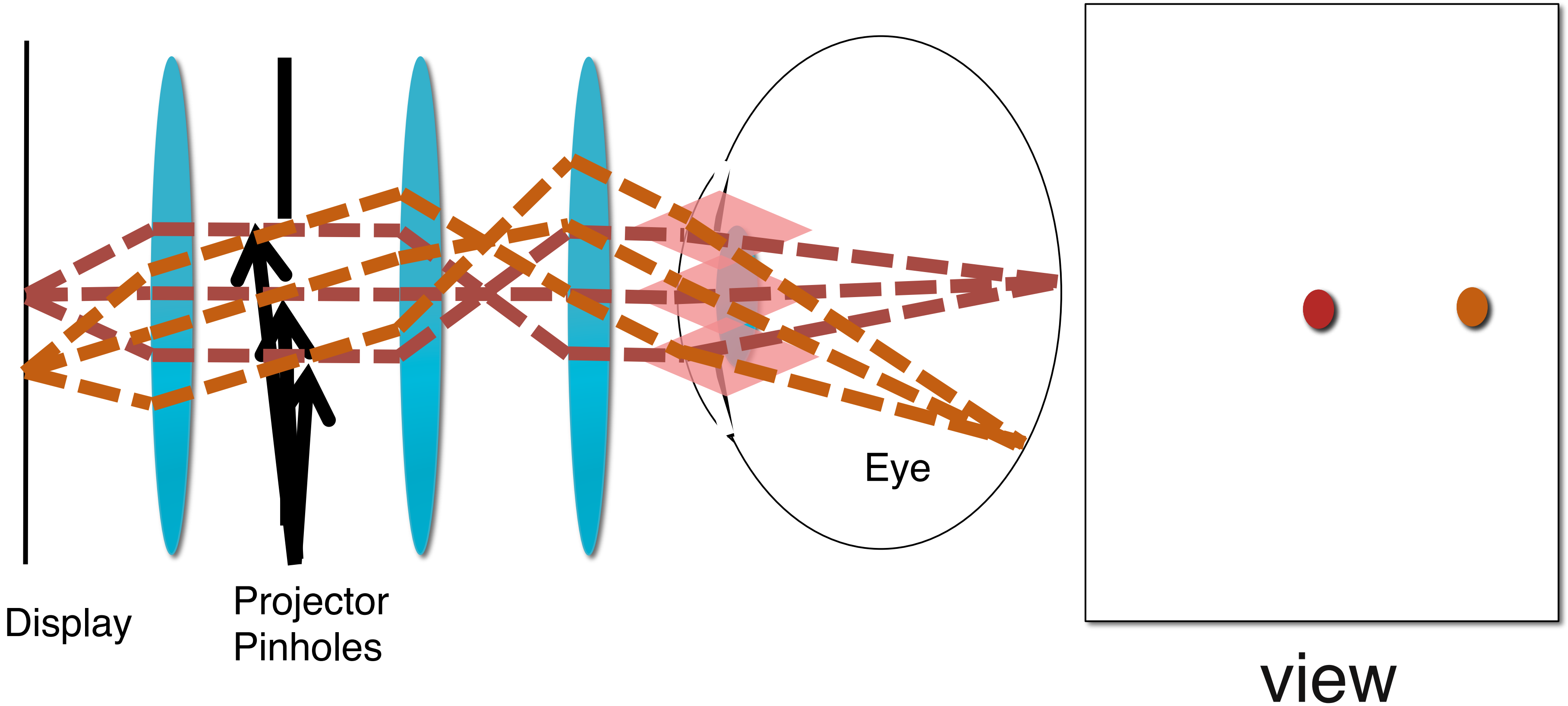

Pupil forming display

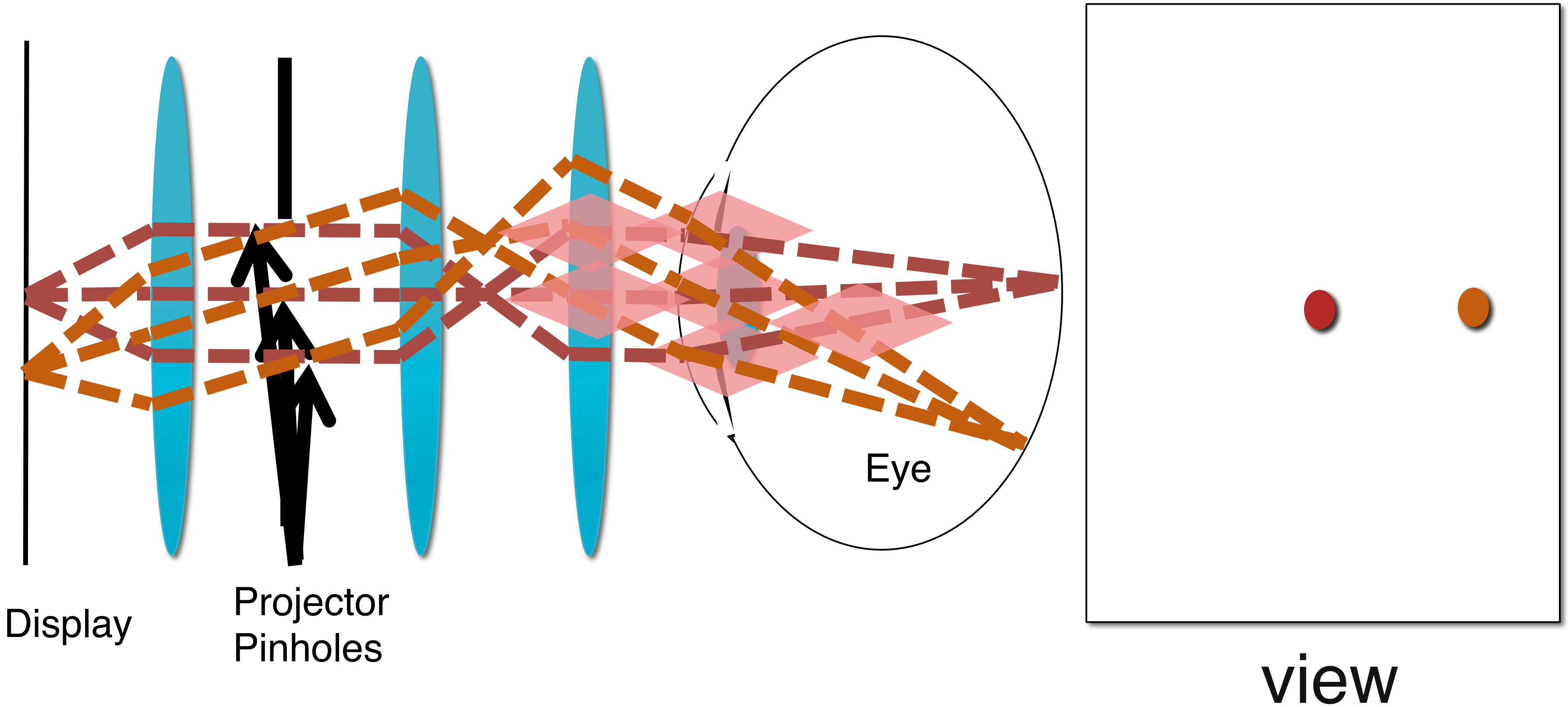

Pupil forming display

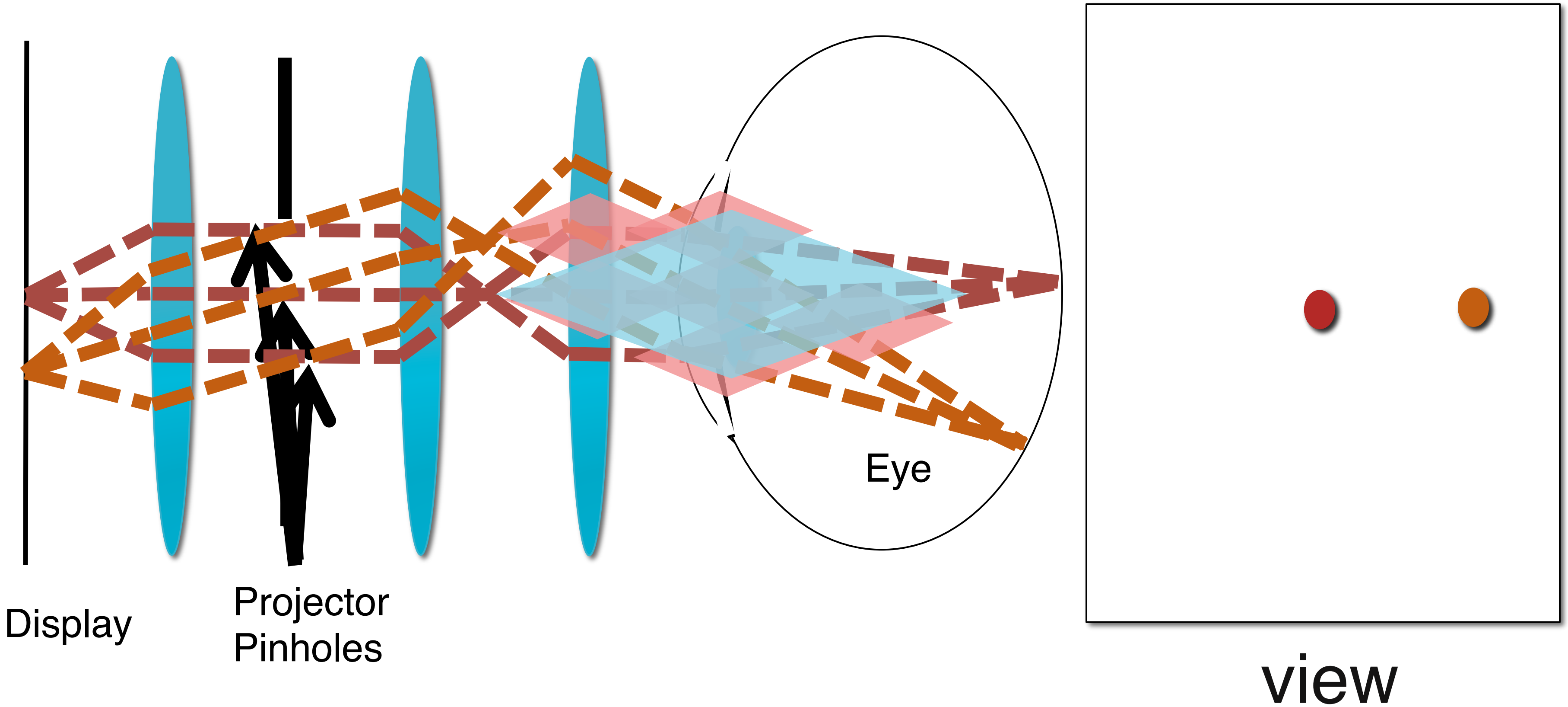

Pupil forming display

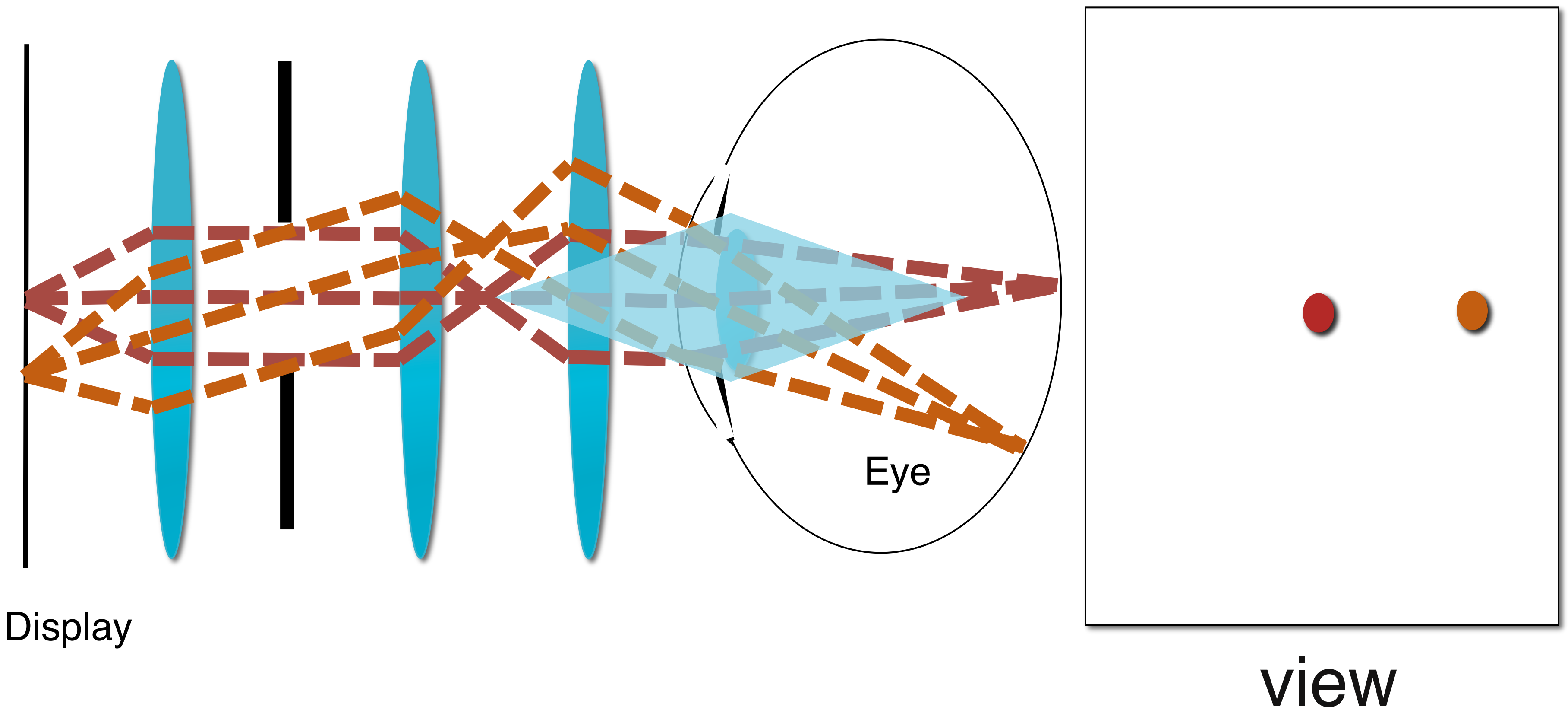

Light Field Eye Boxes

Defining eye box of heterogeneous pupil images

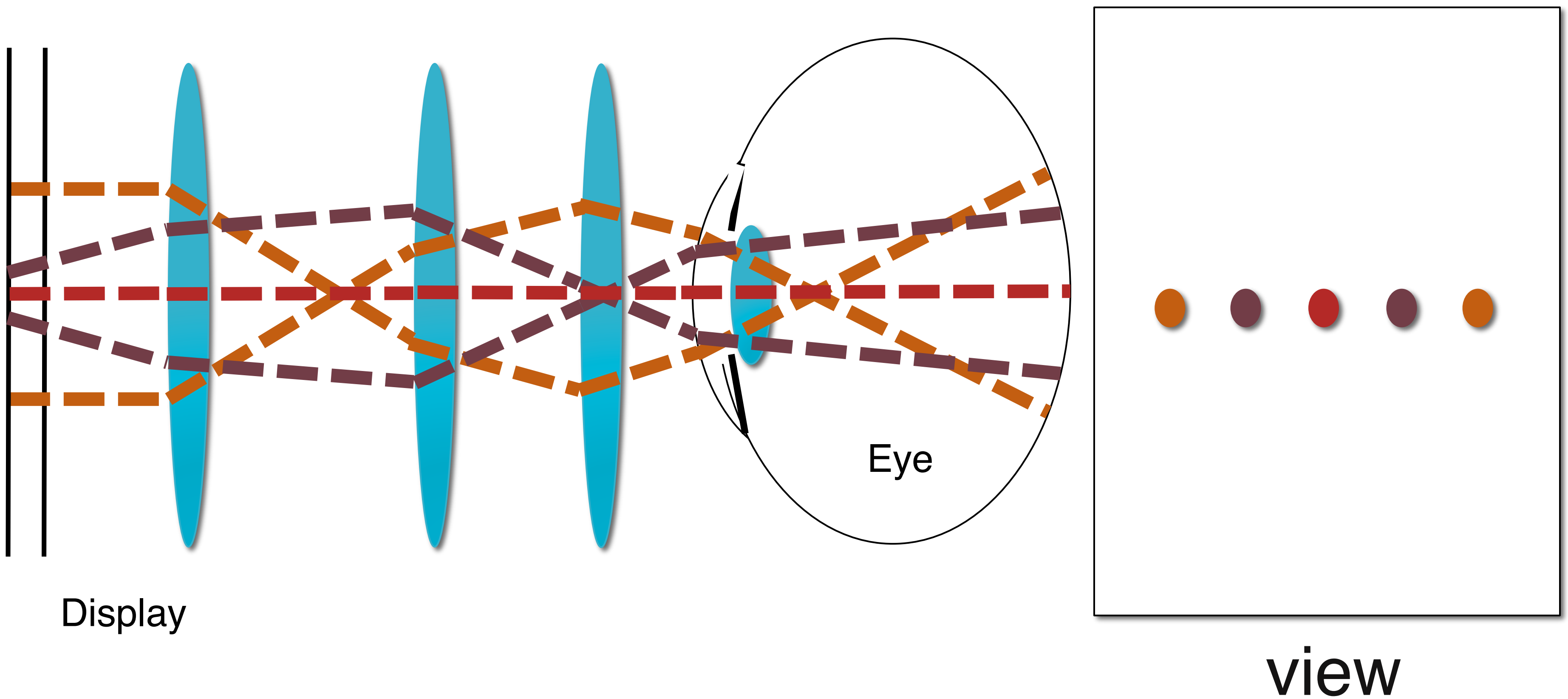

Defining eye box of heterogeneous pupil images

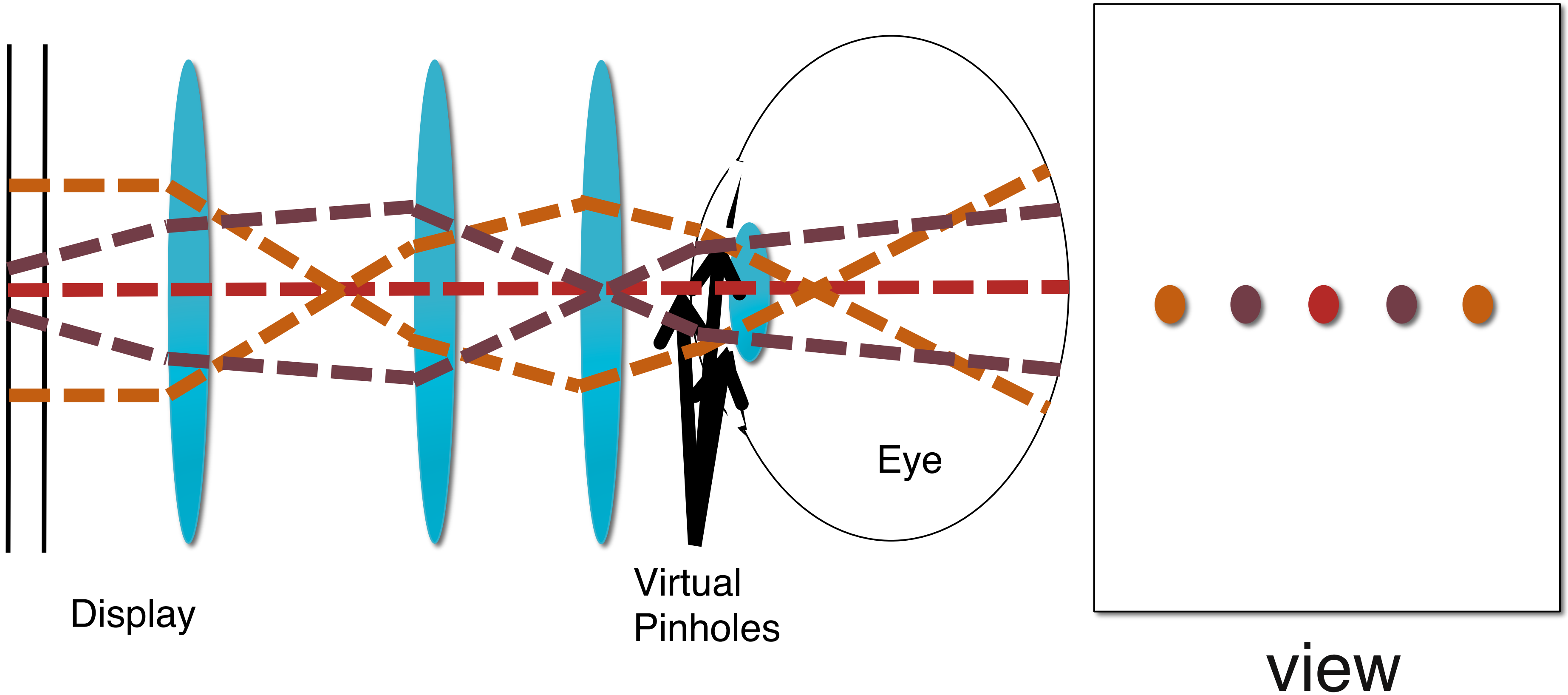

SIGGRAPH2016

Defining eye box of heterogeneous pupil images

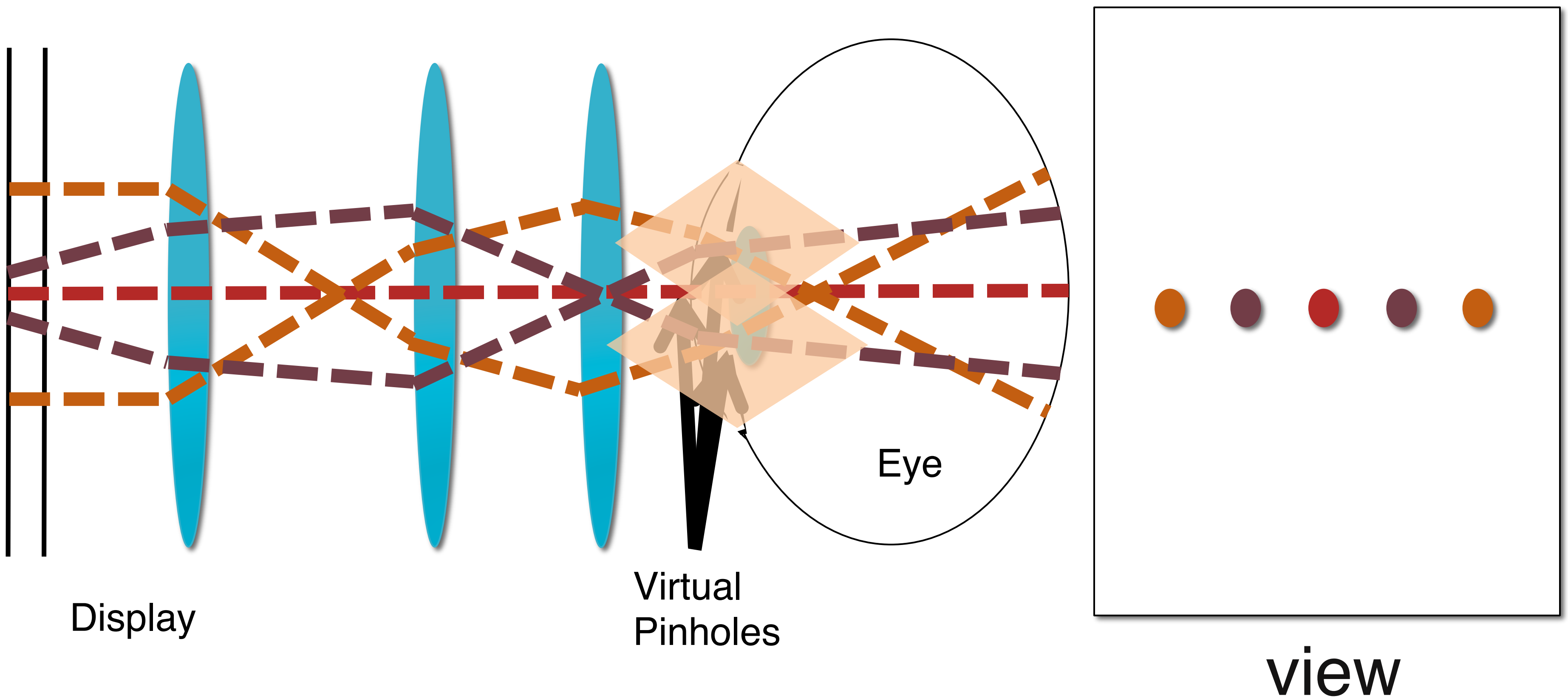

Defining eye box of heterogeneous pupil images

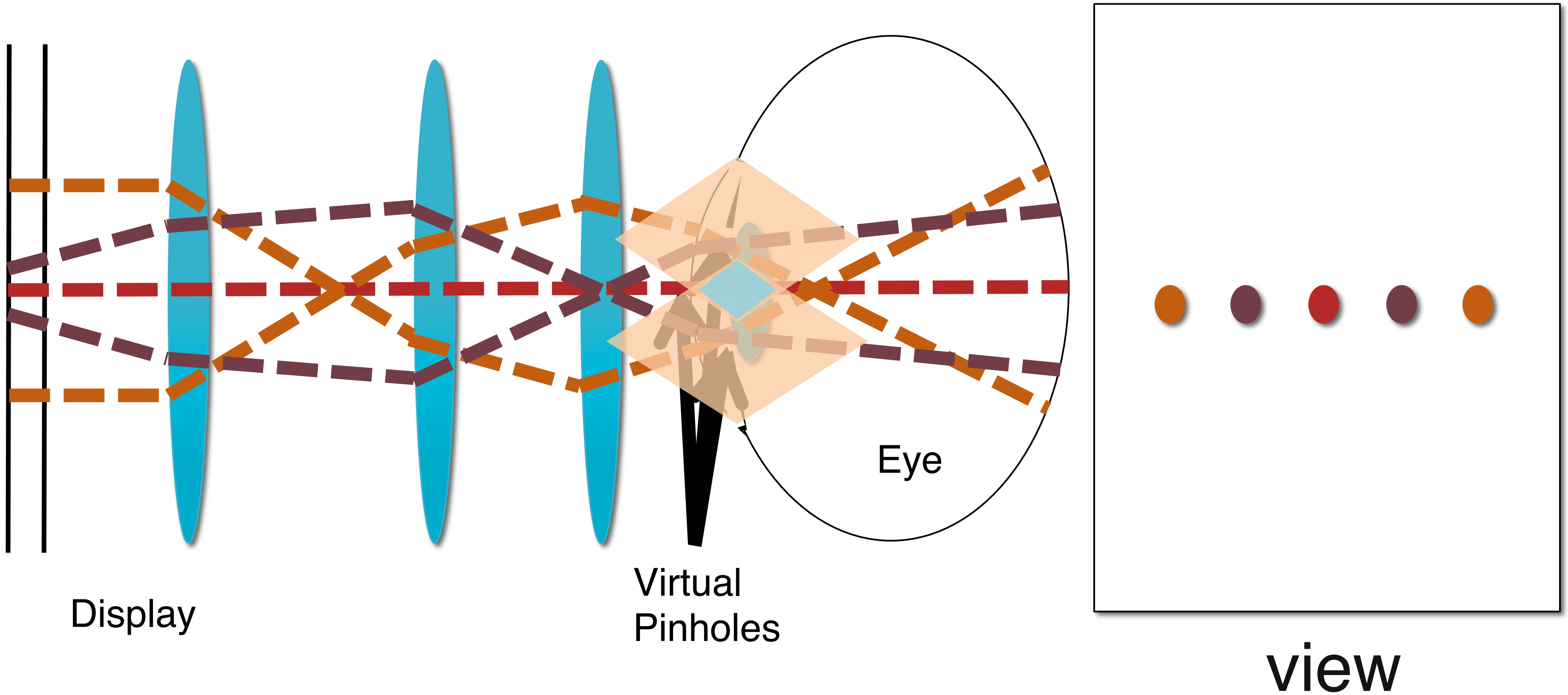

Defining eye box of heterogeneous pupil images

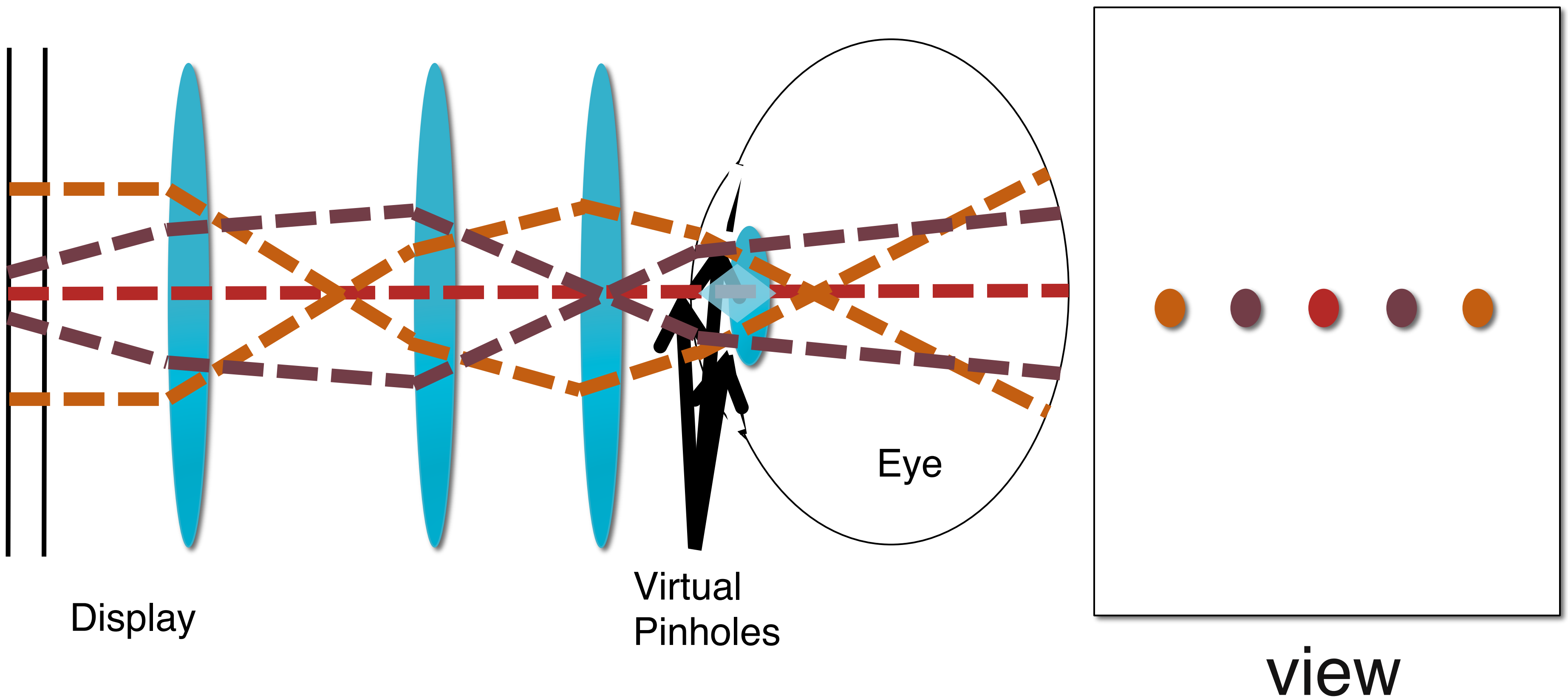

Light Field notation

Light Field: essential description

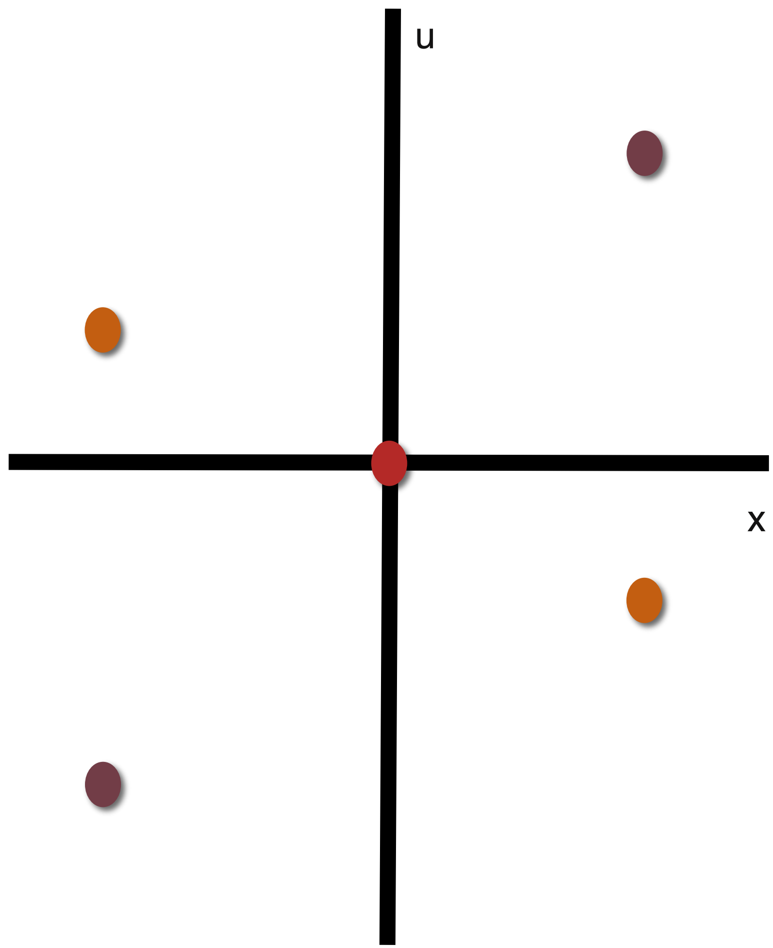

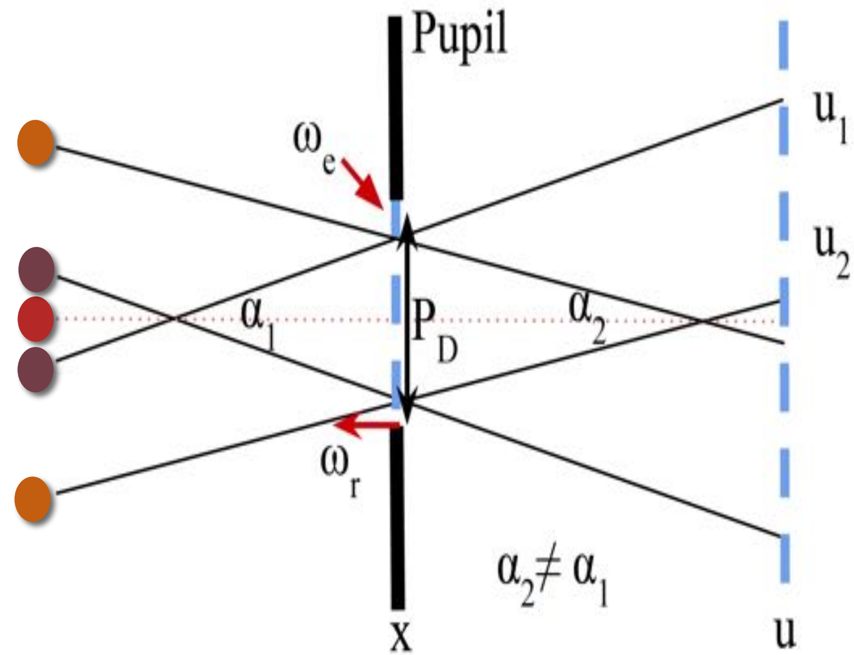

Light Field: essential description

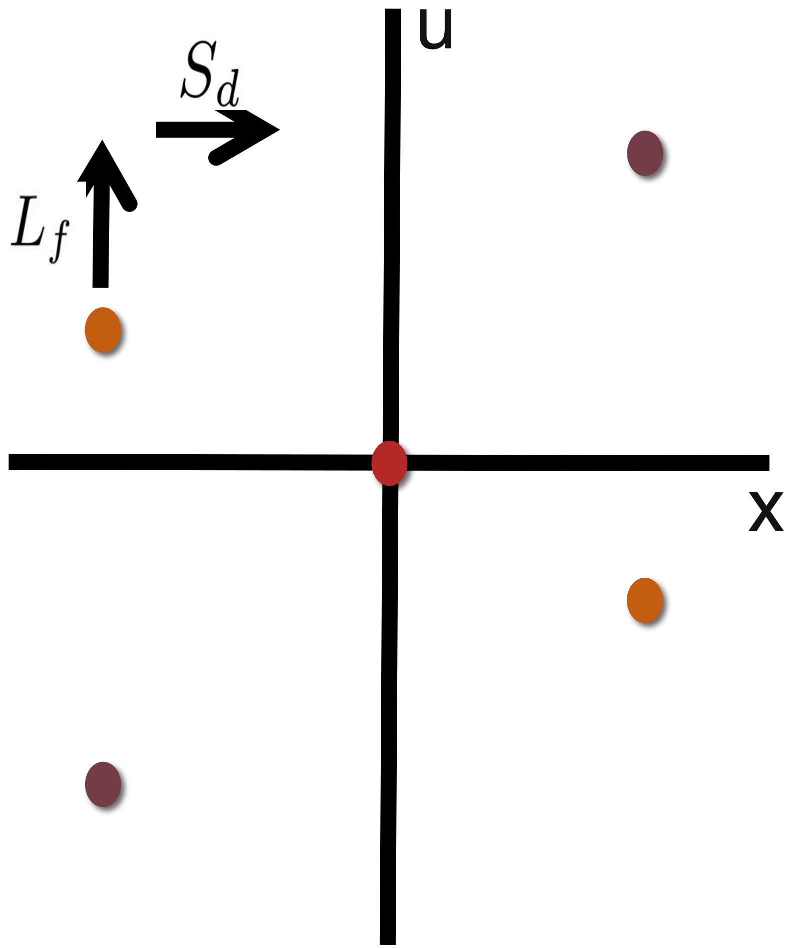

$$S_d = \begin{bmatrix} 1 & d \\ 0 & 1 \end{bmatrix} \quad L_f = \begin{bmatrix} 1 & 0 \\ -1/f & 1 \end{bmatrix}$$

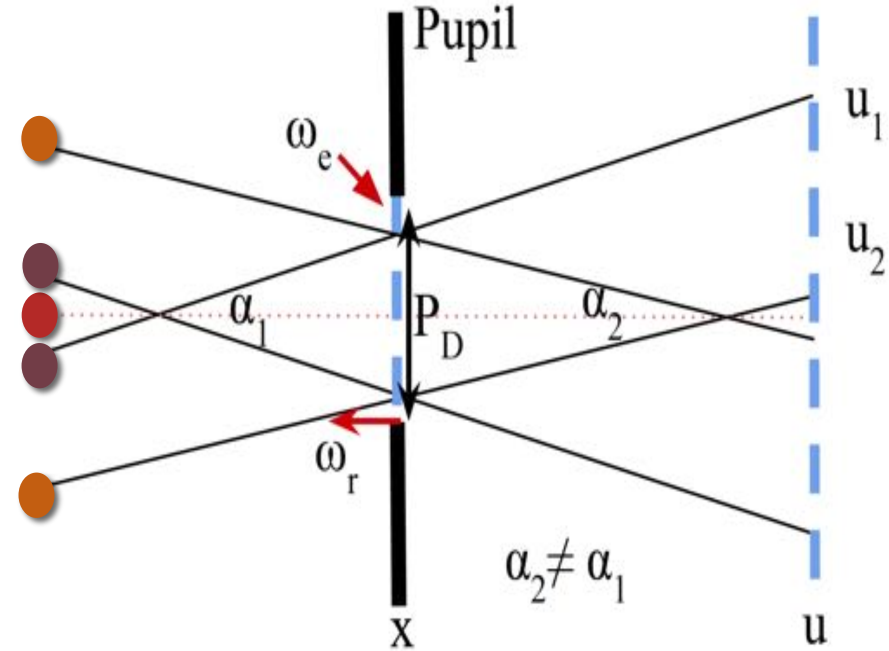

Light Field: simple eye model

$$\begin{bmatrix} x'' \\ u'' \end{bmatrix} = \begin{bmatrix} 1 & d \\ 0 & 1 \end{bmatrix} \begin{bmatrix} 1 & 0 \\ -1/f & 1 \end{bmatrix} \begin{bmatrix} x' \\ u' \end{bmatrix}$$

“Fourier Transform”:

90° rotation

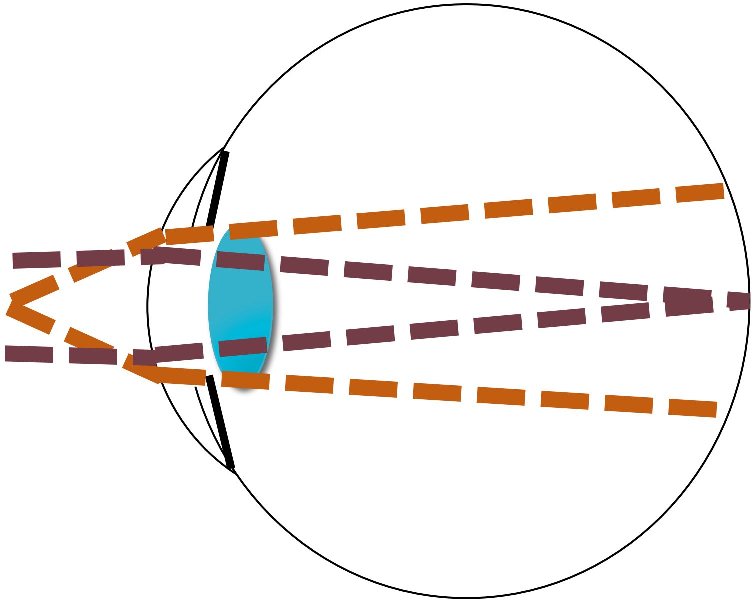

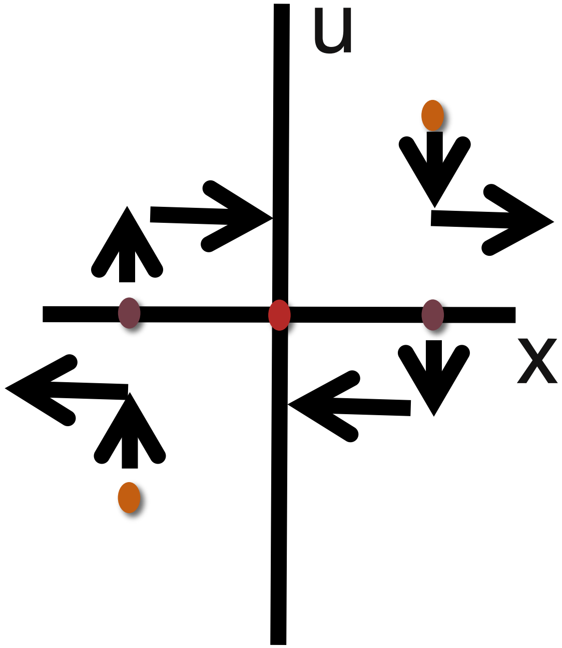

Light Field: simple eye model

$$\begin{bmatrix} x'' \\ u'' \end{bmatrix} = \begin{bmatrix} 1 & d \\ 0 & 1 \end{bmatrix} \begin{bmatrix} 1 & 0 \\ -1/f & 1 \end{bmatrix} \begin{bmatrix} x' \\ u' \end{bmatrix}$$

"Fourier Transform":
90° rotation

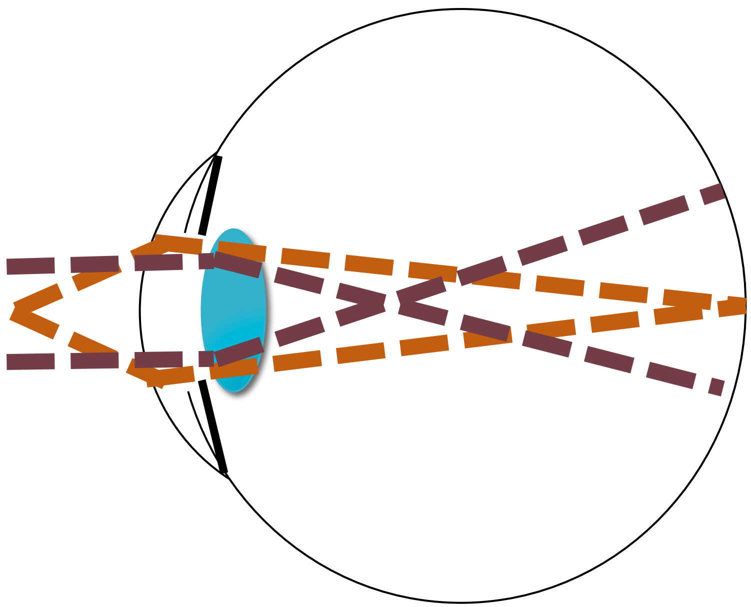

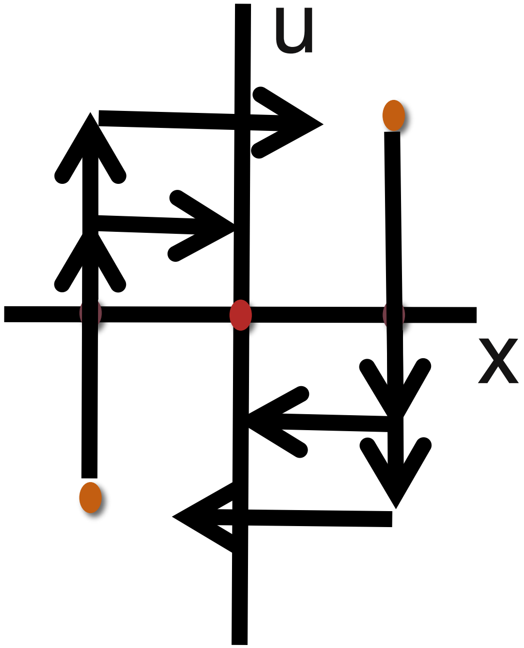

Accommodation vs. alignment display

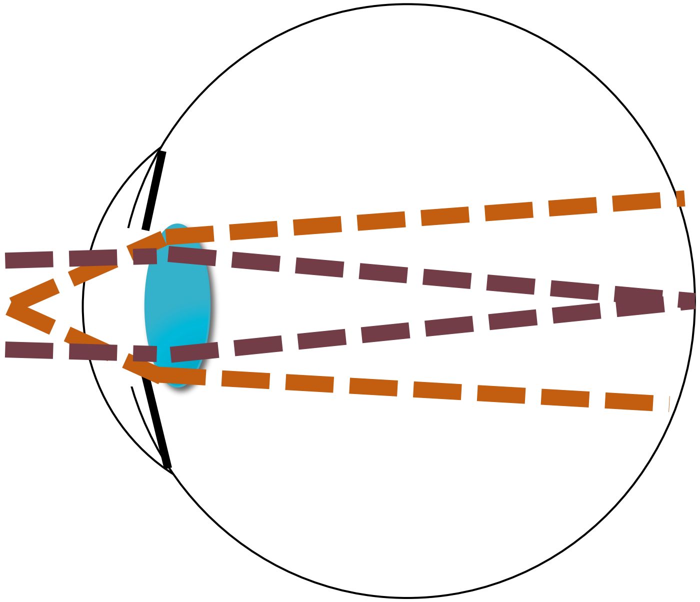

Accommodation:
Same scene but different views across pupil

Alignment:
Different view for each pupil position

Alignment Display: pupil size independence

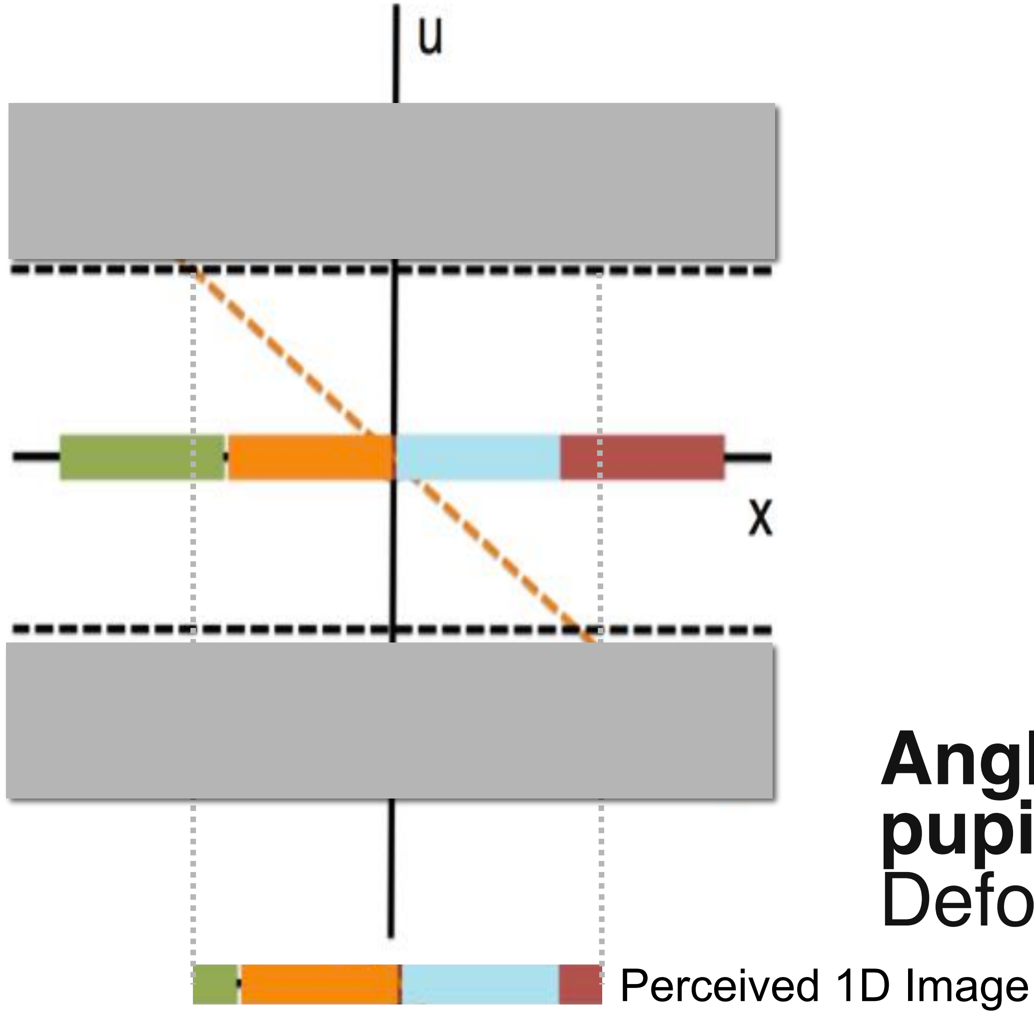

Aligned

Angle unique across pupil:
Defocused point source

Alignment Display: pupil size independence

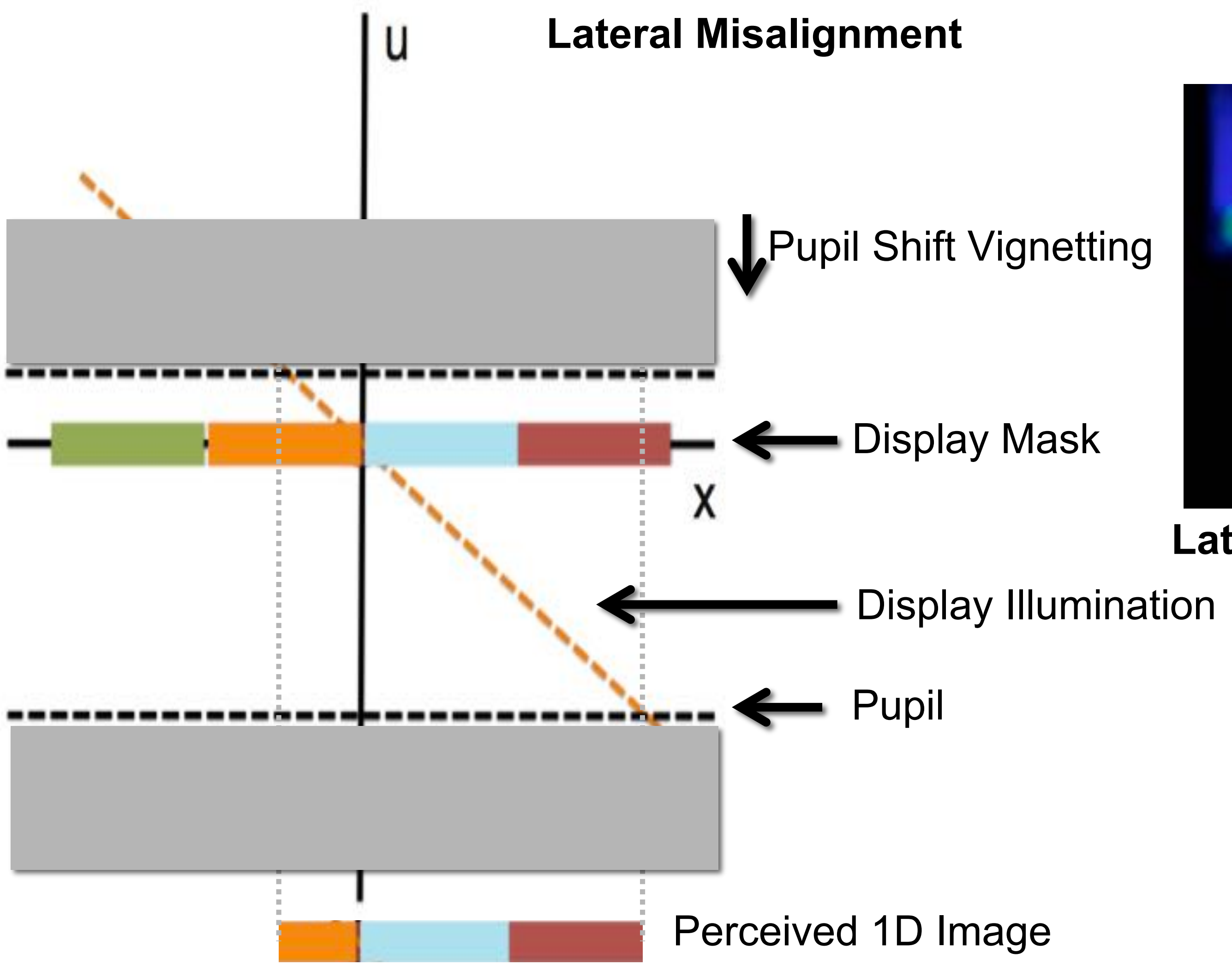

Lateral Misalignment

Corneal Reflection Channels

Corneal Reflection: illumination

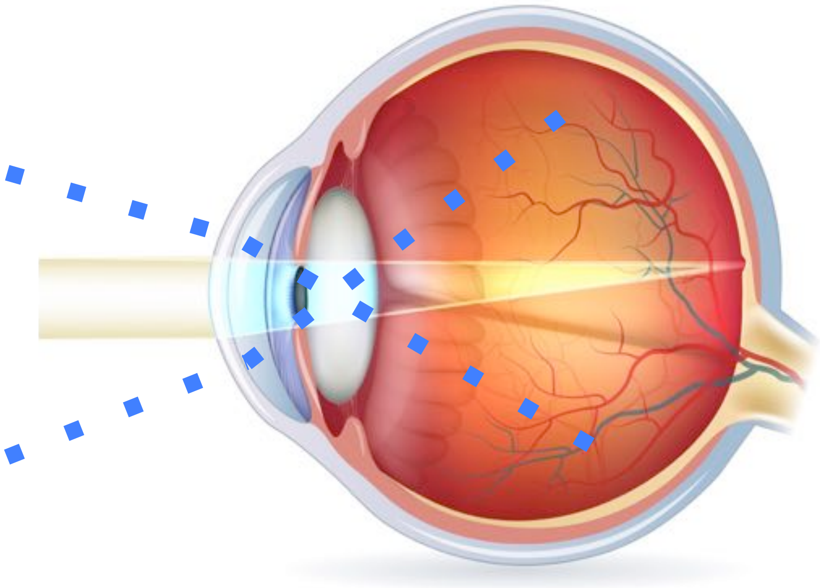

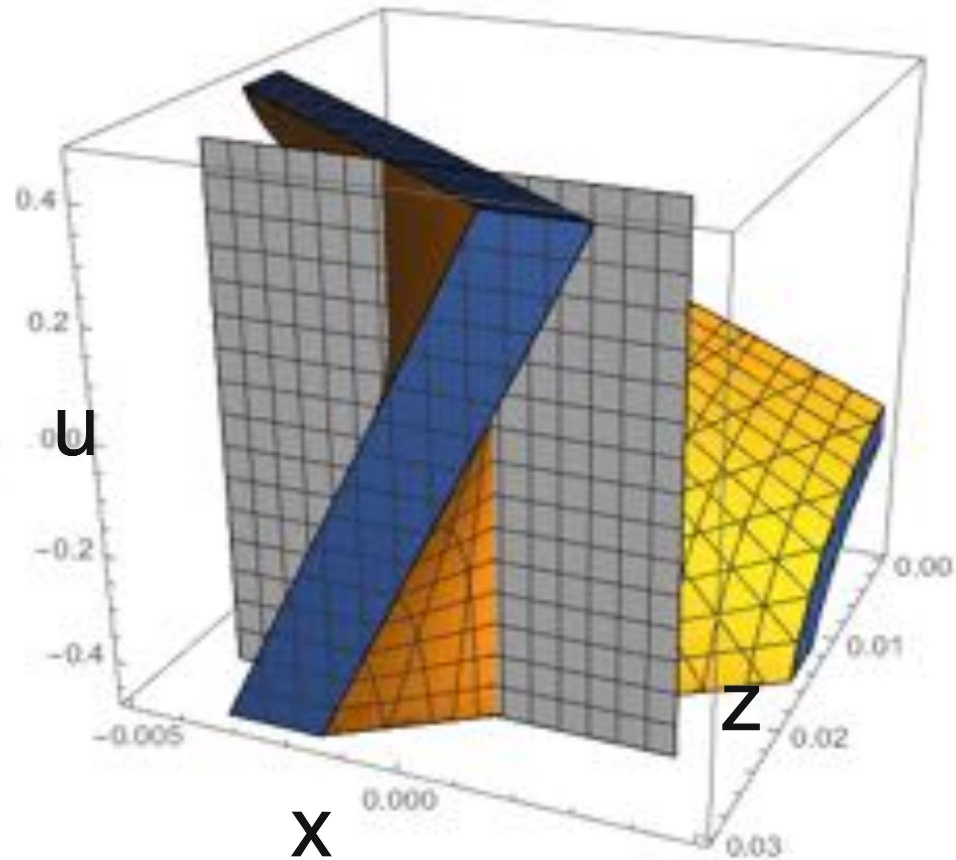

Corneal Reflection: light transport channel

Reflected at Image Plane

$$\begin{bmatrix} x'' \\ u'' \end{bmatrix} = \begin{bmatrix} f_L(-\frac{x}{f_c} + u) \\ x(\frac{1}{f_c} - \frac{2}{f_L}) + u(1 + f_L) \end{bmatrix}$$

Objective Lens

$$-\frac{D}{2f_L} + \frac{x}{f_c} < u < \frac{D}{2f_L} + \frac{x}{f_c}$$

Image Plane

$$\cap$$

$$-\frac{D}{2f_L} - x\left(\frac{1}{f_L} - \frac{1}{f_c}\right) < u < \frac{D}{2f_L} - x\left(\frac{1}{f_L} - \frac{1}{f_c}\right)$$

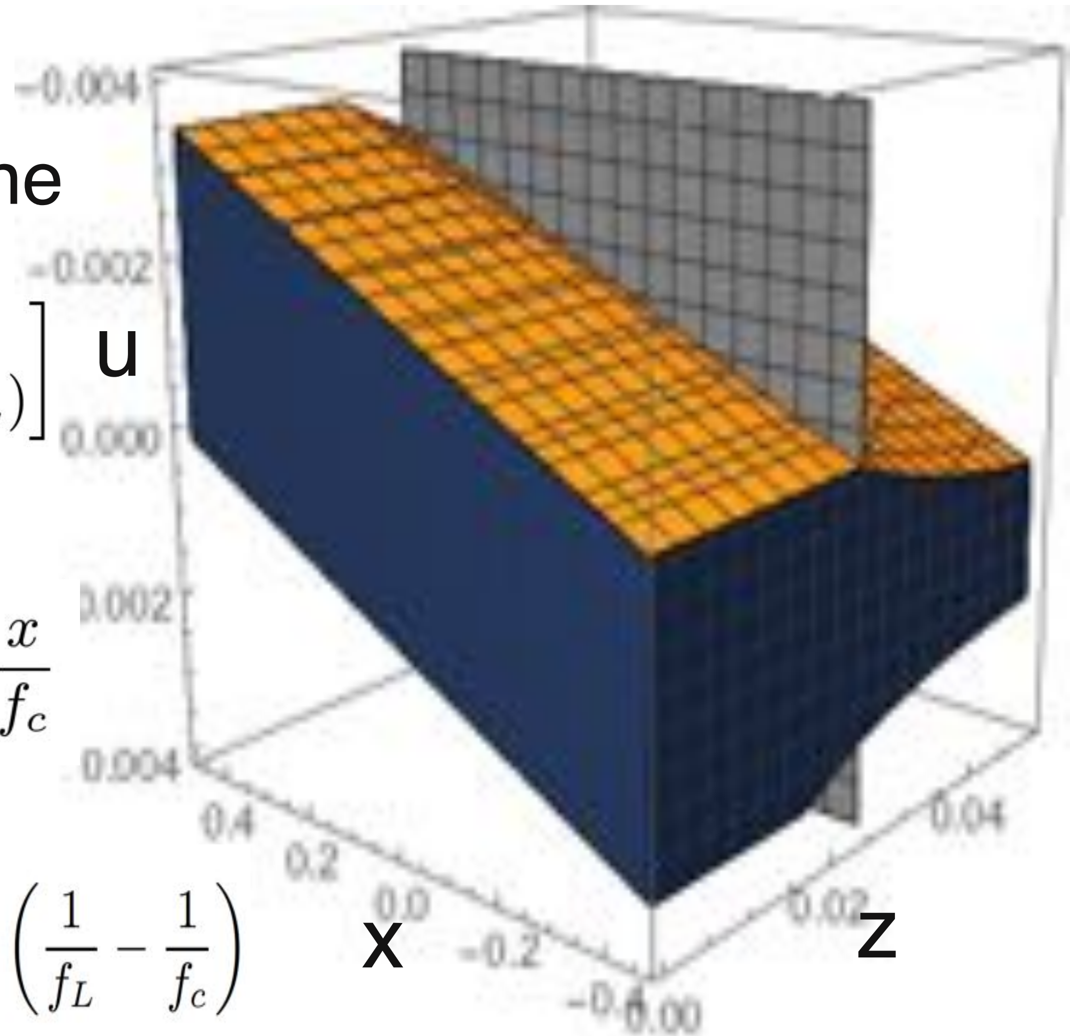

Corneal Reflection: light transport

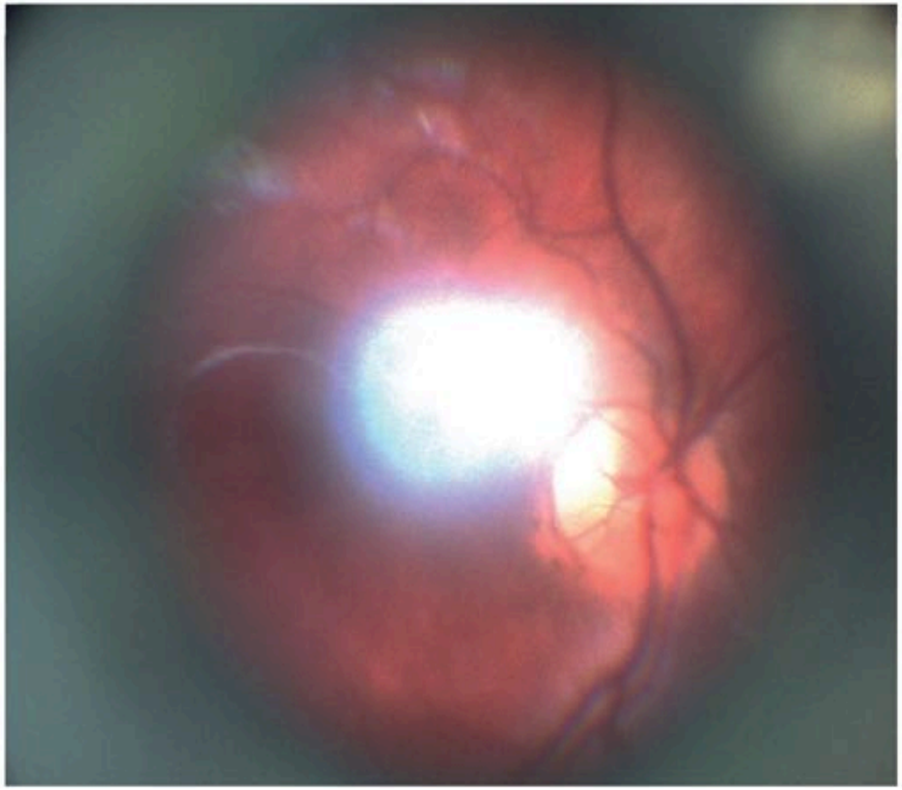

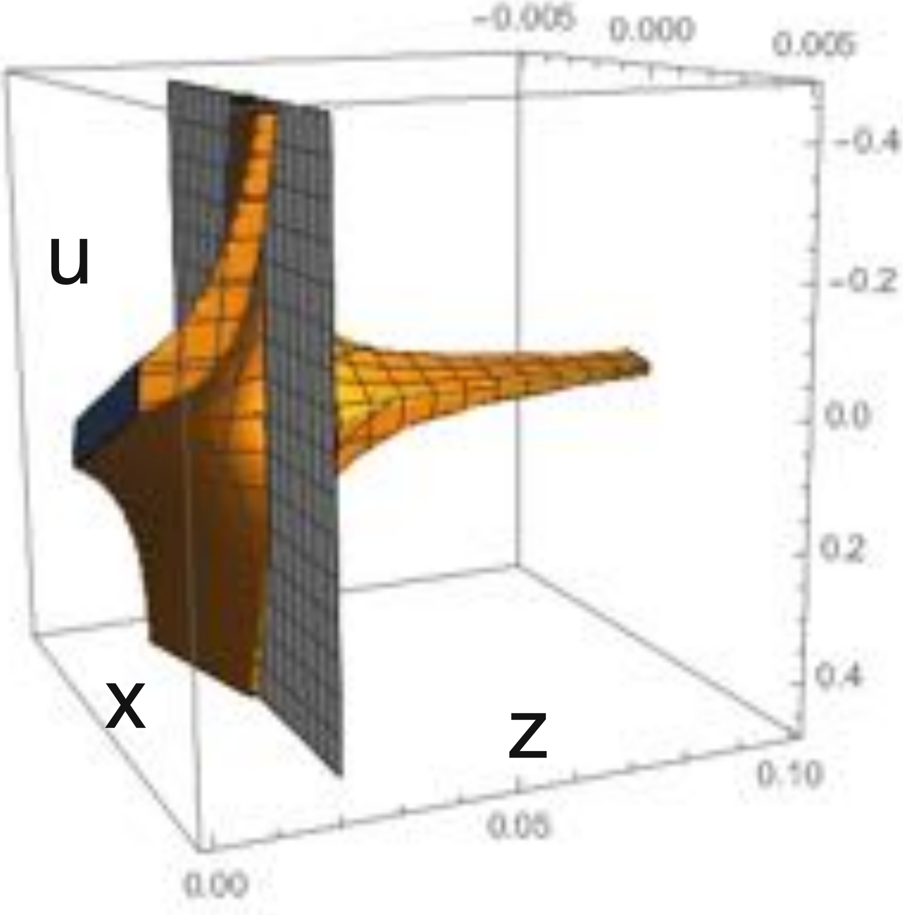

Corneal Reflection: light transport

$$u_{max} = \frac{f_c f_L (D_L/2)}{{r_e}^2 + f_c f_L - r_e(2f_c + f_L)}$$

$$x' = -u_{max}\left(\frac{f_c + f_L - r_e}{f_c}\right)$$

Reflection size and pupil or lens occlusion mapped to eye relief

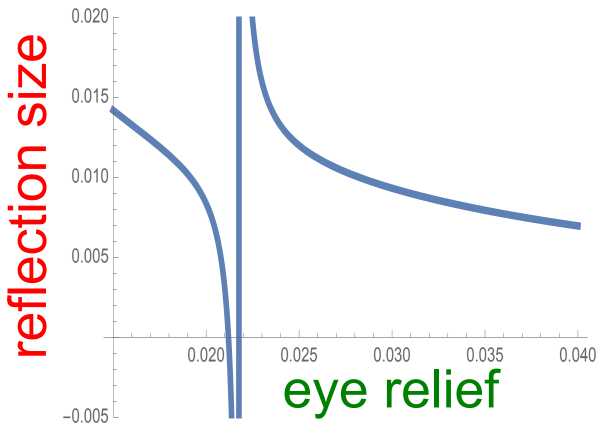

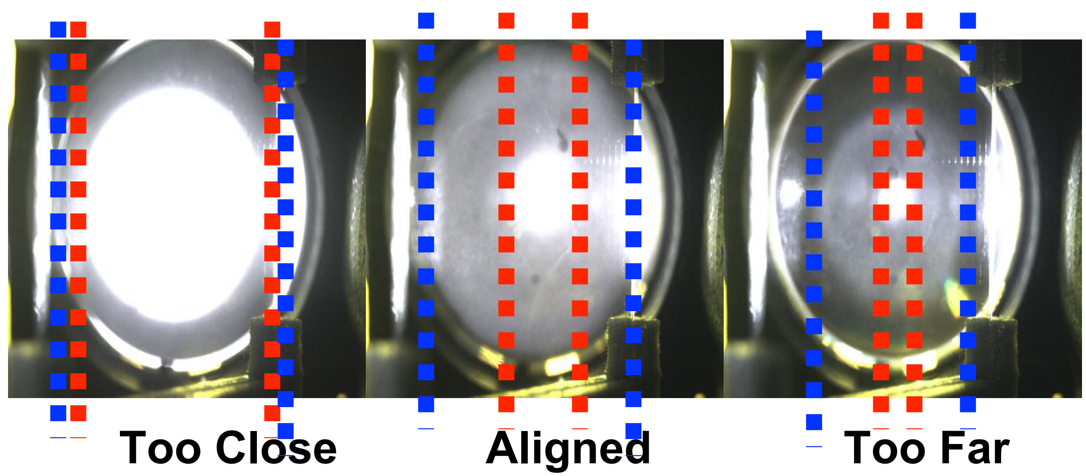

Retinal Imaging: “Inverse VR”

Eye box: near eye pinhole projector

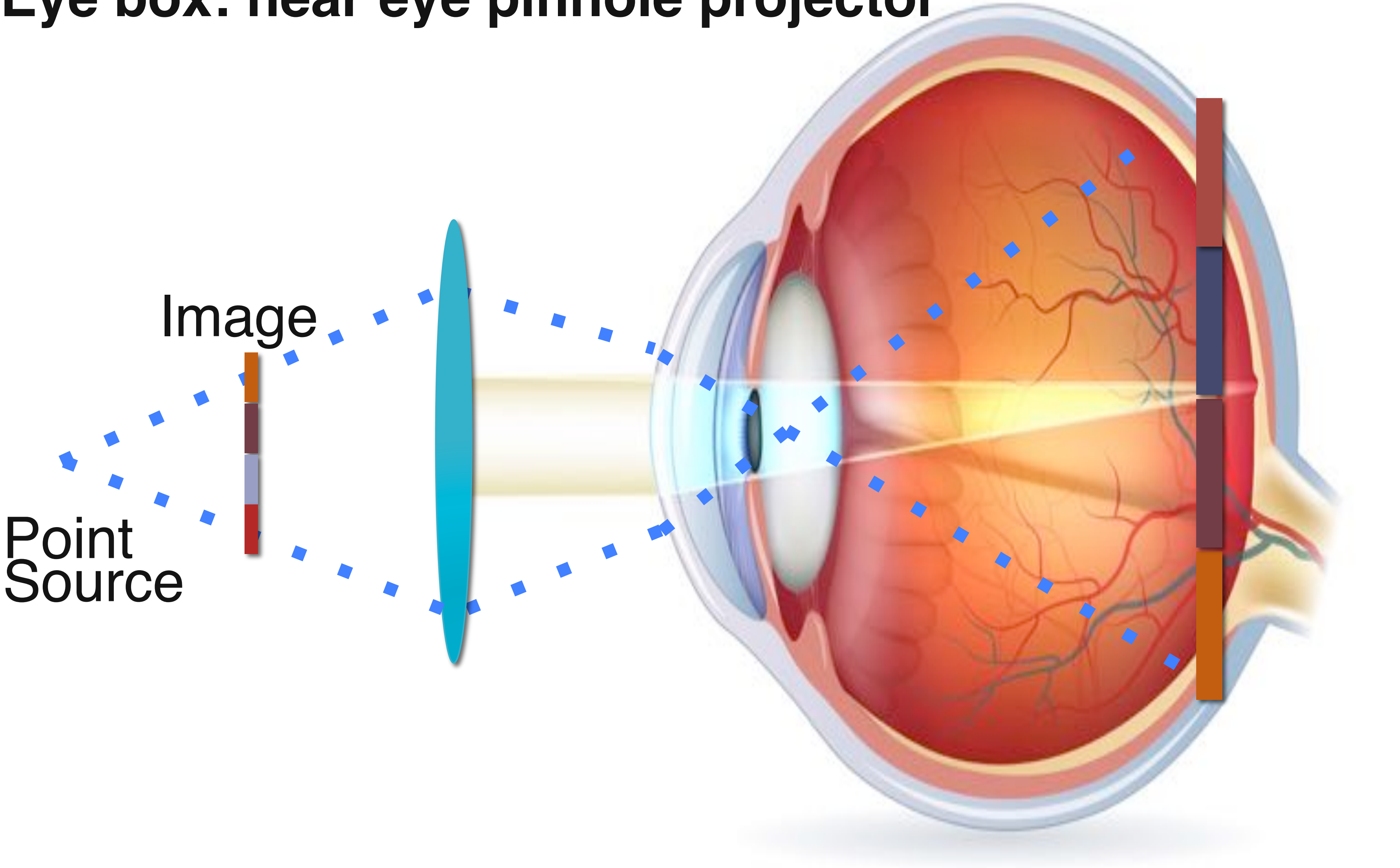

Retinal imaging optics

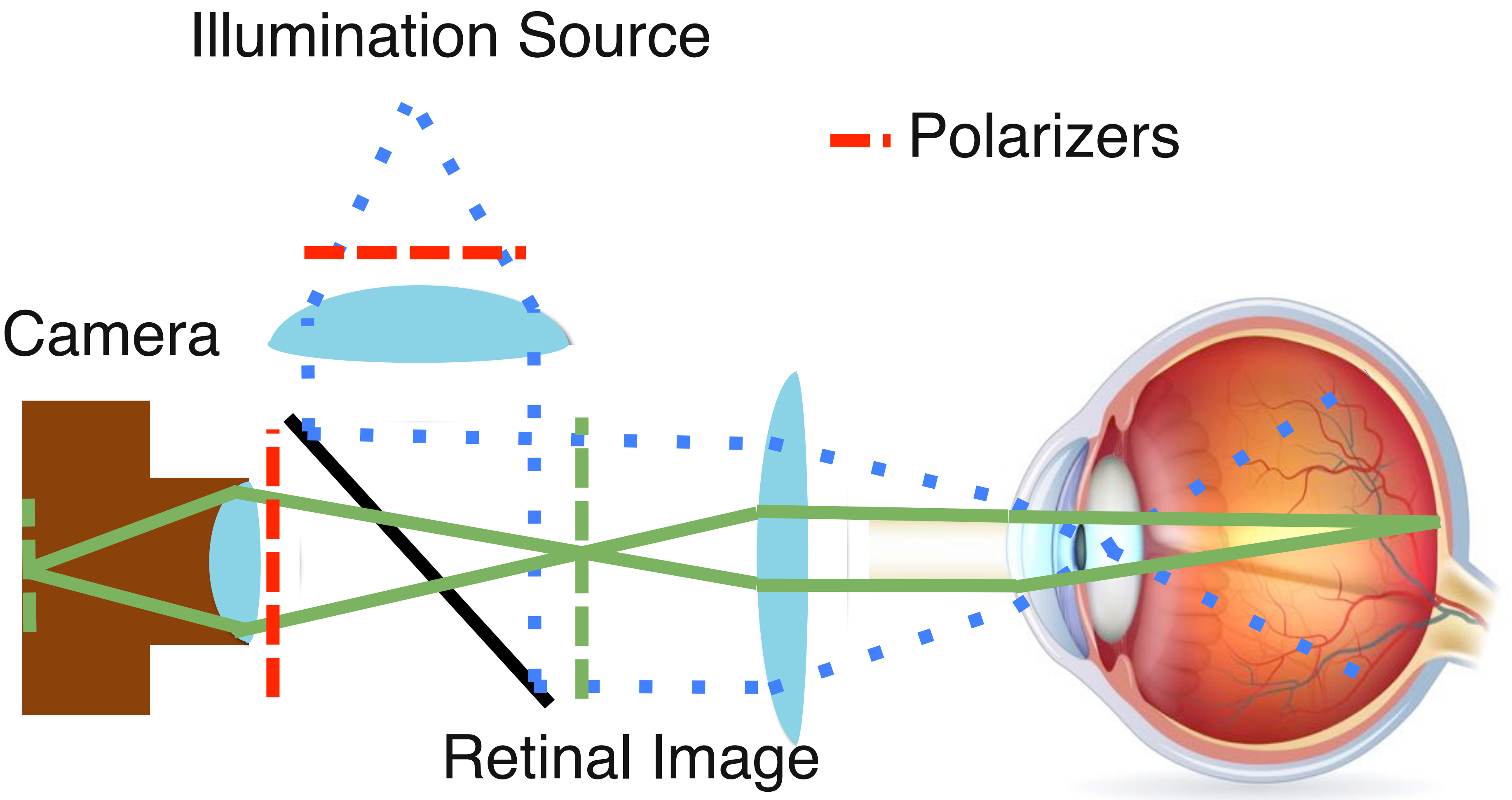

Image capture user experience

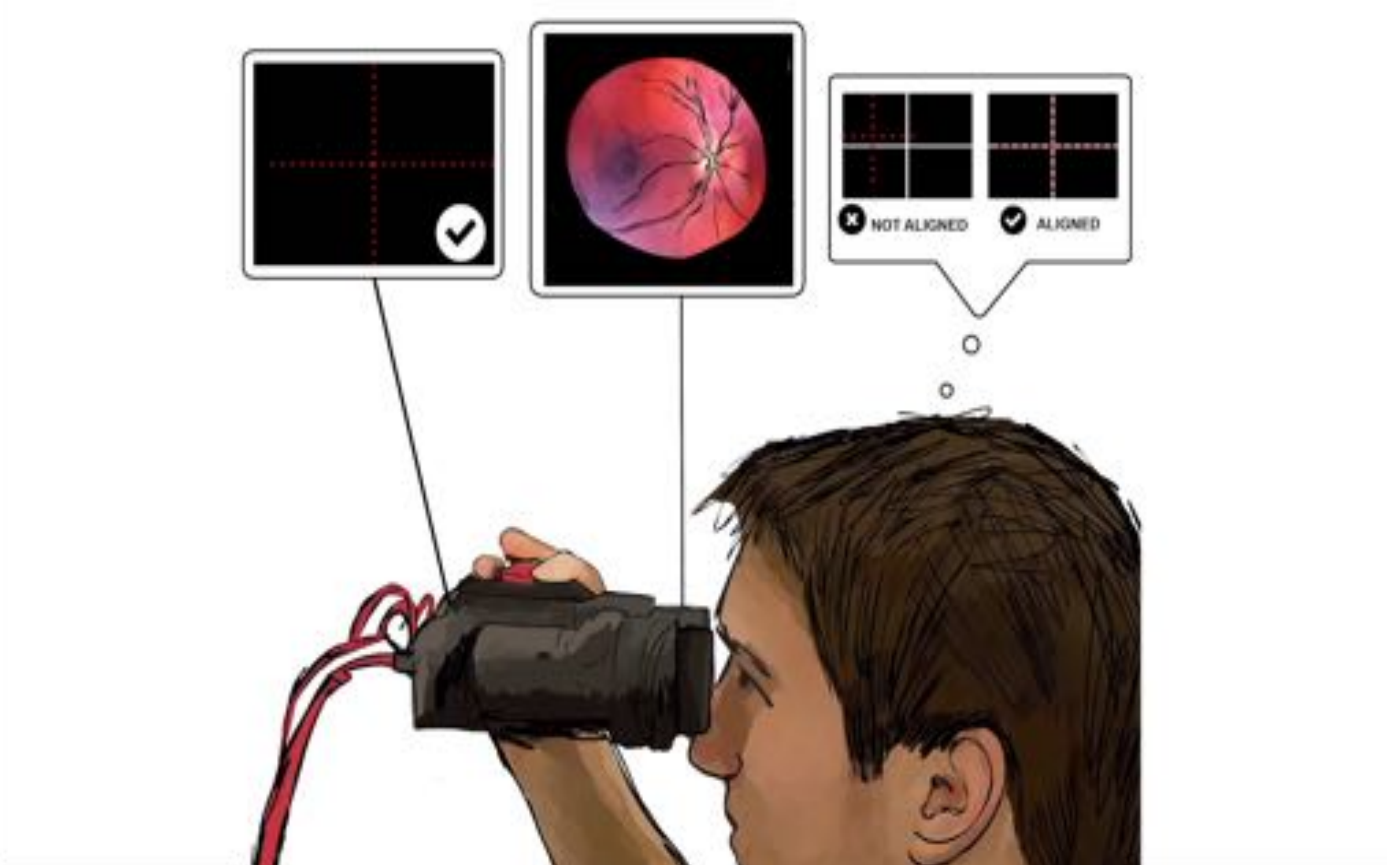

[T. Swedish, et al. eyeSelfie. ACM Trans. Graph (34, 4), 2015.]

Optical design of prototype

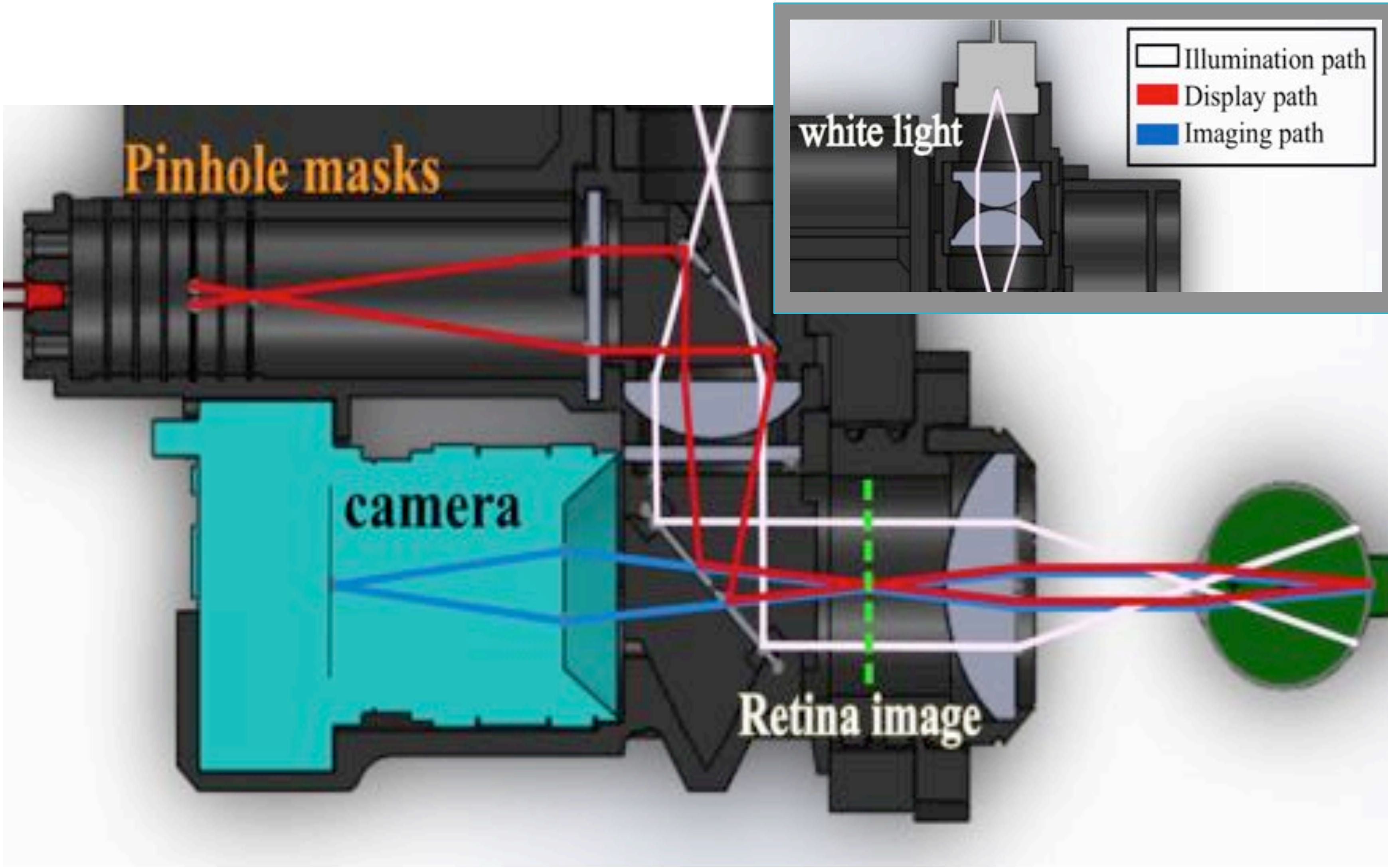

[T. Swedish, et al. eyeSelfie. ACM Trans. Graph (34, 4), 2015.]

Double ray cone display design

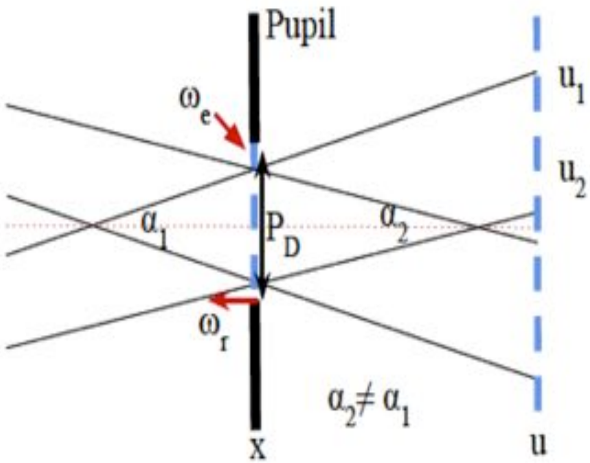

$$l_c = \begin{pmatrix} \frac{P_D}{2} & \frac{P_D}{2} & -\frac{P_D}{2} & -\frac{P_D}{2} \\ -u_1 & u_2 & u_1 & -u_2 \end{pmatrix}$$

$$T = S_1 L_1 S_2 L_2 ... S_n L_n$$

$$l_d = T^{-1} l_c$$

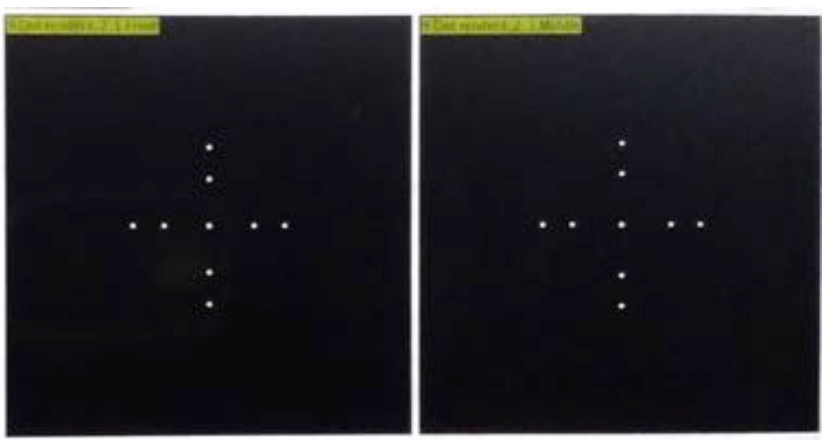

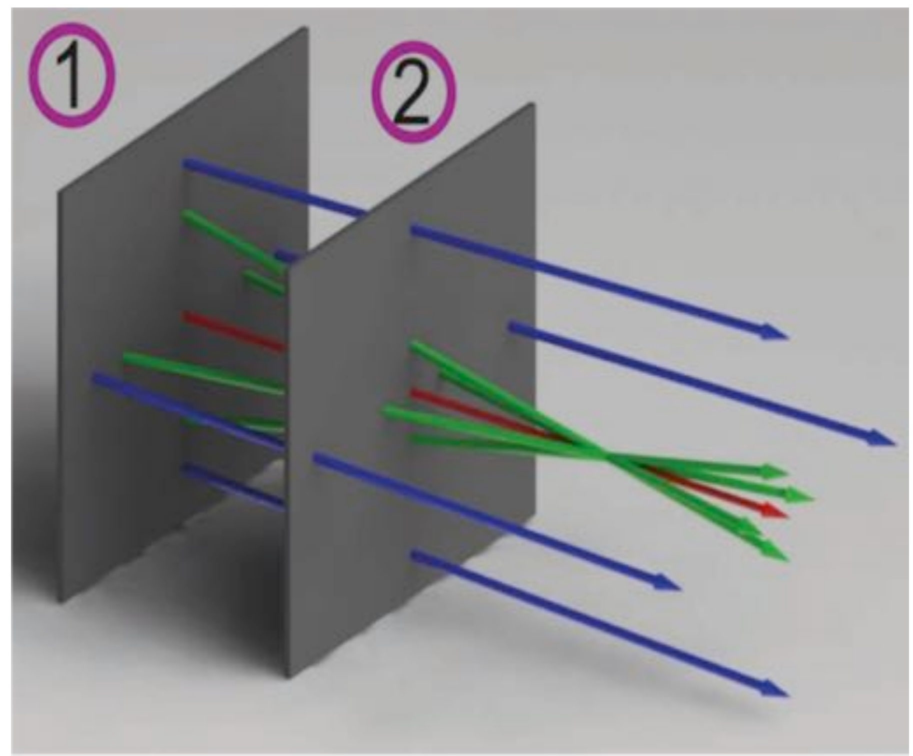

[T. Swedish, et al. eyeSelfie. ACM Trans. Graph (34, 4), 2015.]

Validation of alignment accuracy

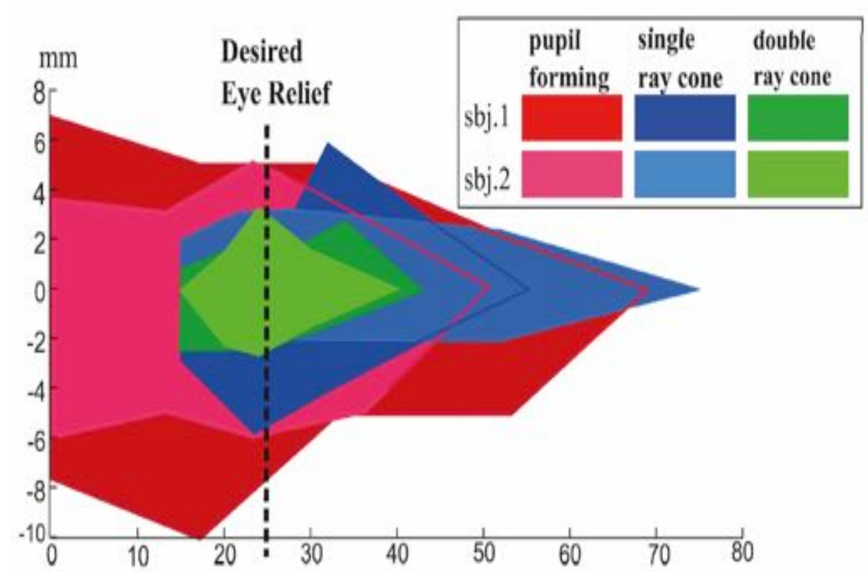

[T. Swedish, et al. eyeSelfie. ACM Trans. Graph (34, 4), 2015.]

Repeat alignment results

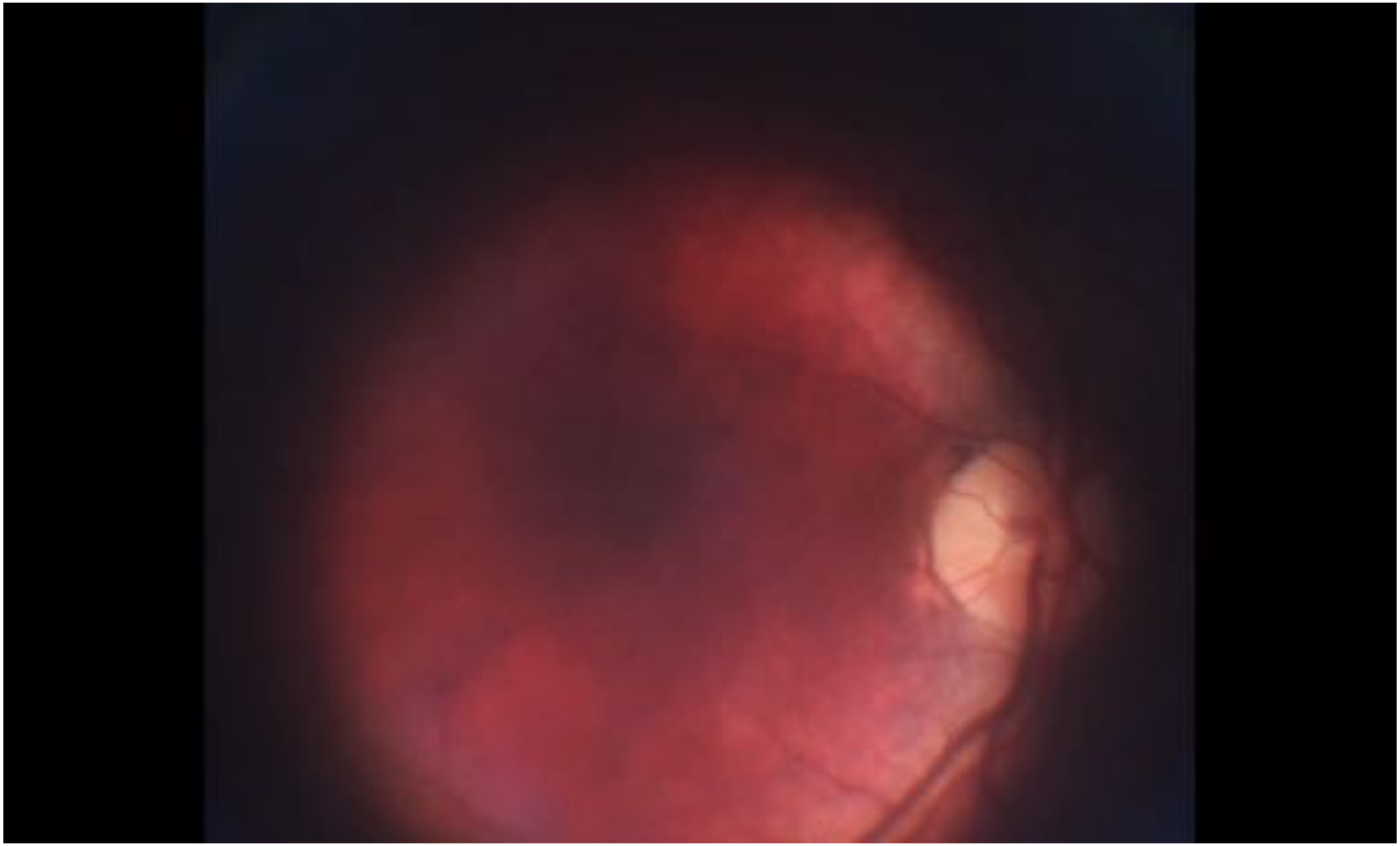

[T. Swedish, et al. eyeSelfie. ACM Trans. Graph (34, 4), 2015.]

Repeat alignment results: HDR Application

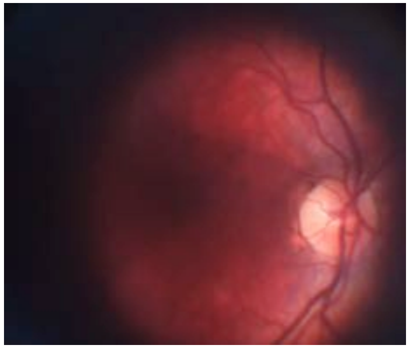

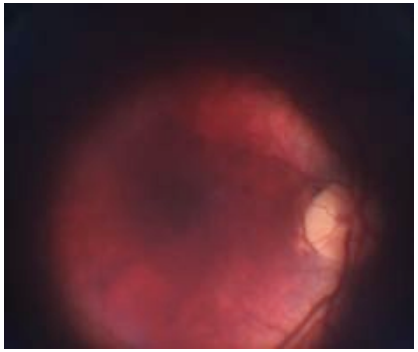

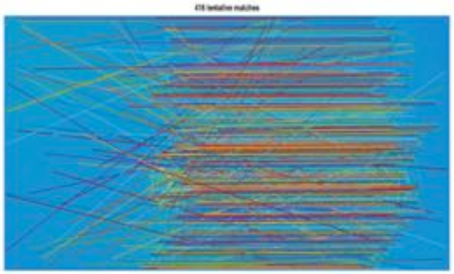

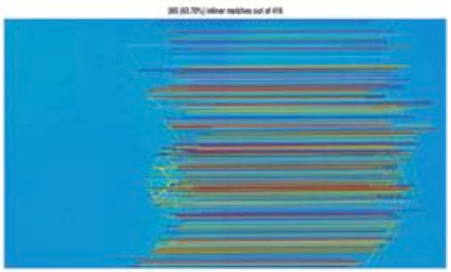

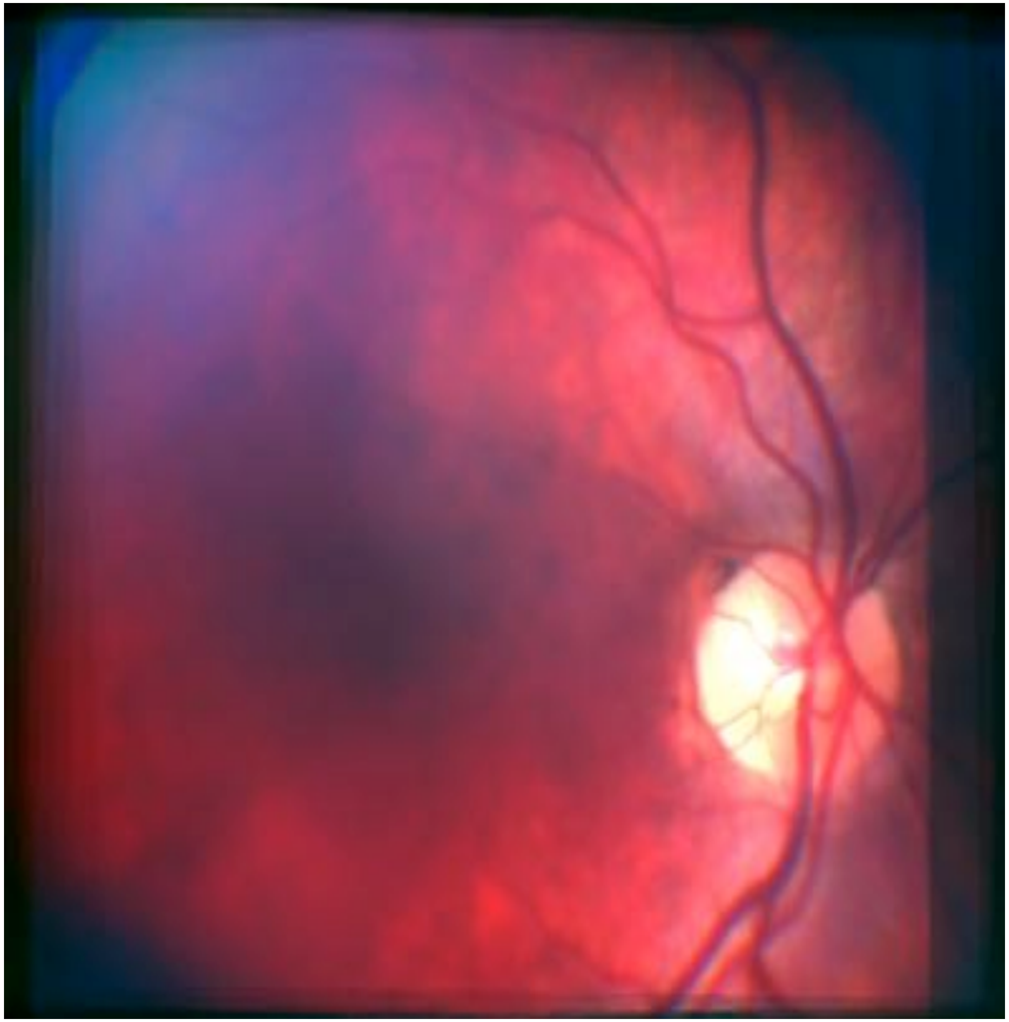

Future Applications: light efficient displays

AR VR

Future Applications: predictive health

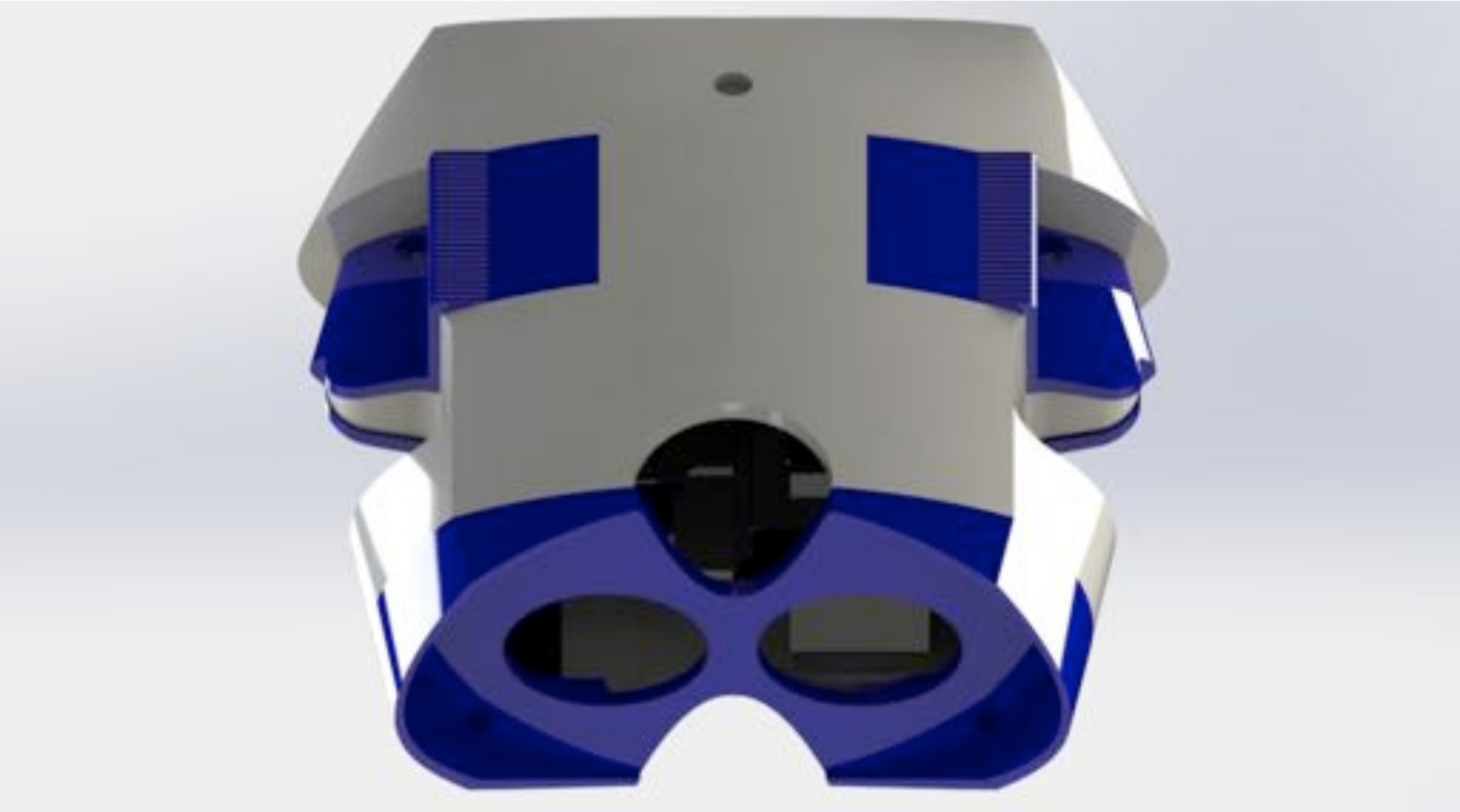

Future Applications: predictive health

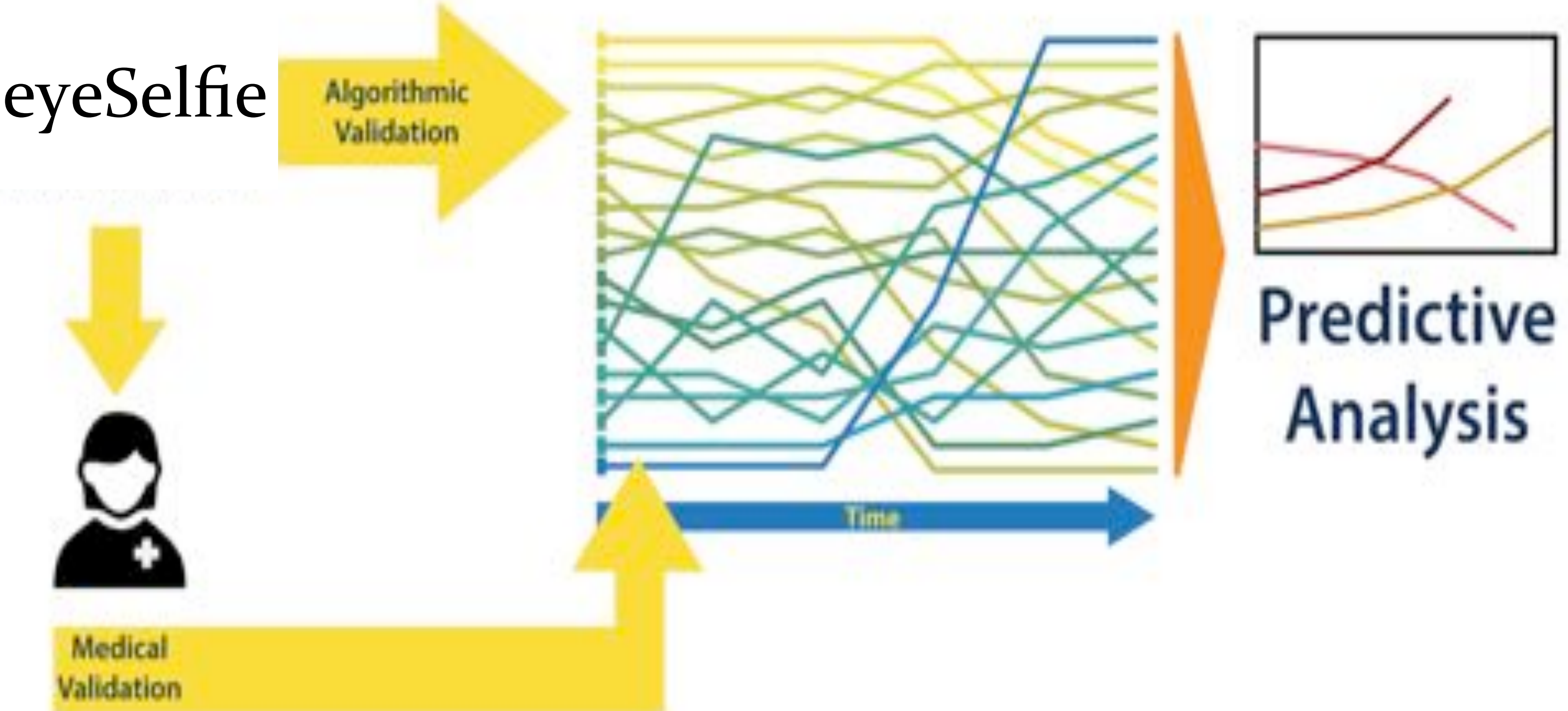

Summary

tinyurl.com/eyeSelfie

eyeSelfie enables accurate self-alignment to the eye

Various near eye displays evaluated in terms of alignment

We demonstrate this alignment through retinal imaging

Repeatable alignment useful for VR/AR and Predictive Health

BIOMEDICAL IMAGING AND HUMAN IMAGE CAPTURE

Anshuman Das
MIT Media Lab

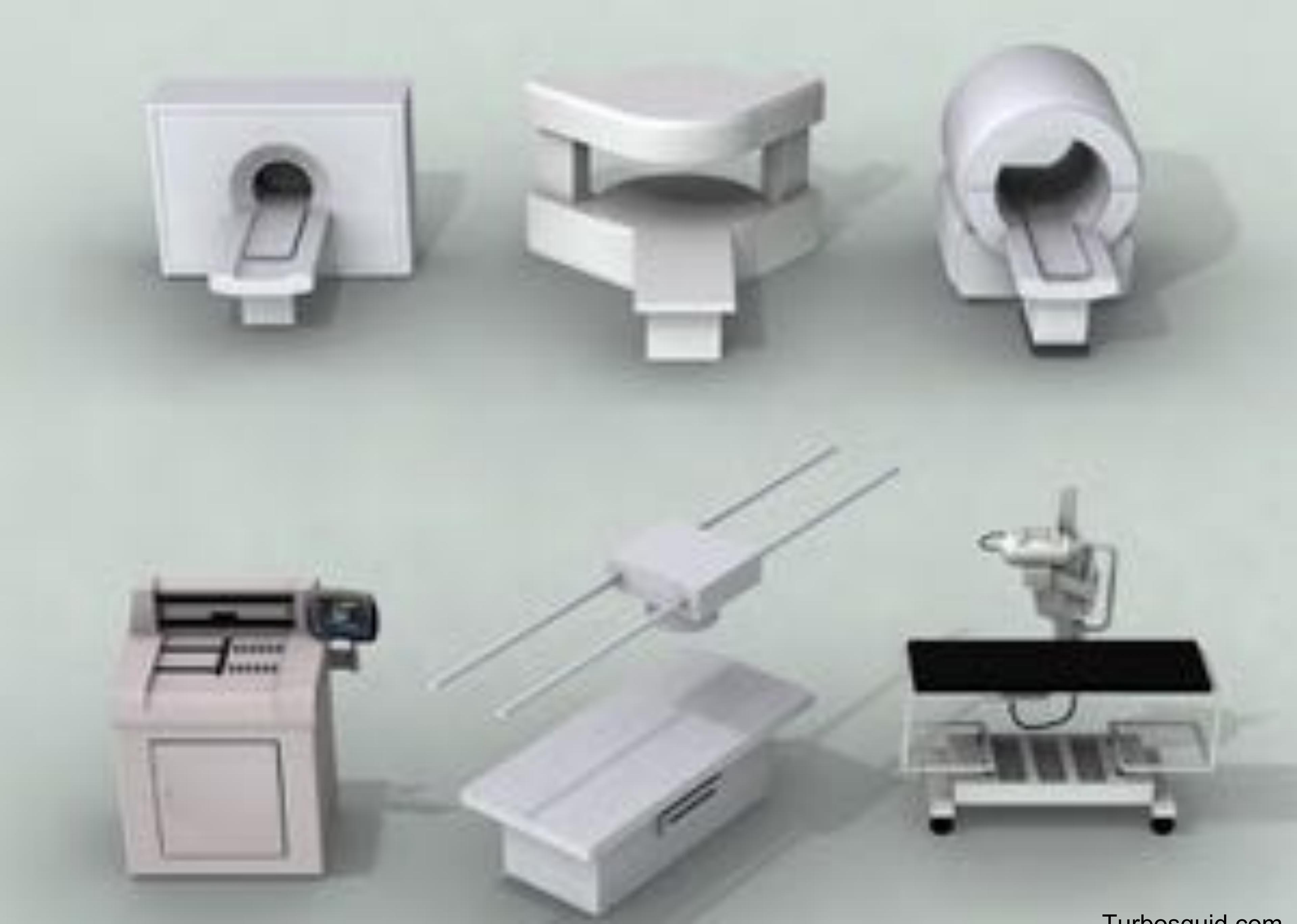

Turbosquid.com

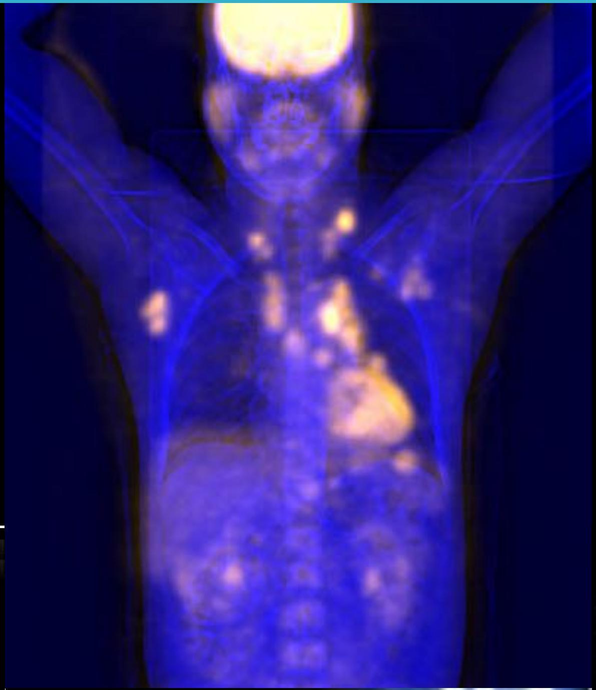


11.08.1984
GA=12w3d
RAB4-8-D/OB
8.3cm/1.4/16Hz
MI 1.1
Tis 0.1
Dr. Moroder ecofetale.com
02.02.2012
12:41:36
Routine
Har-high
97
Gn 10
C6 / M7
P6 / E3
SRI II 5
CRL
CRL 6.51cm
GA 12w6d 71.8%

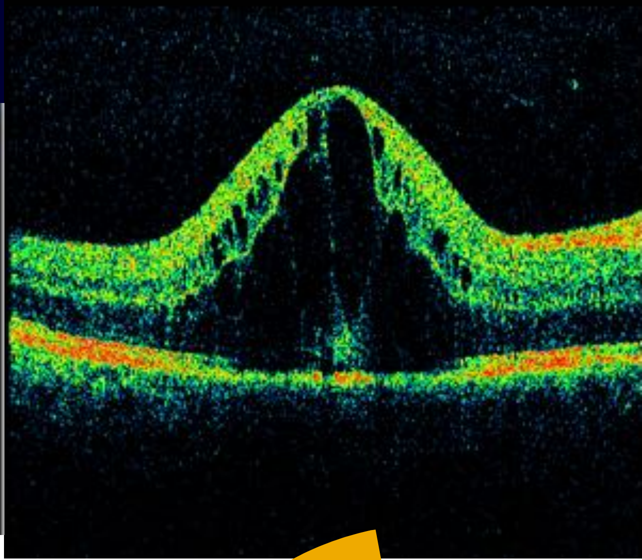

Faces, hair, furniture, art….macro objects

3D Imaging

Time of flight

Lightfield

Single-pixel

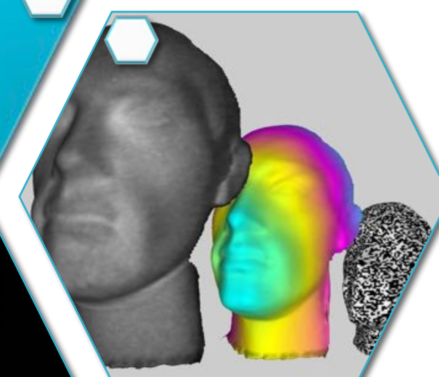

Structured light/ speckle

Wikipedia, WH.gov, http://www.gla.ac.uk/, http://www.3dunderworld.org/

3D Imaging …
-MICRO-IMAGING,
-LOOKING WITHIN THE HUMAN BODY?
-IMAGING SMALL OBJECTS

Challenges: From macro to micro…

- Depth resolution
- Optical design: very limited space for triangulation schemes to work

- Depth resolution of different 3D imaging devices
- Laser line scan: 1 micron depth (expensive, bulky, time consuming)
- Kinect: mm to cm (low resolution for imaging small objects)
- Phase-shifting method (sub mm resolution, easy to implement but multi-shot process)

Triangulation and depth estimation

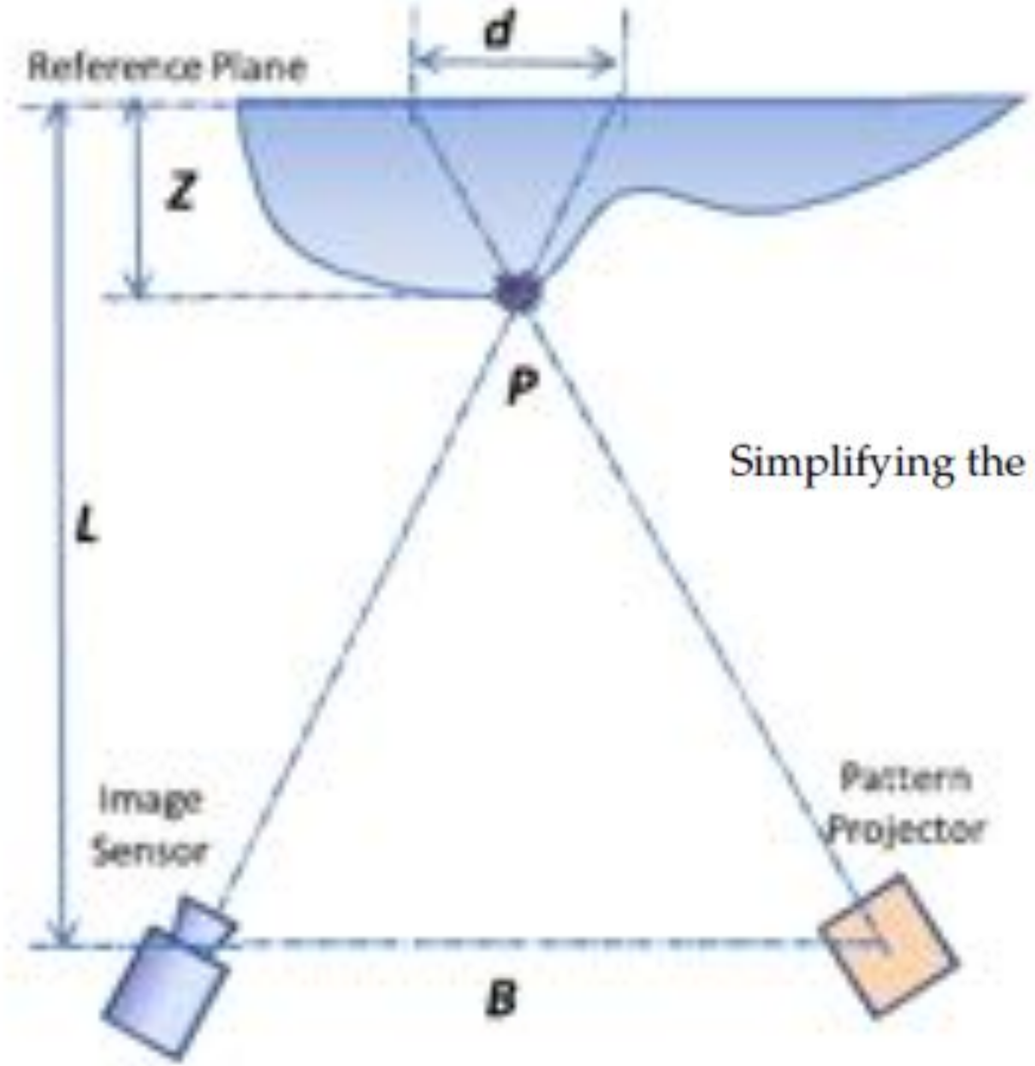

$$\frac{Z}{L-Z} = \frac{d}{B}, \quad \text{or} \quad Z = \frac{L-Z}{B} d.$$

Simplifying the relationship leads to

$$Z \approx \frac{L}{B} d \propto \frac{L}{B}(\phi - \phi_0).$$

Jason Geng, "Structured-light 3D surface imaging: a tutorial," Adv. Opt. Photon. 3, 128-160 (2011)

Phase estimation by phase shifting method

A set of 3 or 5 phase shifted images are sequentially projected,

Captured images can be modeled as,

$$I_n(x,y) = a(x,y) + b(x,y)\cos\left(\phi(x,y) + \omega_x \mathrm{x} + \omega_y y + \frac{\pi}{2}\mathrm{n}\right)$$

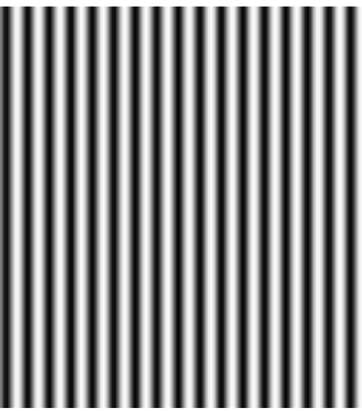

$$I_1(x,y) = I_0(x,y) + I_{mod}(x,y)\cos(\phi(x,y) - \theta),$$
$$I_2(x,y) = I_0(x,y) + I_{mod}(x,y)\cos(\phi(x,y)),$$
$$I_3(x,y) = I_0(x,y) + I_{mod}(x,y)\cos(\phi(x,y) + \theta),$$

$$\phi' = \arctan\left[\sqrt{3}\frac{I_1(x,y) - I_3(x,y)}{2I_2(x,y) - I_1(x,y) - I_3(x,y)}\right].$$

$$\phi(x,y) = \phi'(x,y) + 2k\pi,$$

Jason Geng, "Structured-light 3D surface imaging: a tutorial," Adv. Opt. Photon. 3, 128-160 (2011)

Process flow

Fringe Projection Sequence

↓

Capture each pattern

↓

Threshold and segment images

↓

Phase unwrapping

↓

Conversion from phase to height

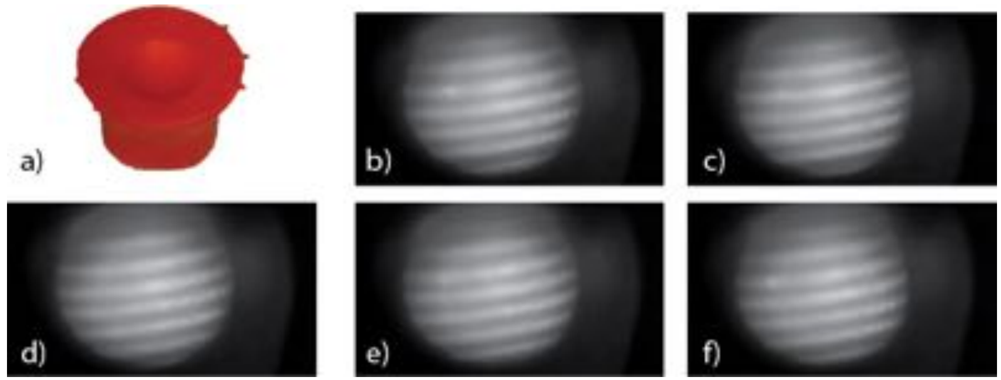

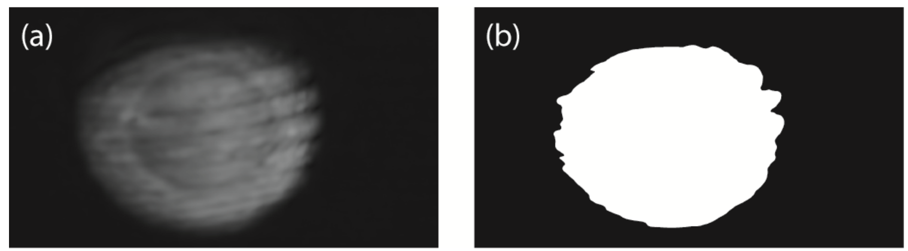

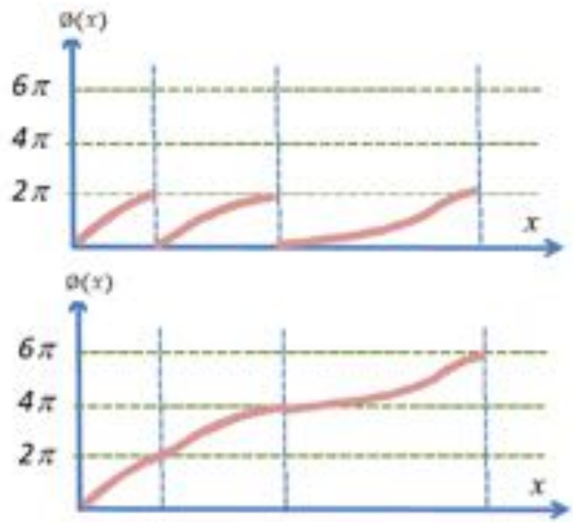

$$\phi(x, y) = \phi'(x, y) + 2k\pi,$$

$$Z \approx \frac{L}{B} d \propto \frac{L}{B}(\phi - \phi_0).$$

Jason Geng, "Structured-light 3D surface imaging: a tutorial," Adv. Opt. Photon. 3, 128-160 (2011)

Case study of middle ear imaging

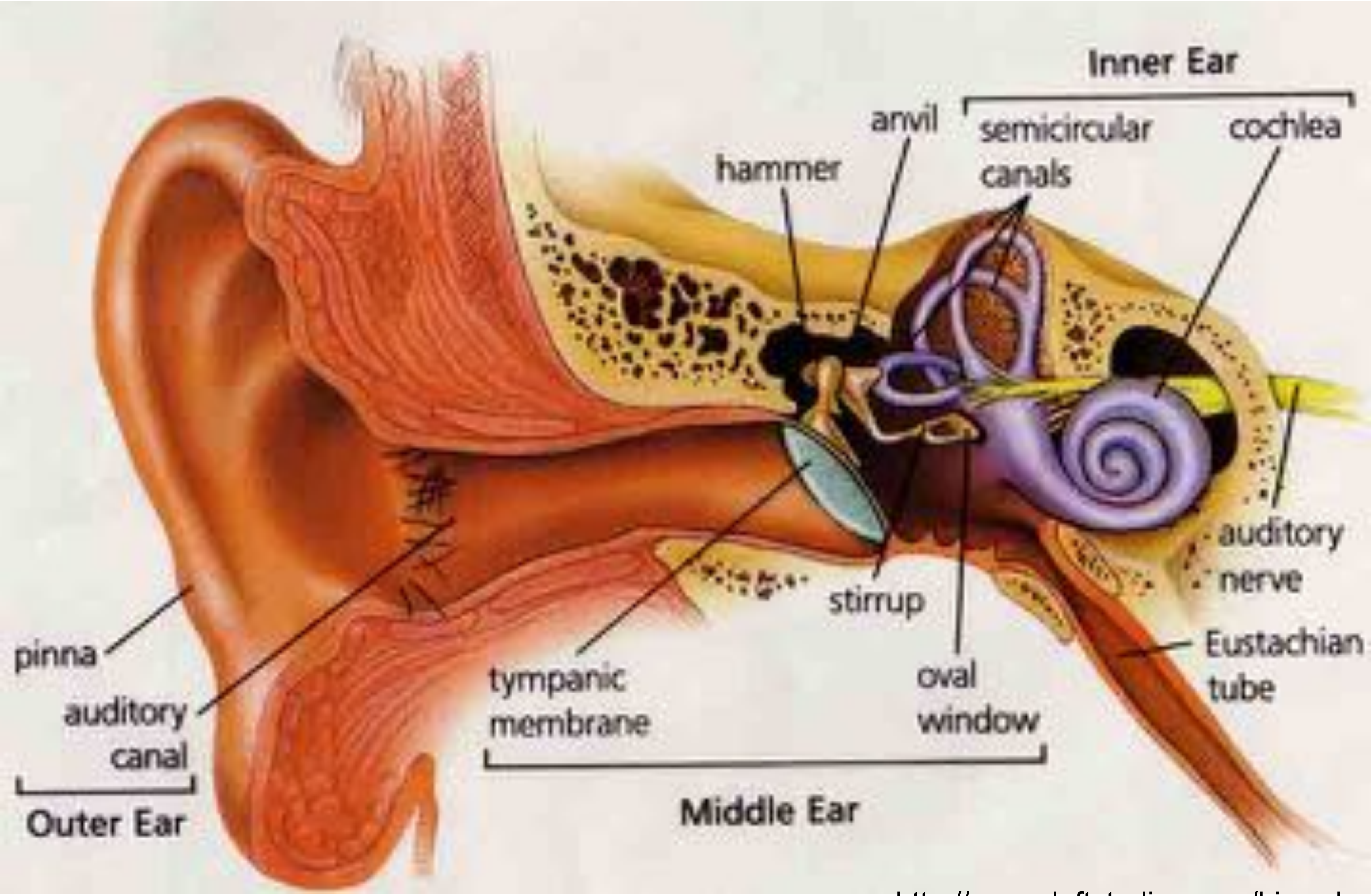

http://www.deftstudios.com/bioweb

Pressure changes in the middle ear

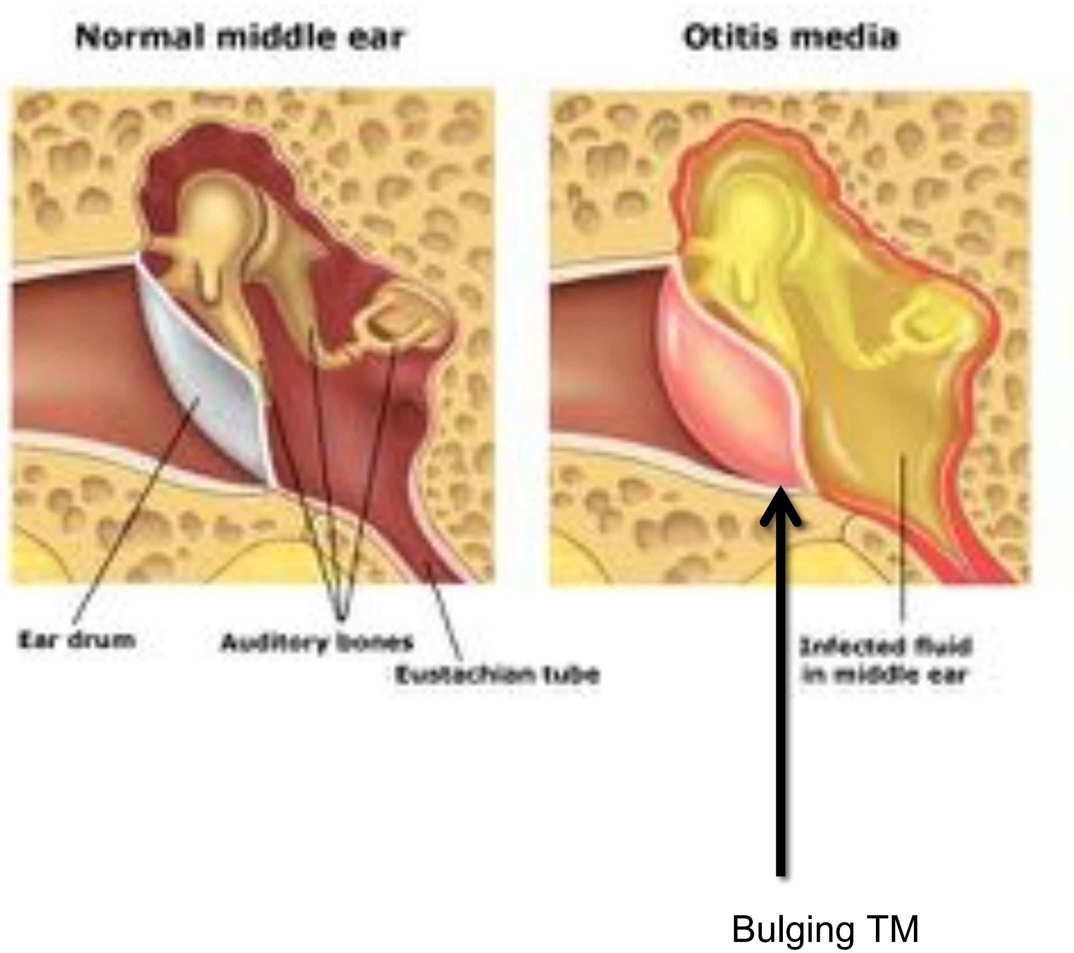

Otitis Media with Effusion

Diagnostic challenge: presence of colorless fluid can go undetectable

- **Standard procedure to diagnose is pneumatic otoscopy and tympanometry**
- **Huge problem in children (>3 million cases in US per year)**

Rayur.com

Ear drum in detail

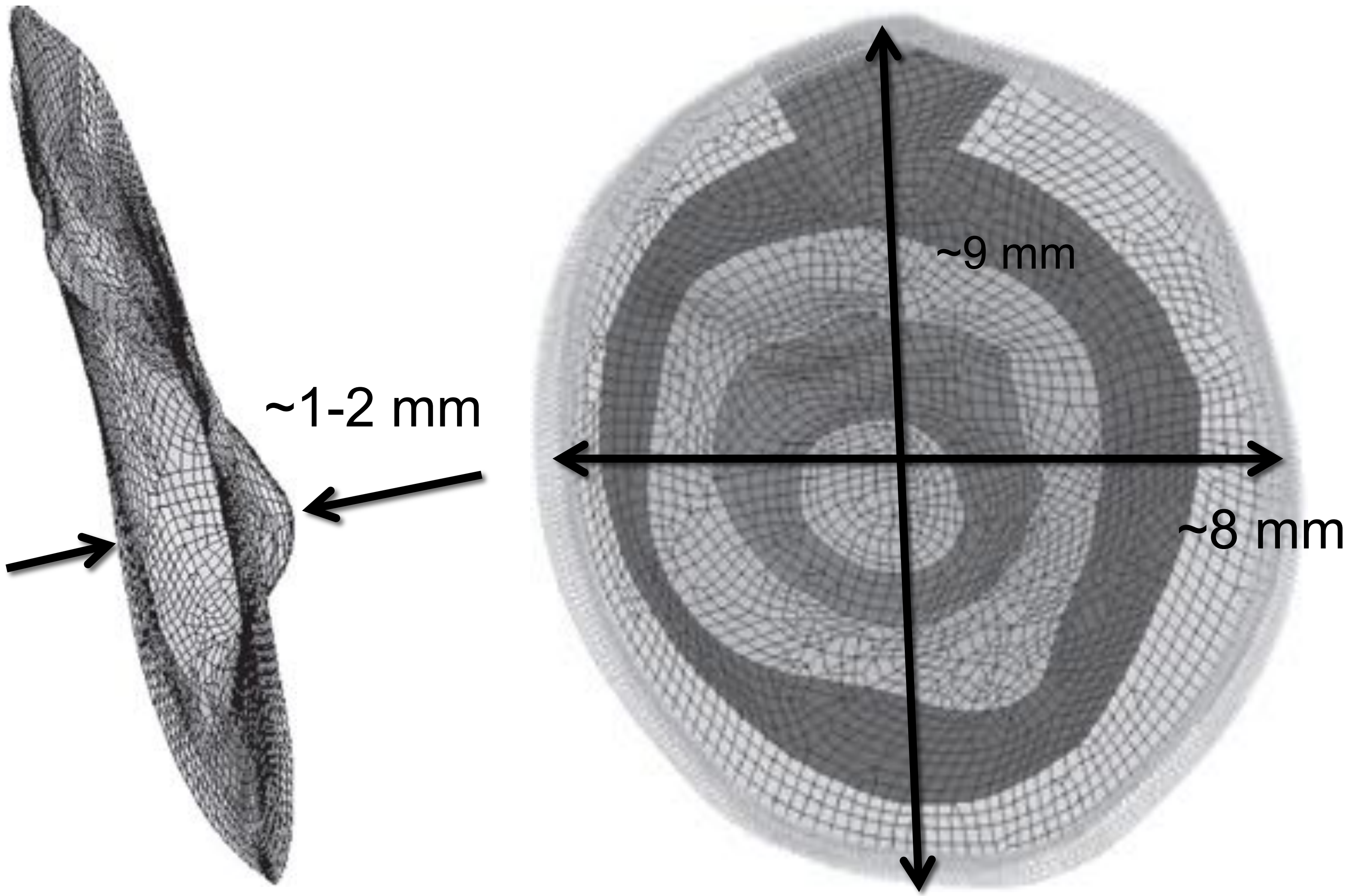

Volandri et. al, Journal of Biomechanics 44 (2011) 1219–1236

Imaging device: The otoscope



- 2D Imaging with a speculum and simple lens arrangement
- Subtle pressure changes cause the tympanic membrane to bulge or retract
- In cases where this depth cannot be imaged, 3D information may be useful

Recent developments in otoscopy

- New methods like Fluorescence otoscopy for cholesteotoma detection
- Cellscope oto

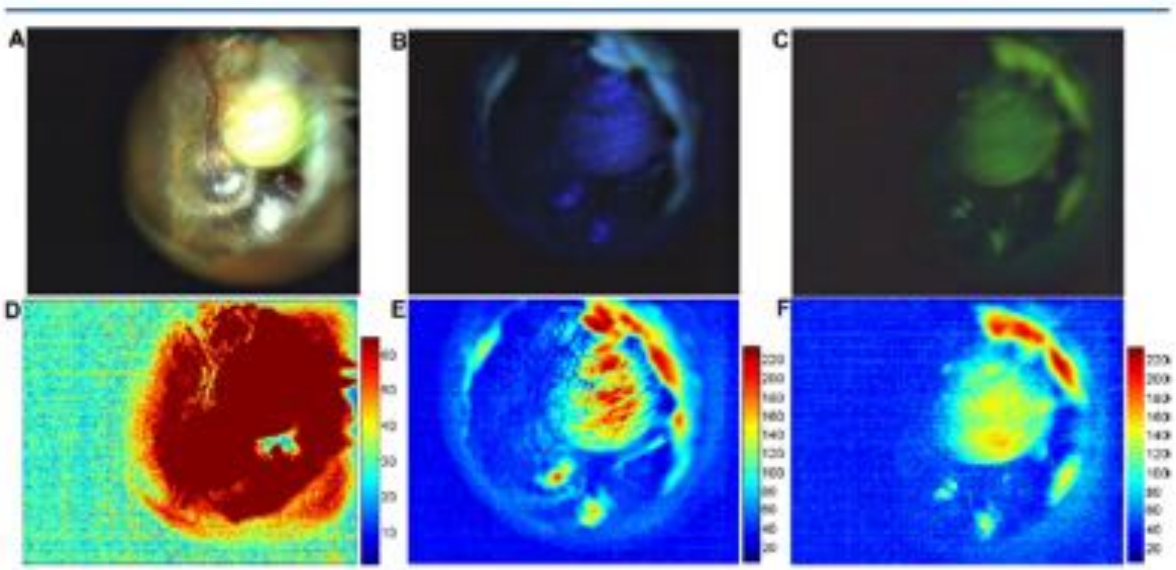

Tulio A. Valdez, et. al, *Analytical Chemistry* **2014** *86* (20), 10454-10460

Optical Coherence Tomography

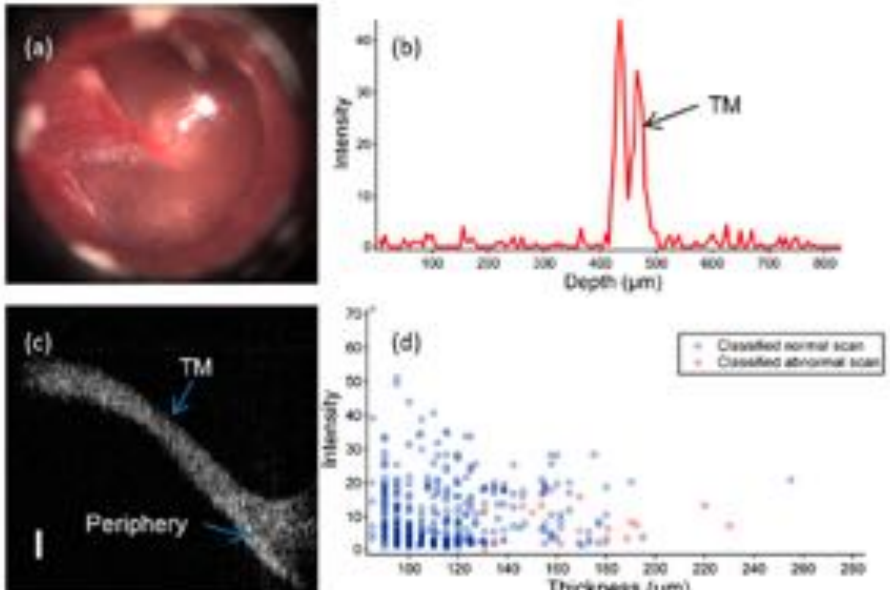

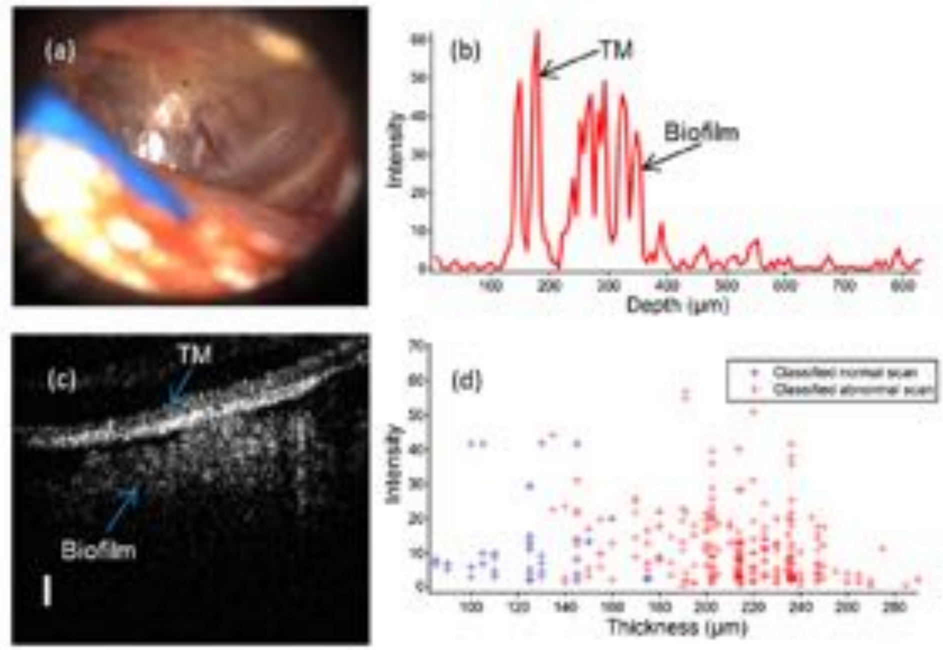

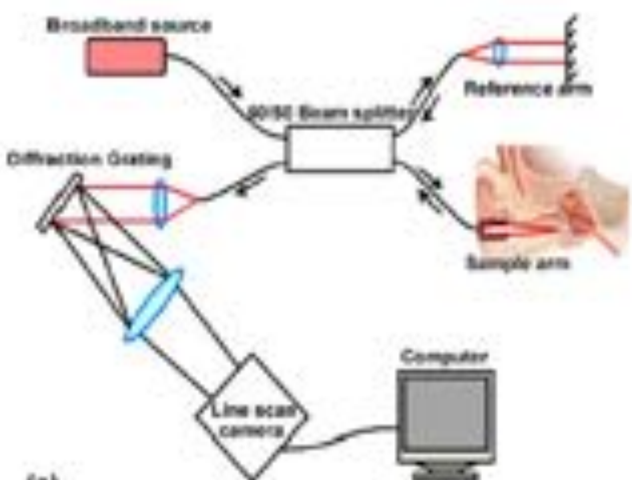

Cac T. Nguyen, et. al, Noninvasive in vivo optical detection of biofilm in the human middle ear, PNAS 2012 109 (24) 9529-9534

Recent advance: Light field Otoscope

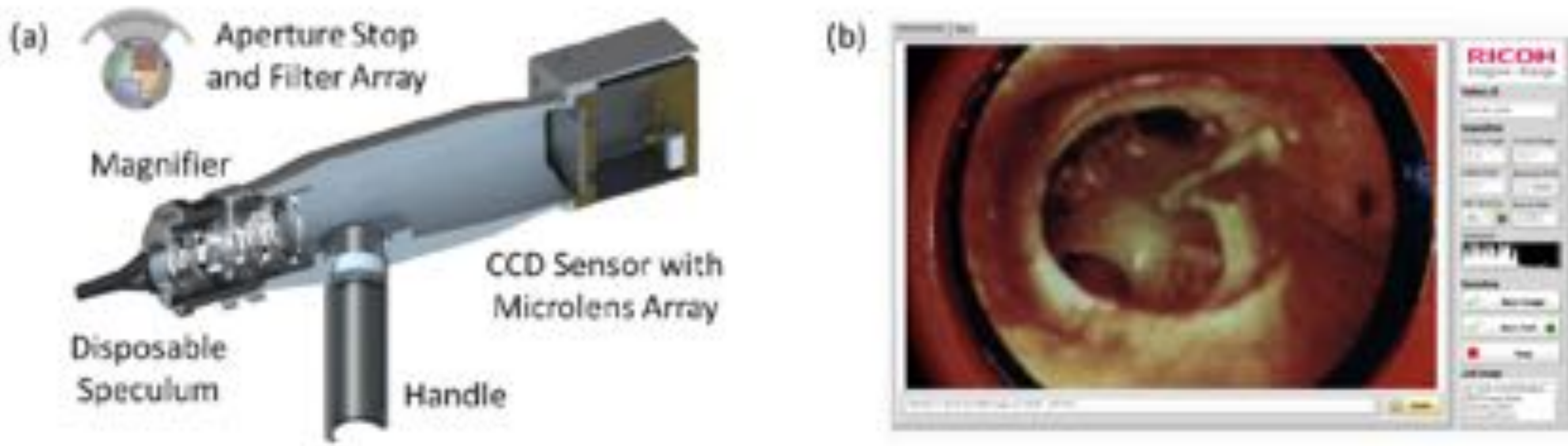

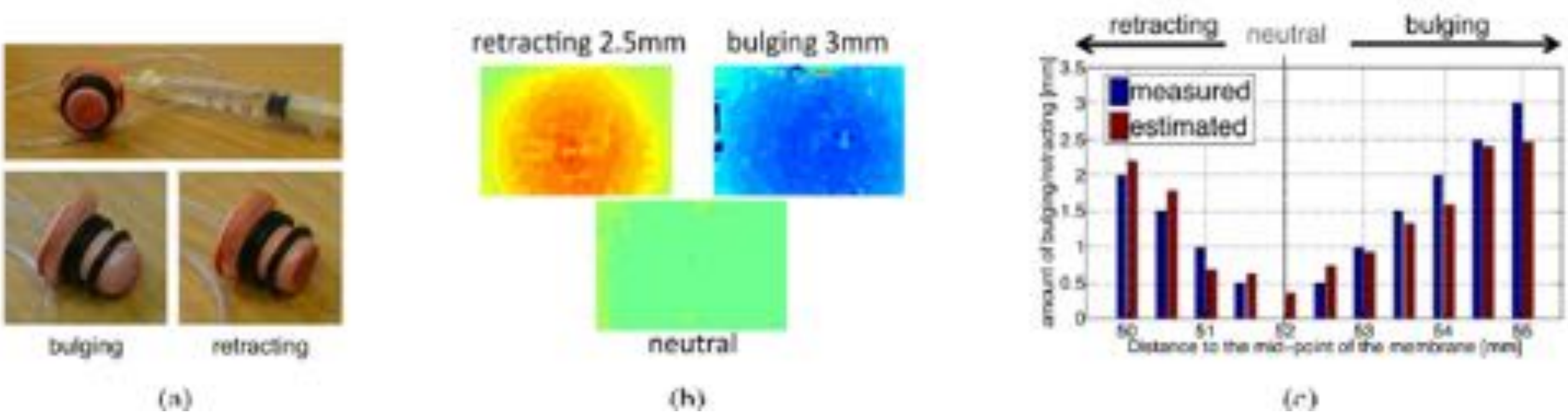

. Bedard, I. et.al , Imaging and Applied Optics 2014, OSA Technical Digest 2014, paper IM3C.6.

Our approach: otoscope with structured light

- Optical system specs:
- Focal plane about 1cm from tip of speculum
- 1080p webcam
- Telephoto lens with aperture control
- DLP Projector
- Front surface mirror
- Otoscope head

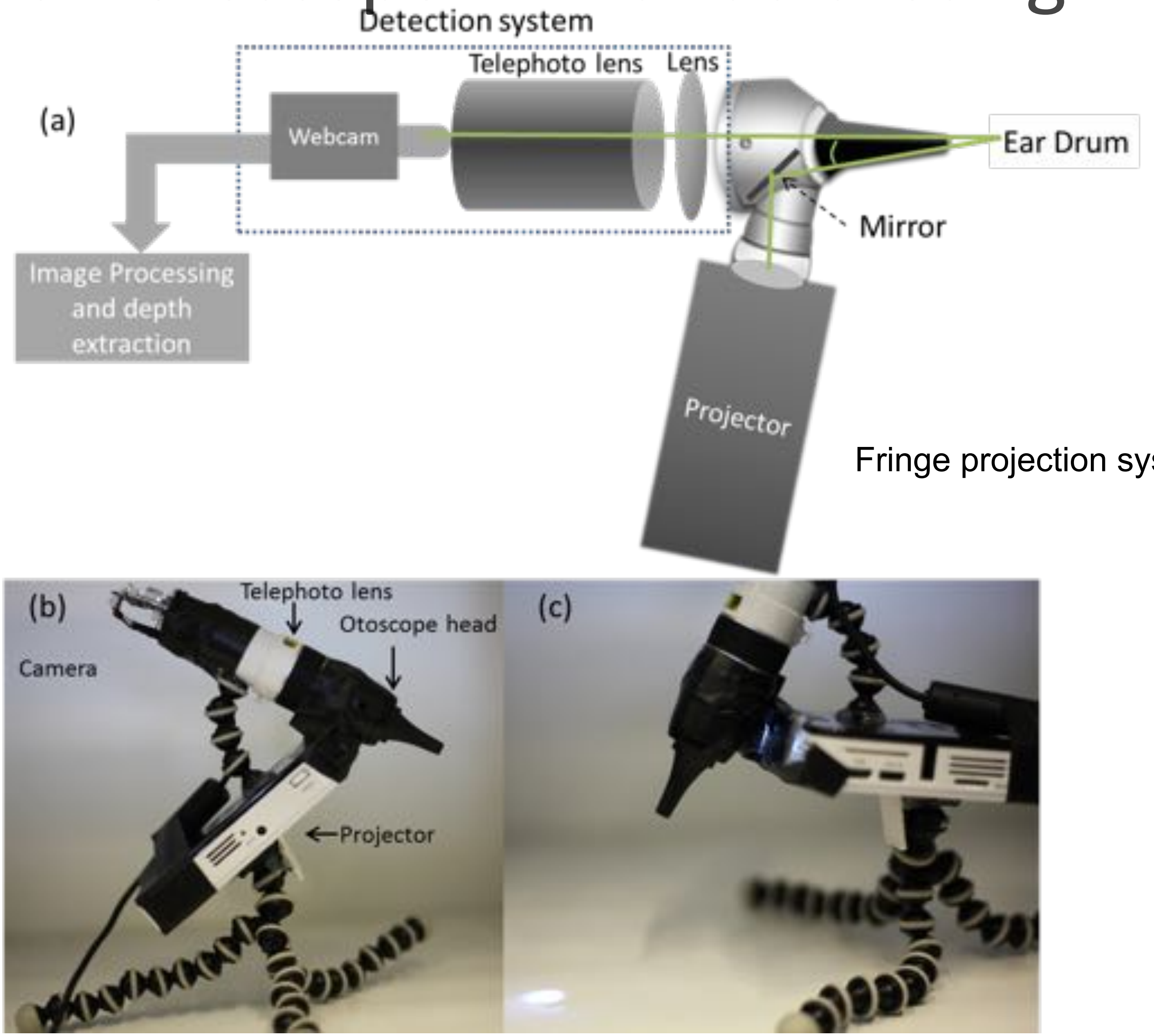

Fringe projection system

A. J. Das, et al., "A compact structured light based otoscope for three dimensional imaging of the tympanic membrane", Proceedings of SPIE Vol. 9303, 93031F (2015)

Fringe projection based 3D imaging

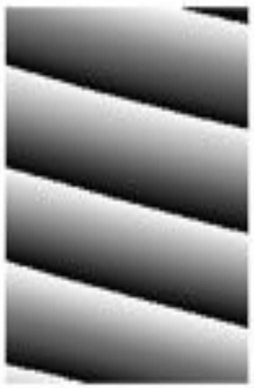

Reference projected fringe

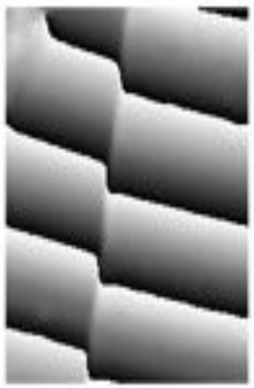

Fringe on object

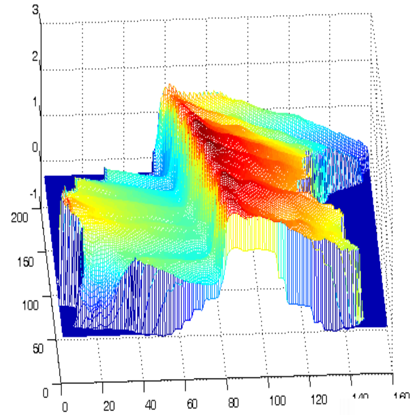

Depth resolution ~ 25 microns!

Calibration of our device with spacers of known depths

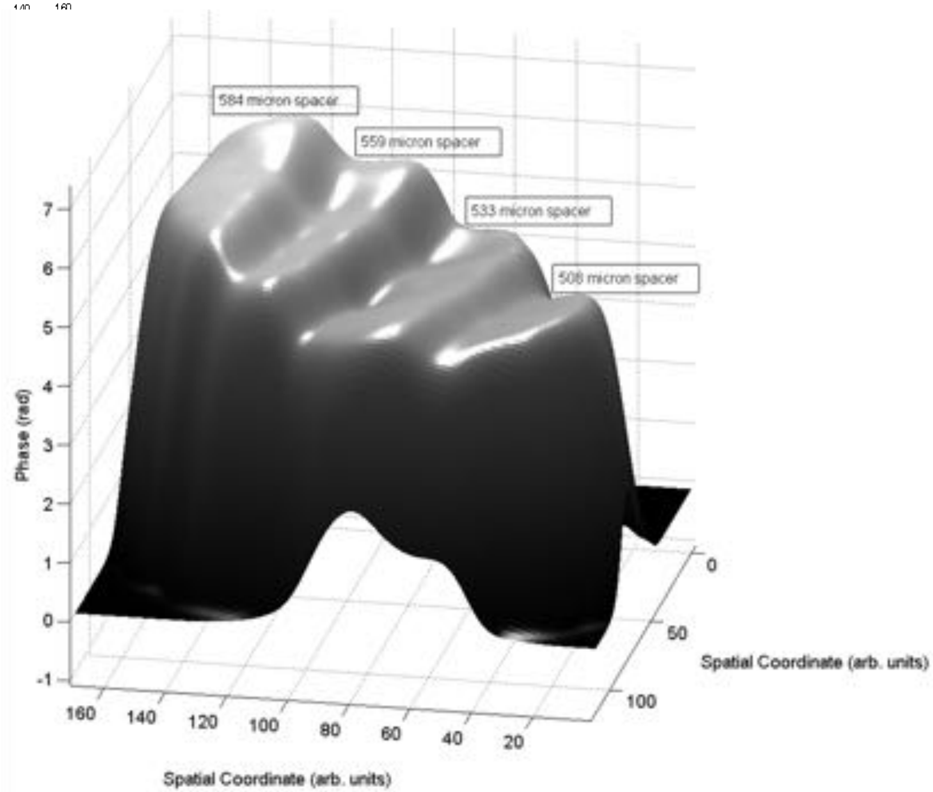

3D Imaging of Tympanic Membrane Phantom

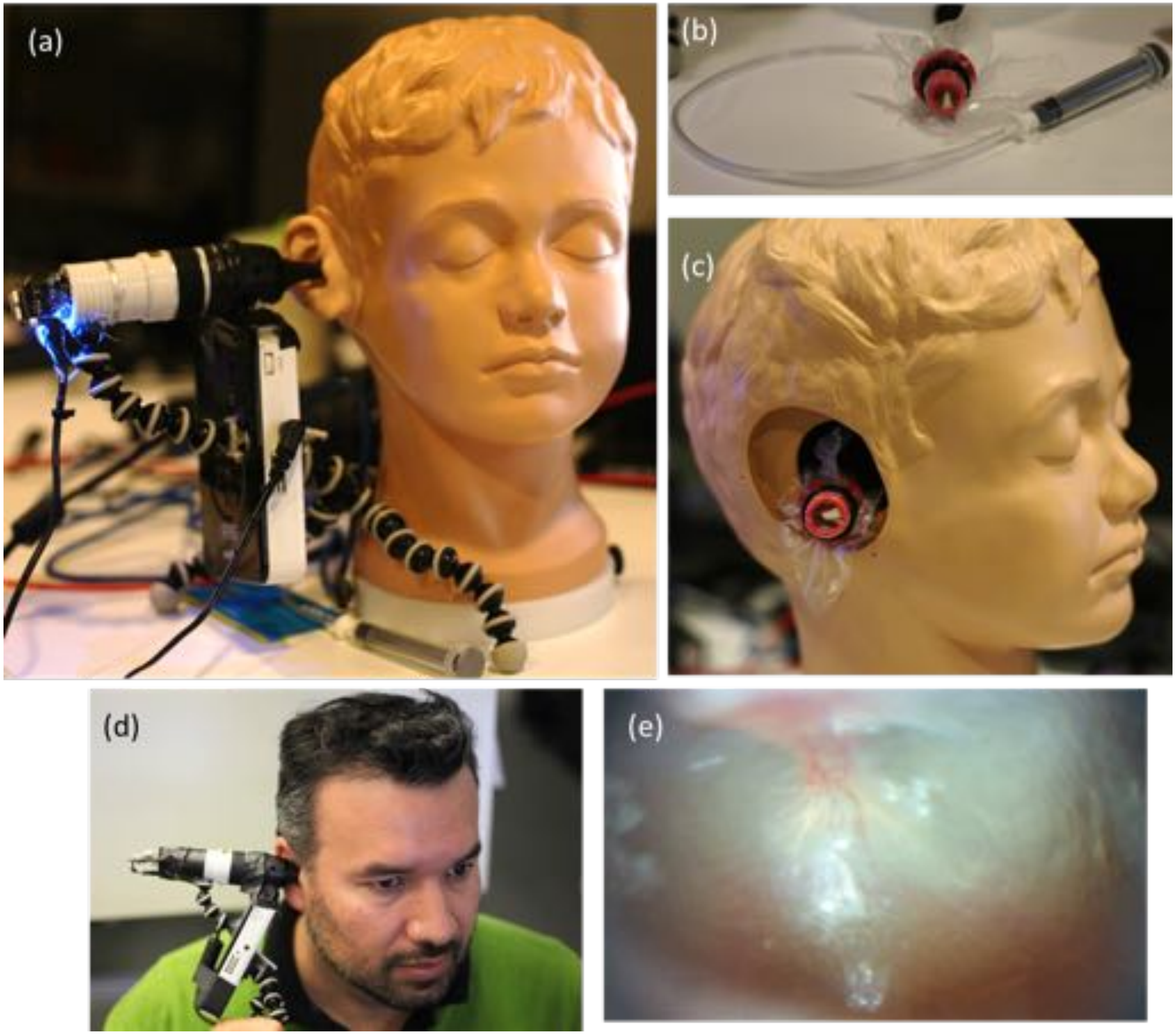

Image of TM captured by our device

Results: Ear phantom

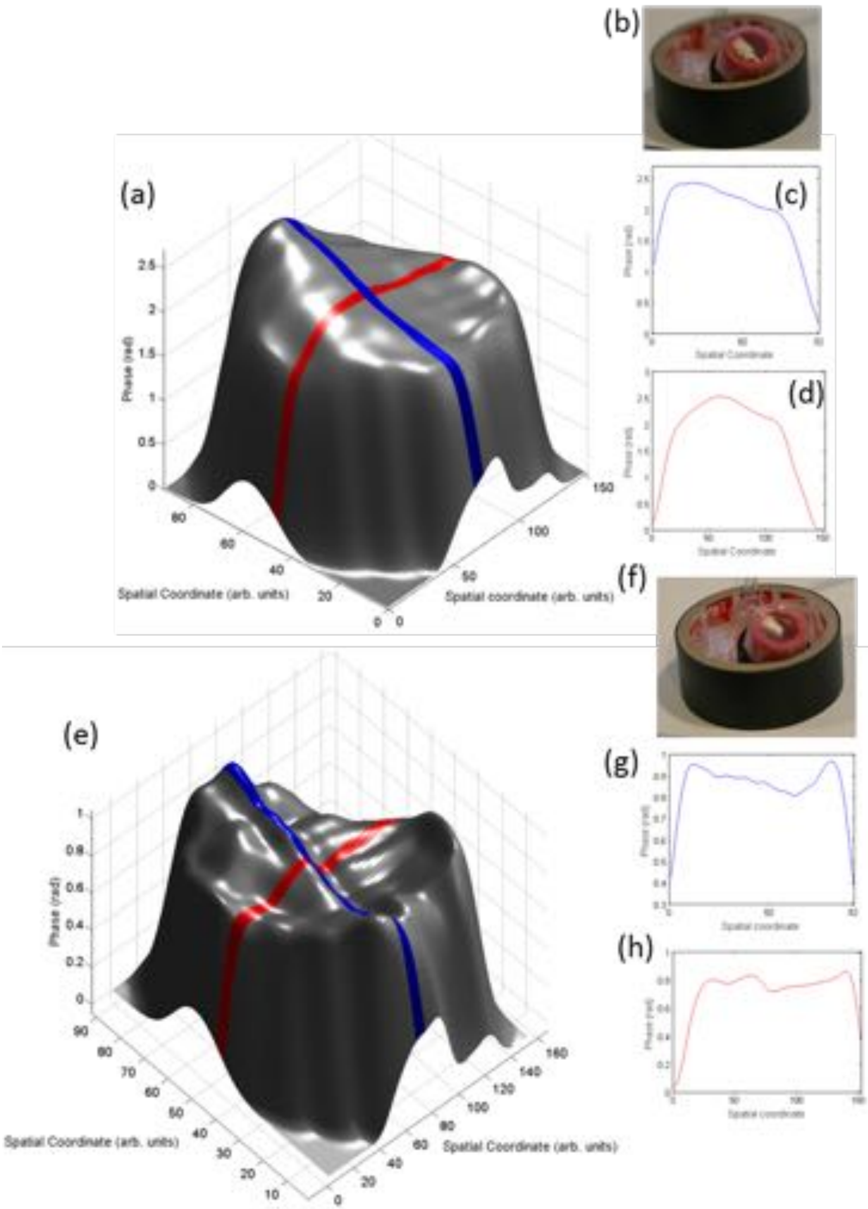

Pressure in the phantom was changed with a syringe attached to the TM

Positive pressure

Negative pressure

Results: In vivo imaging in human subject

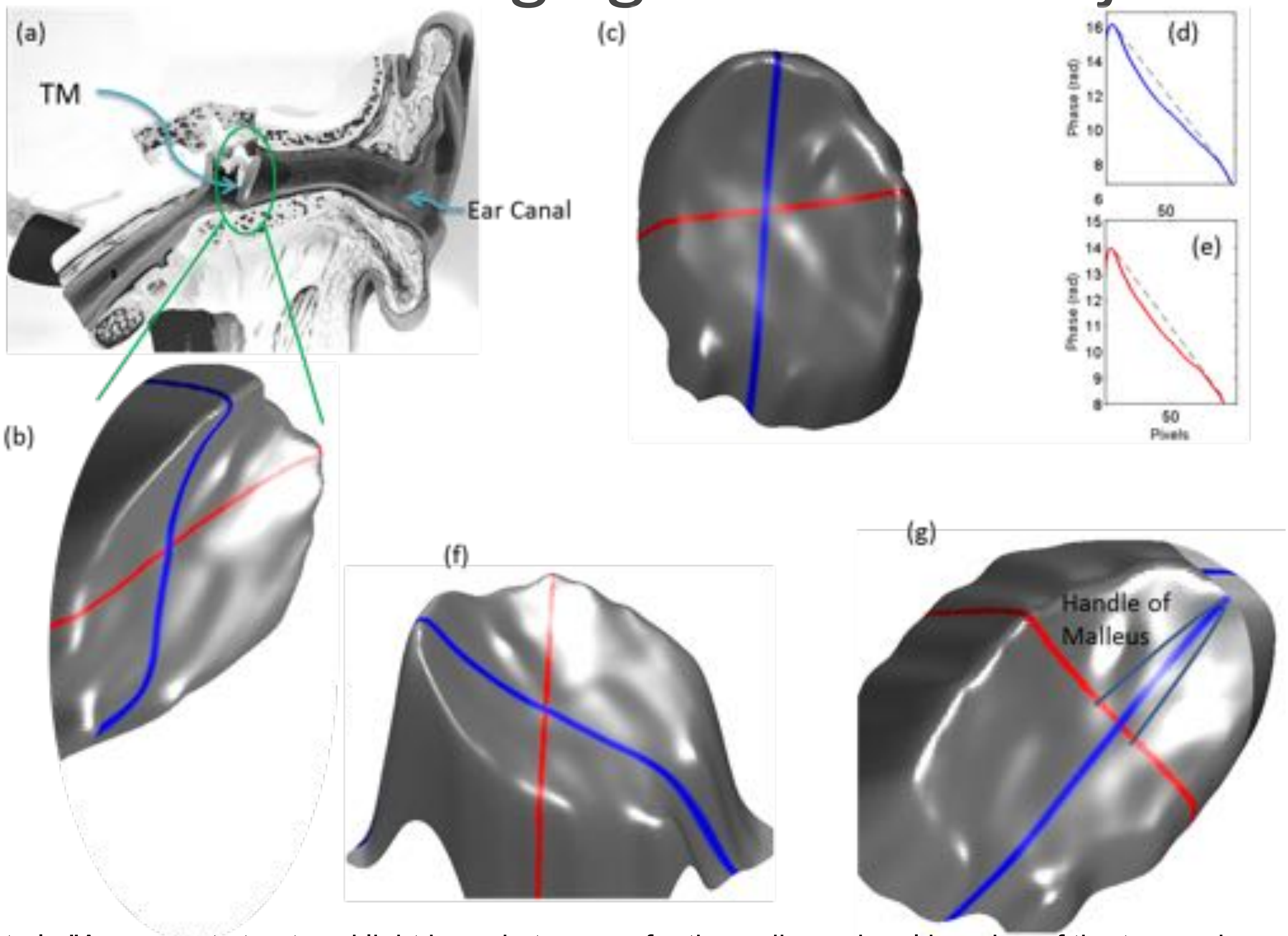

A. J. Das, et al., "A compact structured light based otoscope for three dimensional imaging of the tympanic membrane", Proceedings of SPIE Vol. 9303, 93031F (2015)

Things to keep in mind...

- Suppressing motion related noise in fringe projection
- Faster image acquisition for real time processing
- Quantification of the depth map
- Clinical tests to determine range of TM depths that are normal and classify TM into healthy and unhealthy categories
- Machine learning algorithms to carry out automated diagnosis
- Global-direct separation could be used to improve fringe contrast in cases of diffuse surfaces like the tympanic membrane

Thanks to…

- Dr. Julio Estrada, CIO, Mexico
- Dr. Ayesha Khalid and Dr. Ellen Weinberg at Cambridge Health Alliance, Harvard Medical School, Cambridge
- MIT Tata Center for Technology + Design

In the future...

- Look at throat imaging, vocal chords, nose-implications in sleep quality
- 3D endoscopy: TOF, structured light: pushing boundaries
- Reconstructing internal organs will help in surgery
- Training in surgery, simulations of internal organs

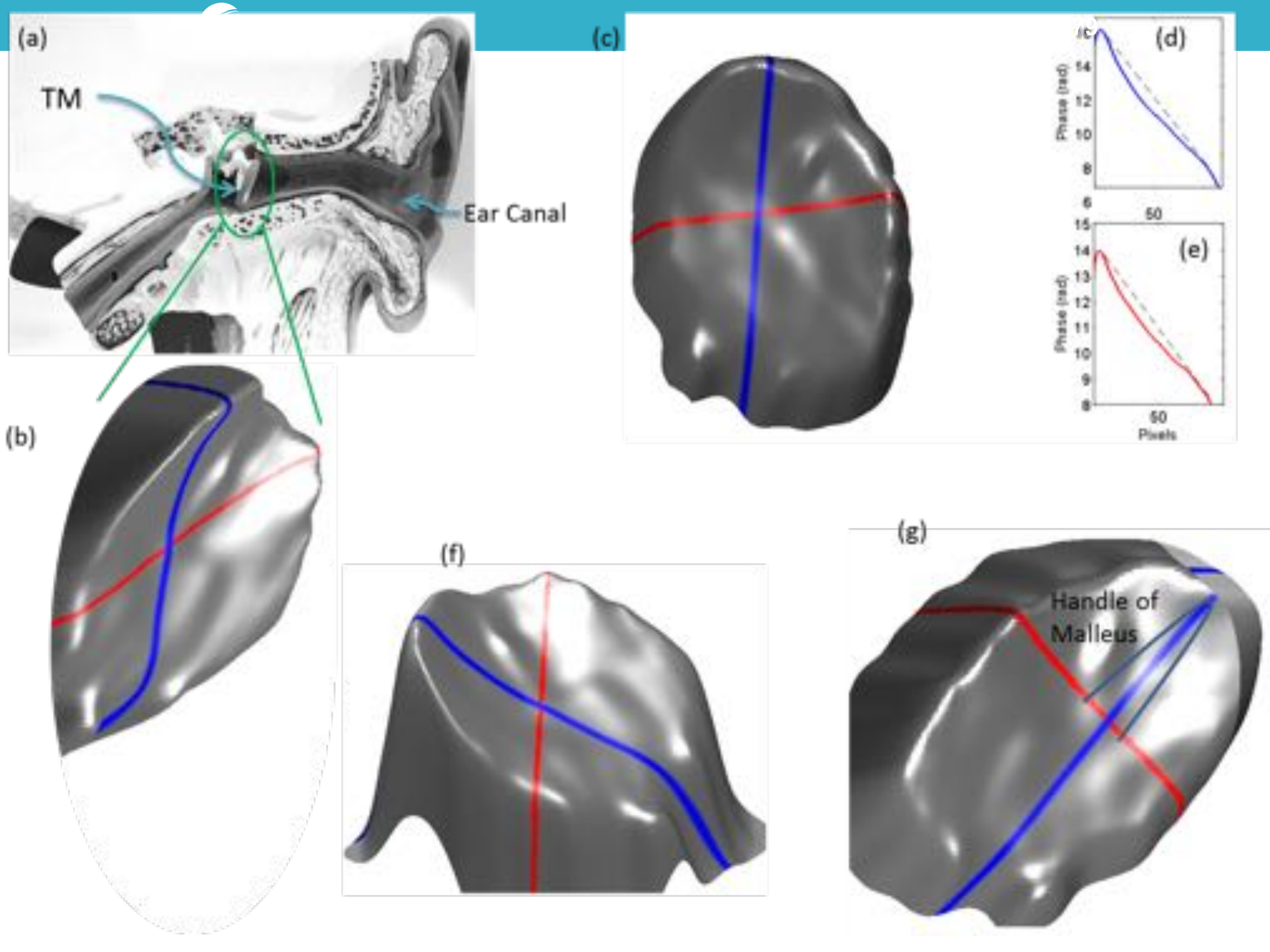

(a)
TM
Ear Canal
(b)
(c)
(d)
Phase (rad)
50
(e)
Phase (rad)
50
Pixels
(f)
(g)
Handle of
Malleus

ORAL IMAGING, RENDERING, DIAGNOSIS

Pratik Shah
USC

Imaging of the oral cavity

- How can we detect shape and color of teeth?
- How can we monitor the health of teeth and gums?
- How can we get X-ray like images of teeth with non-ionizing radiations?
- How can we use biomarker imaging and rendering to improve clinical medicine?

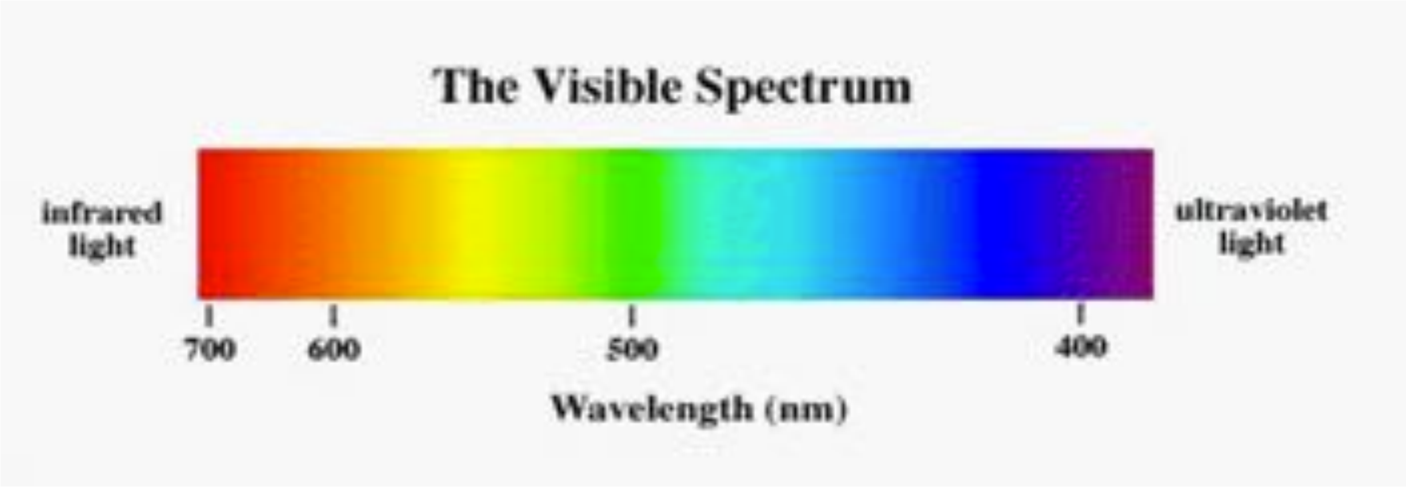

Translucent dentin
(Caries)

Porphyrin/ Color magnification
/Loss of fluorescence
(Plaque/Caries/Gingivitis)

Collagen/
NADH
(Cancer)

Visible Spectrum

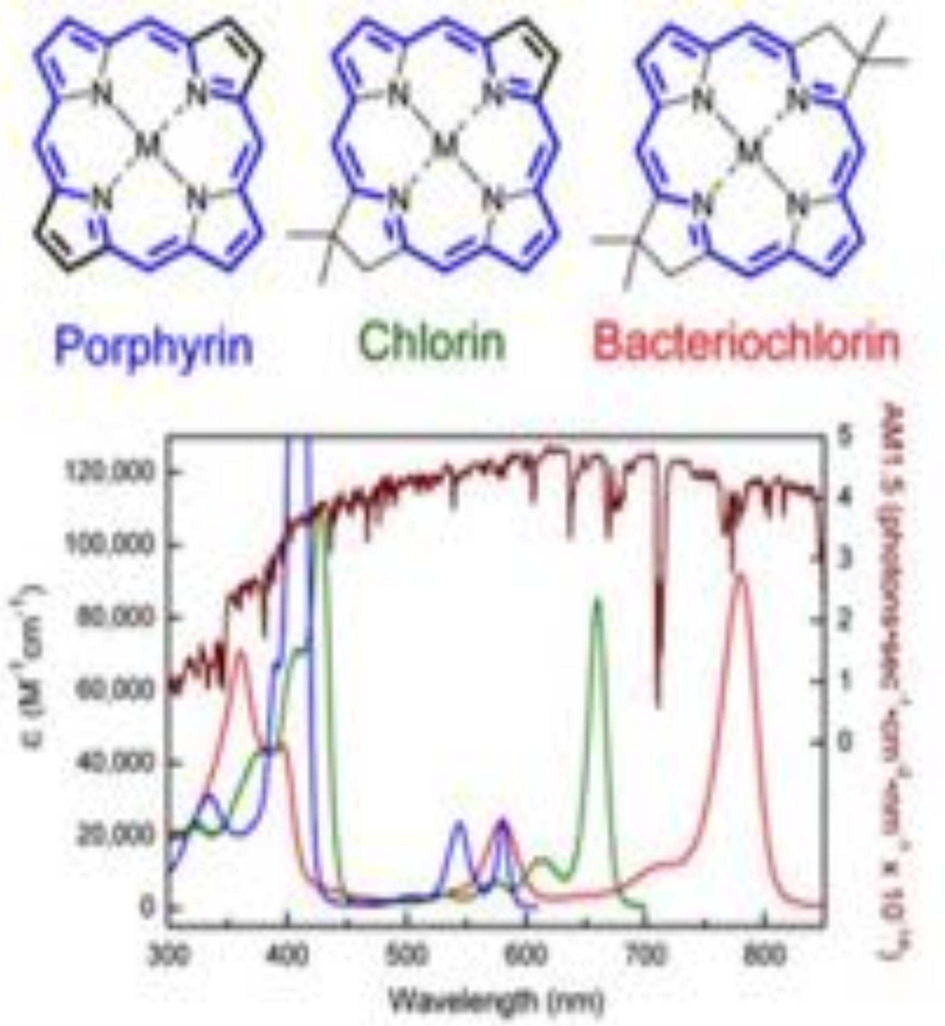

Quantitative Light Induced Fluorescence (QLF™)

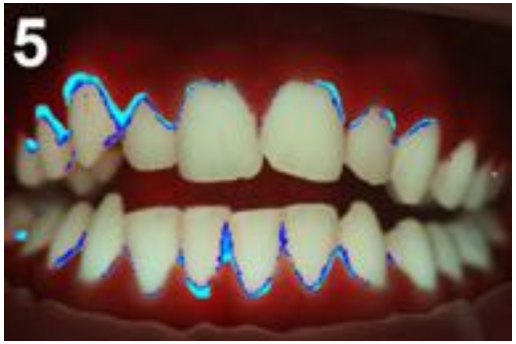

Image source:
Inspektor Research Systems
http://www.inspektor.nl/

Infrared Spectrum

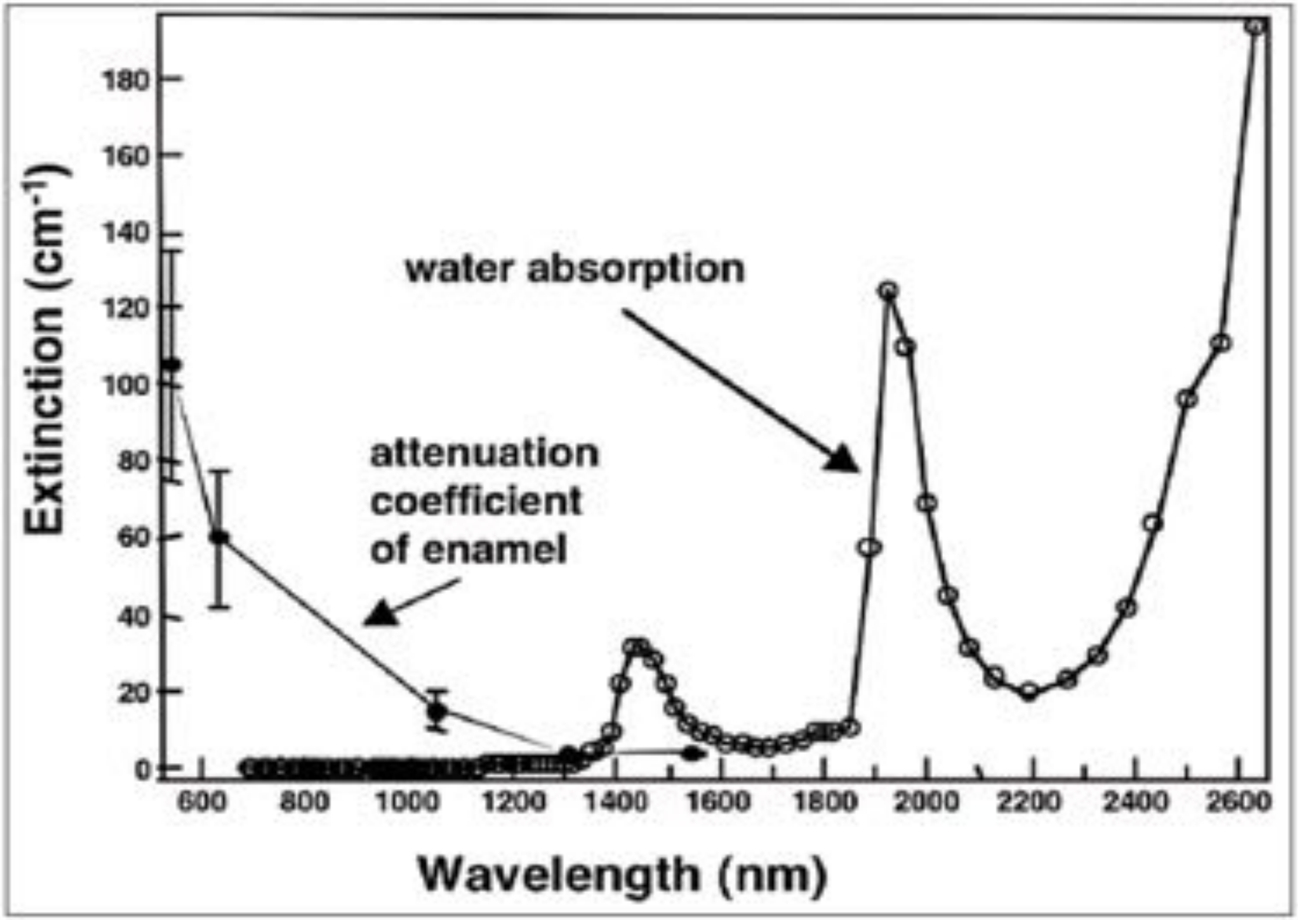

Jones R, Huynh G, Jones G, Fried D., “Near-infrared transillumination at 1310-nm for the imaging of early dental decay.”, Opt Express. 2003 Sep 8;11(18):2259-65.

Infrared Spectrum

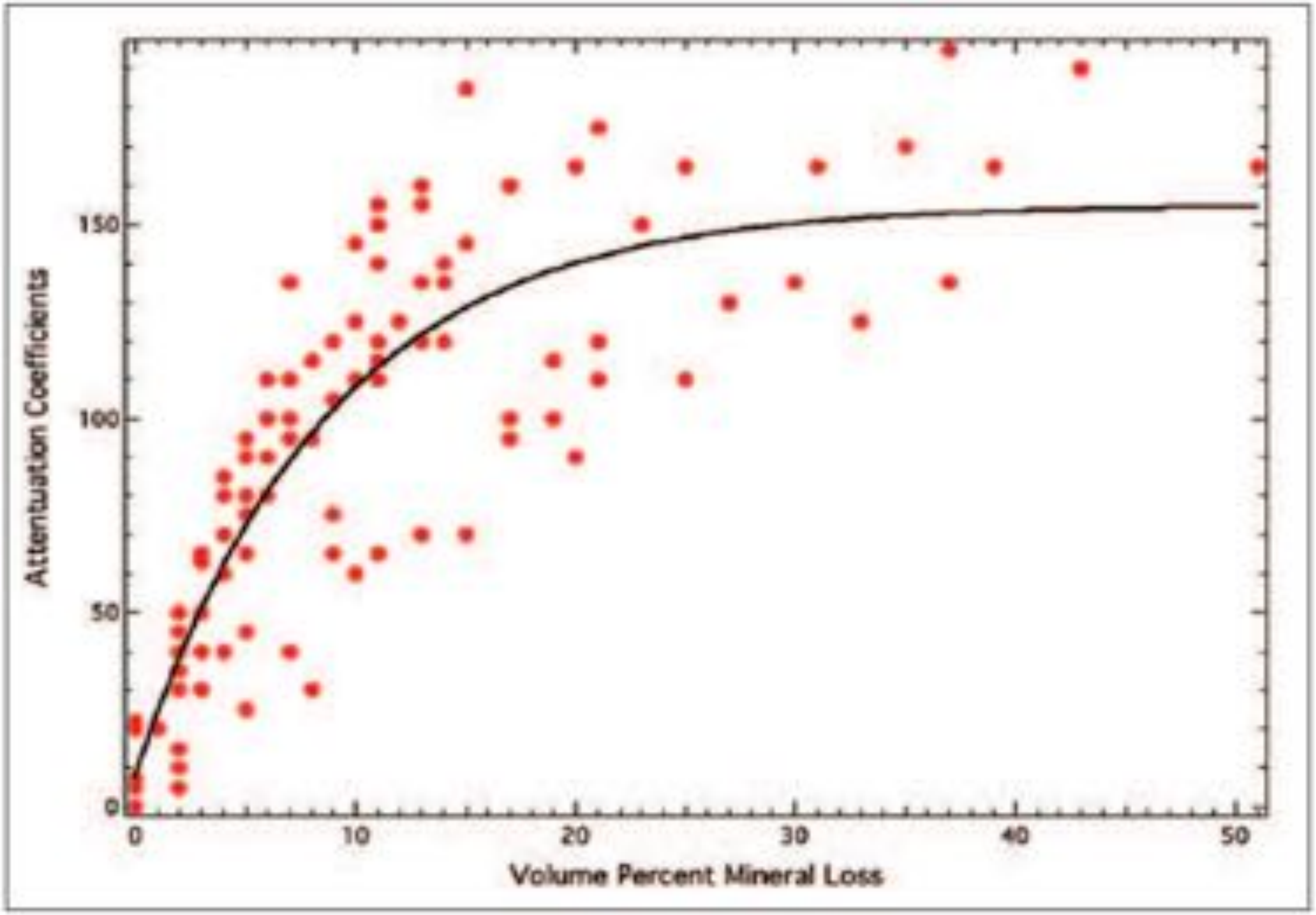

Jones R, Huynh G, Jones G, Fried D., “Near-infrared transillumination at 1310-nm for the imaging of early dental decay.”, Opt Express. 2003 Sep 8;11(18):2259-65.

Infrared Spectrum

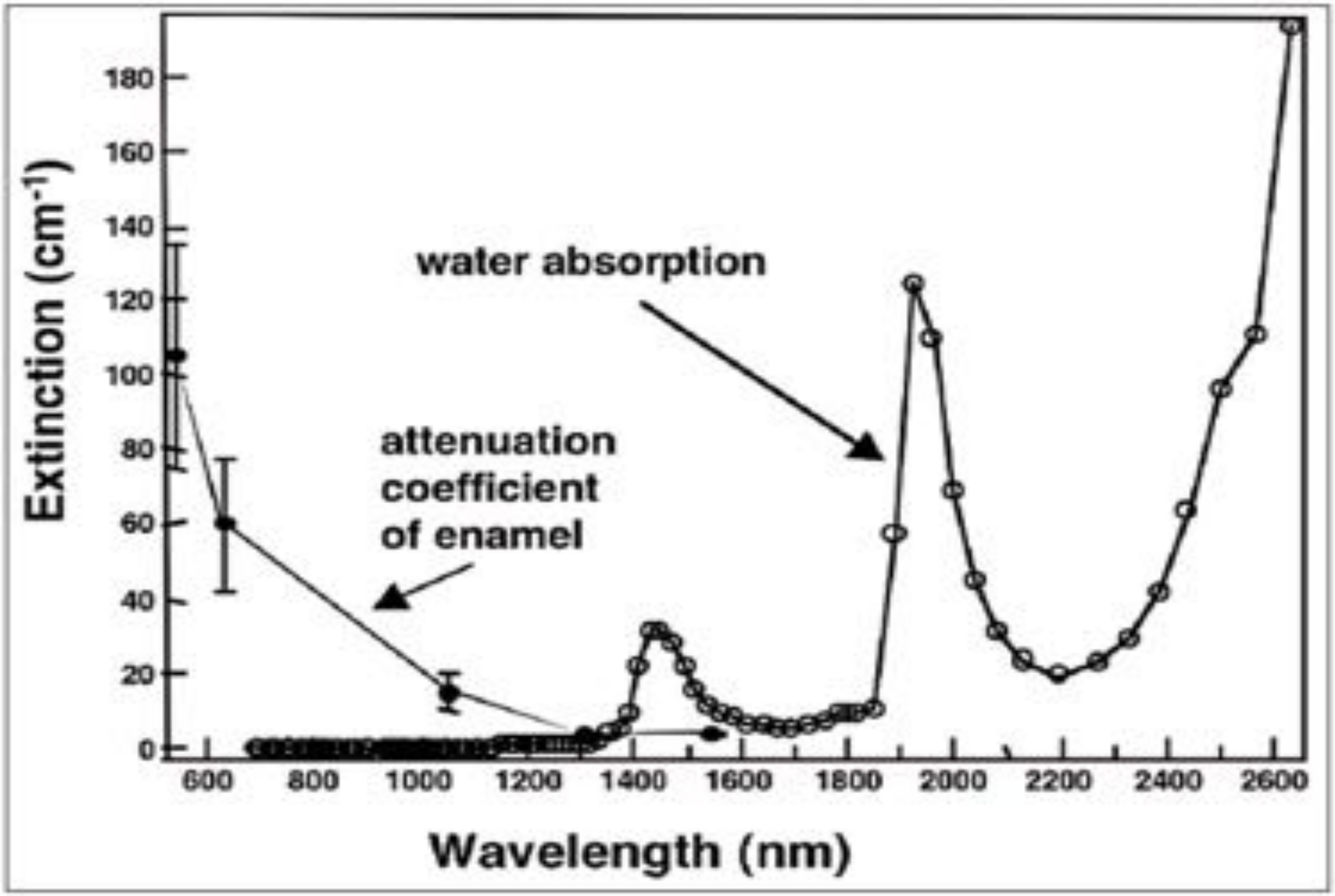

Jones R, Huynh G, Jones G, Fried D., “Near-infrared transillumination at 1310-nm for the imaging of early dental decay.”, Opt Express. 2003 Sep 8;11(18):2259-65.

Caries detection using near-infrared imaging

KaVo's DIAGNOcam

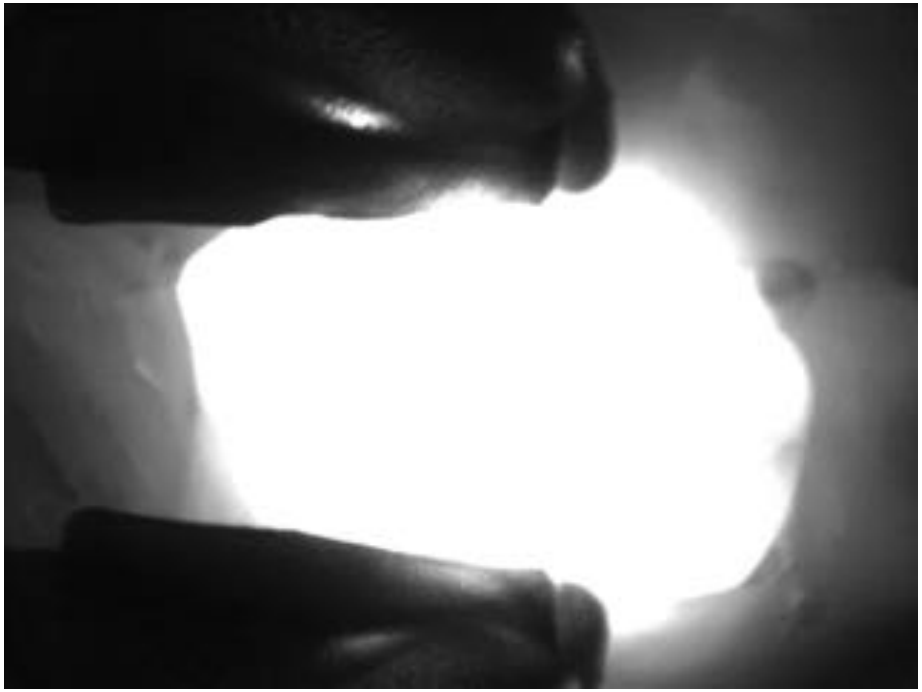

Image source:
http://www.kavo.com/Products/Diagnostics/DIAGNOcam.aspx

DIAGNOcam clinical examples

Color image | NIR | X-ray | Color image after grinding

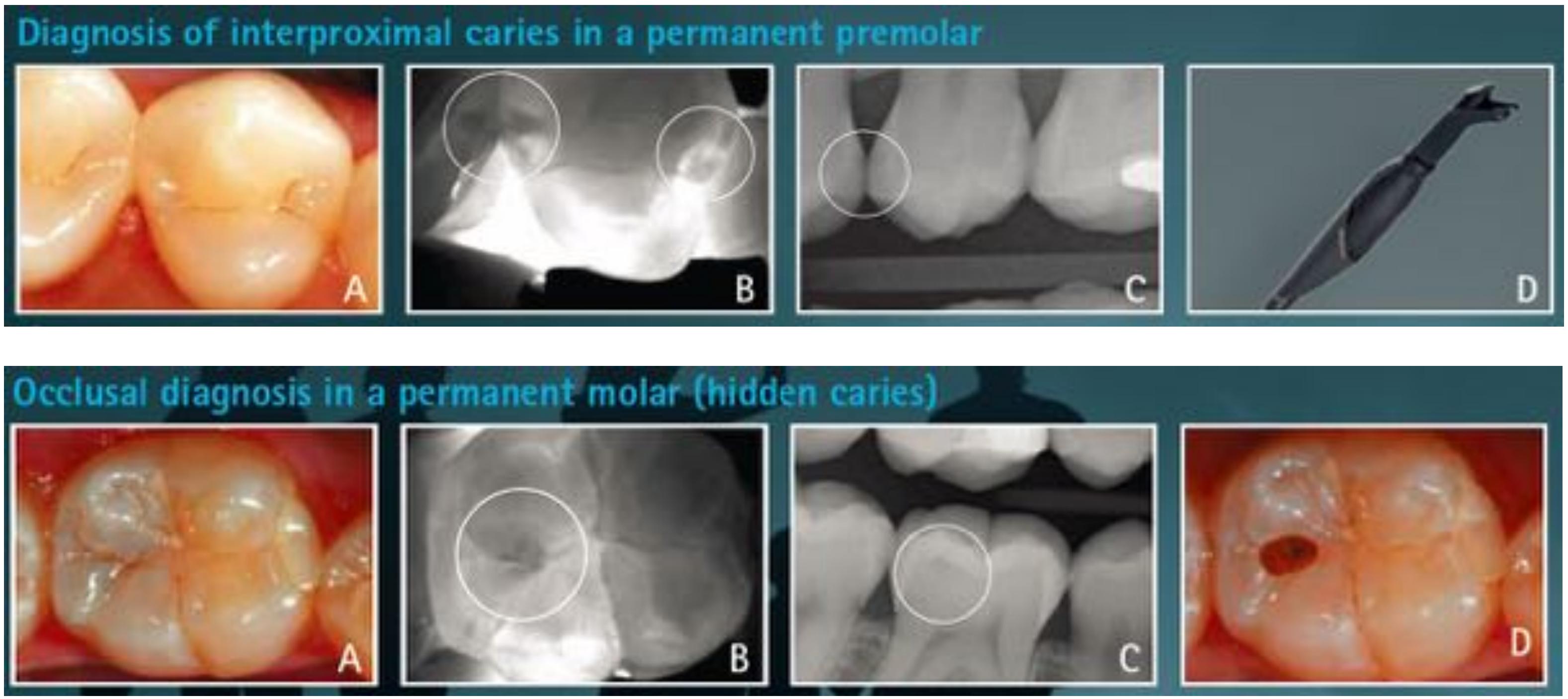

Image source:
Clinical Cases of DIAGNOcam (created by the Ludwig-Maximilian University Munich, Department of Conservative Dentistry, 2012)
http://www.diagnocam.com/

Ionizing Radiation

3D Axial Slices

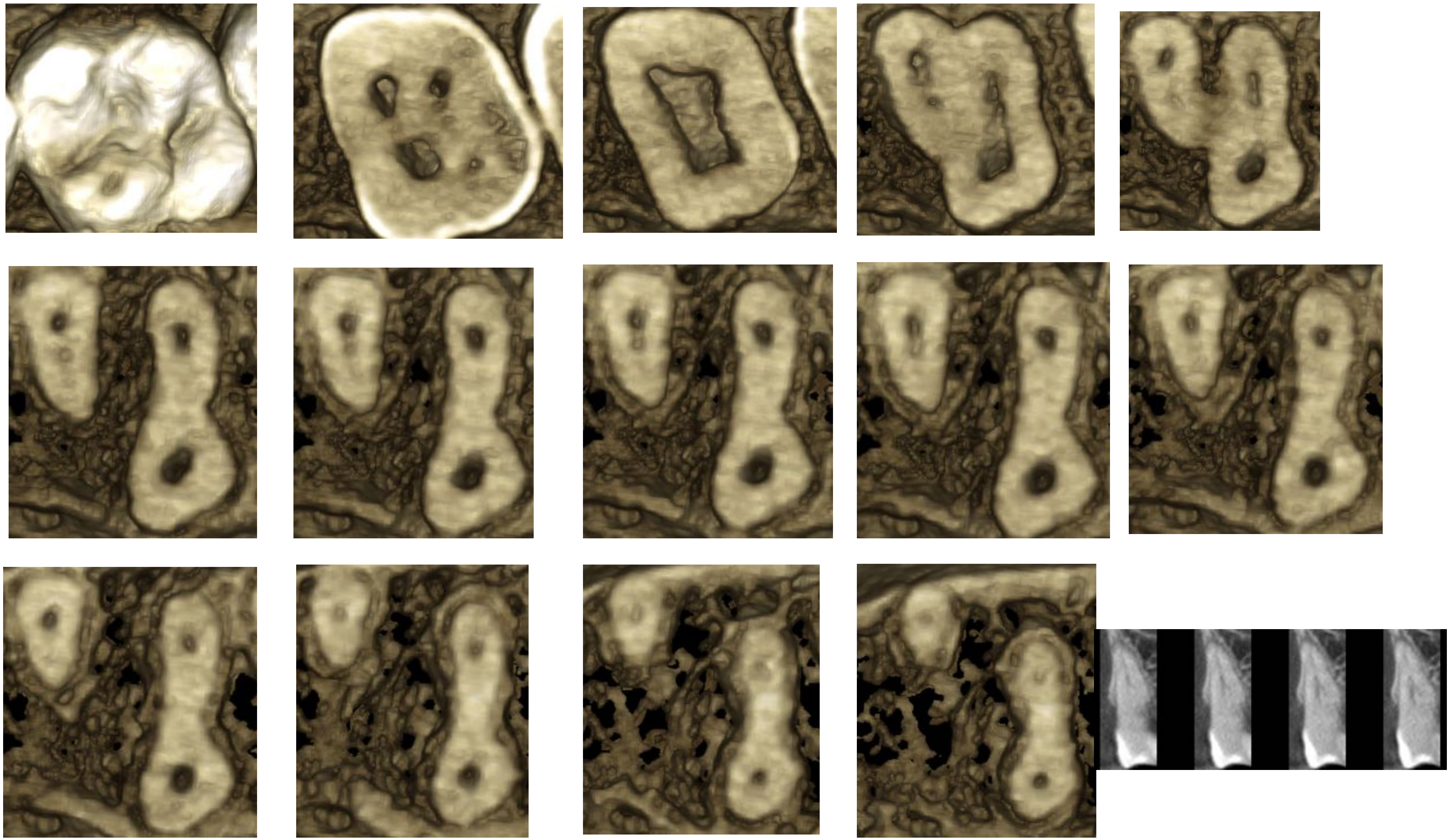

3D Scanning of teeth

Projects a light stripe pattern

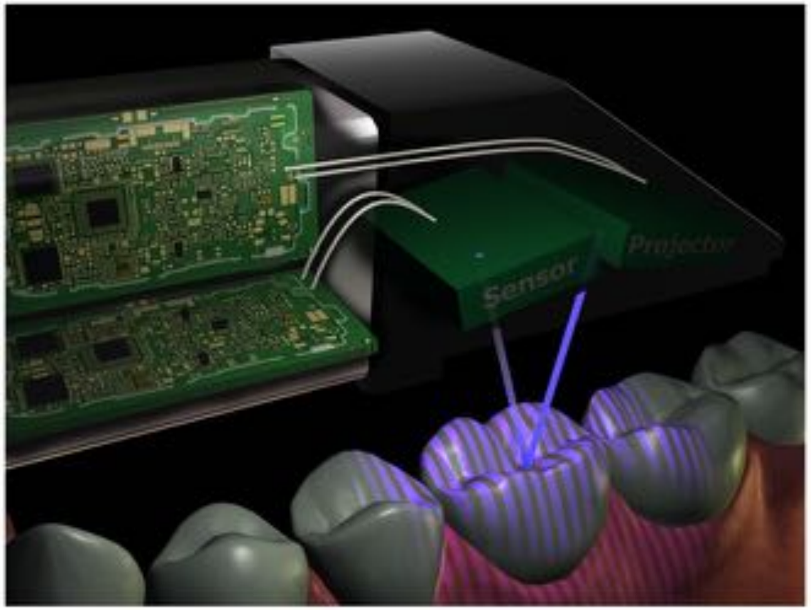

doi:10.1371/journal.pone.0043312.g001

Confocal laser scanning

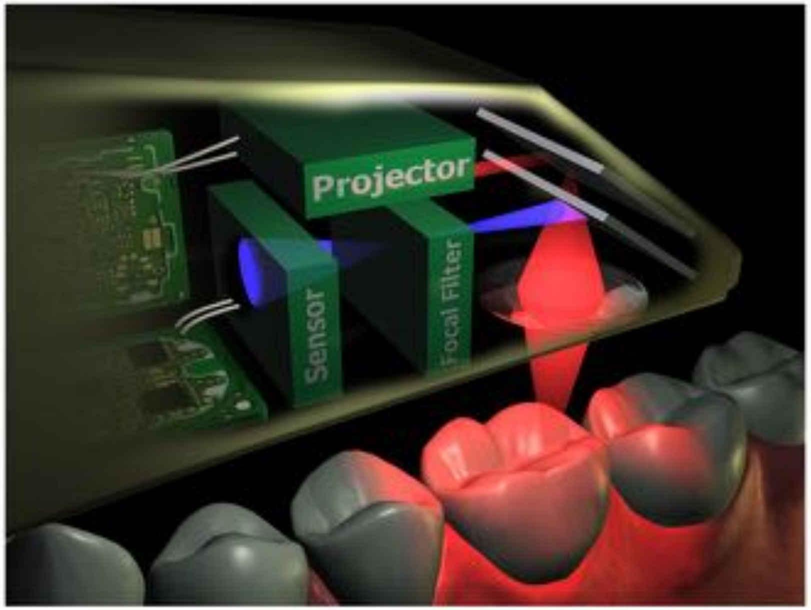

doi:10.1371/journal.pone.0043312.g002

van der Meer WJ, Andriessen FS, Wismeijer D, Ren Y (2012) Application of Intra-Oral Dental Scanners in the Digital Workflow of Implantology. PLoS ONE 7(8): e43312. doi:10.1371/journal.pone.0043312

3D scanned teeth

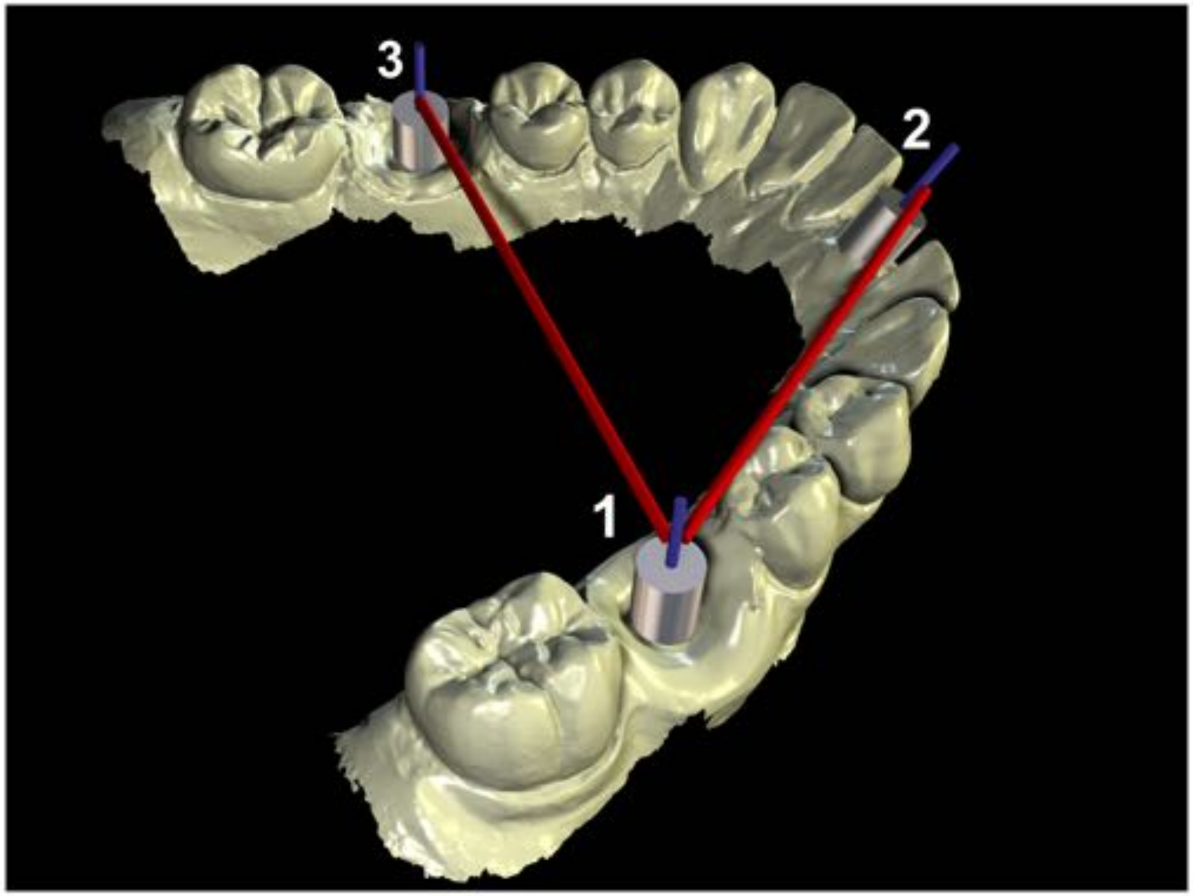

doi:10.1371/journal.pone.0043312.g005

van der Meer WJ, Andriessen FS, Wismeijer D, Ren Y (2012) Application of Intra-Oral Dental Scanners in the Digital Workflow of Implantology. PLoS ONE 7(8): e43312. doi:10.1371/journal.pone. 0043312

Measurement of tooth color

VITA Bleachedguide 3D-MASTER®

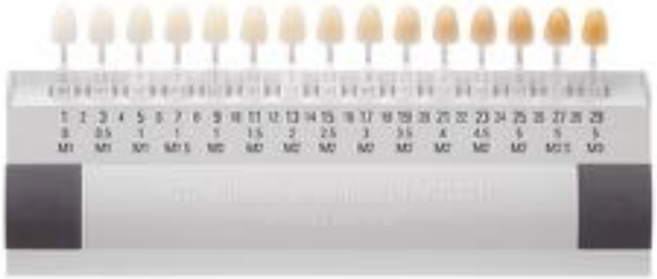

Image source:
https://www.vita-zahnfabrik.com/en/Bleachedguide-3D-MASTER-1081.html

VITA Easyshade®

https://www.vita-zahnfabrik.com/Products/Shade-determination/en/Easyshade-Advance-40-7700,27568,5851.html

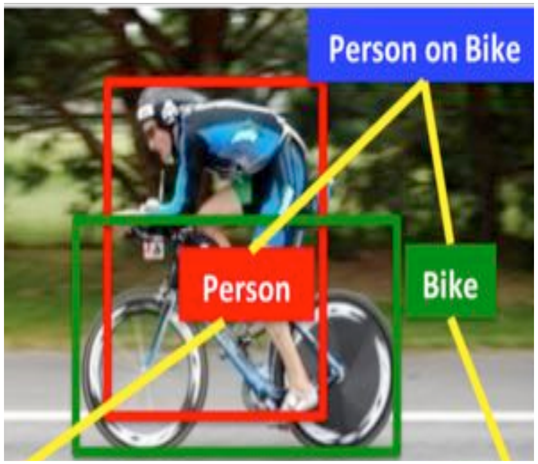

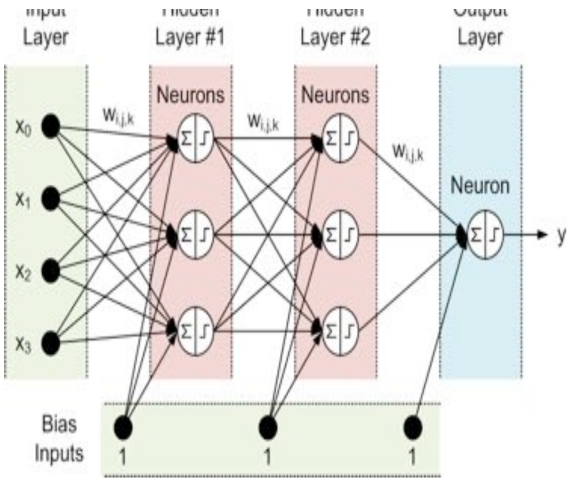

Devices

Clinical Images

Field Trials

Computer Vision → Machine Learning

Detect features in oral images

Correlate with conditions

IMAGES→PROCESSING→PREDICTIONS